Challenges and Opportunities of Membrane Bioelectrochemical Reactors for Wastewater Treatment

Jian Li

Dissertation submitted to the faculty of the Virginia Polytechnic Institute and State University in partial fulfillment of the requirements for the degree of

Doctor of Philosophy
In
Civil Engineering

Zhen He, Chair
Gregory D. Boardman
Zhiwu Wang
Francine Battaglia

March 23, 2016
Blacksburg, VA

Keywords: Microbial fuel cells, Wastewater, Energy recovery, Fouling, Optimization

Challenges and Opportunities of Membrane Bioelectrochemical Reactors for Wastewater Treatment

Jian Li

ABSTRACT

Microbial fuel cells (MFCs) are potentially advantageous as an energy-efficient approach for wastewater treatment. Integrating membrane filtration with MFCs could be a viable option for advanced wastewater treatment with a low energy input. Such an integration is termed as membrane bioelectrochemical reactors (MBERs). Comparing to the conventional membrane bioreactors or anaerobic membrane bioreactors, MBER could be a competitive technology, due to the its advantages on energy consumption and nutrients removal. By installing the membrane in the cathodic compartment or applying granular activated carbon as fluidized bed materials, membrane fouling issue could be alleviated significantly. In order to drive MBER technology to become a more versatile platform, applying anion exchange membrane (AEM) could be an option for nutrients removal in MBERs. Wastewater can be reclaimed and reused for subsequent fermentation use after a series MFC-MBR treatment process. Such a synergistic configuration not only provide a solution for sustainable wastewater treatment, but also save water and chemical usage from other non-renewable resource. Integrating membrane process with microbial fuel cells through an external configuration provides another solution on sustainable wastewater treatment through a minimal maintenance requirement.

ABSTRACT (GENERAL AUDIENCE)

Water is prerequisite to all living organisms. Anthropic activities produce a significant amount of waste every day, certainly including household wastewater. A proper wastewater treatment is a key to sustainable societal development, and this aim can be accomplished by microbial fuel cells (MFCs) technologies. In MFCs, organics in the wastewater are degraded, and the produced bioelectrical energy is harvested through external circuit. Comparing to the conventional wastewater treatment process, MFC offers several advantages, such as less sludge production, operational flexibility, and energy recovery. To optimize MFC system, integrating membrane separation process with MFC, which is termed as membrane bioelectrochemical reactors (MBERs), can produce a high quality effluent with a minimal footprint requirement and energy input. Such an integrated system can effectively remove organic contaminants, accomplish solid and liquid separation, and achieve wastewater reclamation. Therefore, the MBER system can be applied as a decentralized treatment system to remote area residents, who may not have fully developed sanitation system yet. Besides the organic contaminants, nutrients compounds, such as nitrogen and phosphorus, can be controlled by using a two chamber MBER system with anion exchange membrane as a separator material. To sum up, integrating MFC with membrane separation process has been considered as a next generation advanced wastewater treatment in a sustainable way.

ACKNOWLEDGEMENTS

The pathway of earning doctorate degree is a long and struggling process. First and foremost, thank GOD ALMIGHTY for the wisdom he bestowed upon me, the strength, peace of my mind and good health to finish this research.

I would certainly thank Dr. Zhen (Jason) He, my major advisor during my Ph. D training process. Without his help, advice, expertise, and encouragements, this research and dissertation would not have happened. Thanks for offering me such a good opportunity of doing interesting research in microbial fuel cells, membrane filtration, and other fantastic water and wastewater treatment technologies. By working with Dr. He in these four years, my interest on environmental engineering, especially on water/wastewater nexus energy has been stimulated significantly. I would also like to thank other members of my dissertation committee: Drs. Gregory D Boardman, Zhiwu (Drew) Wang and Francine Battaglia. Their insight, advice and feedback helps me a lot on my dissertation writing.

I would also like to thank Gannett Fleming. Inc and National Science Foundation (NSF) grant (#1358145) to financially support my research. I would also thank all of EBBL members for their support and assistance during my Ph. D study, and special thanks for Dr. Zheng Ge.

I would also like to thank my family members and my girlfriend, Dr. Shi. Without their constant support, encouragement and understanding, it would not have been possible for me to achieve my goal. I wish there was room on my diploma to write down their names.

CONTENTS

ATTRIBUTION

Each coauthor is duly credited for his or her contribution to this work, both in their sharing of ideas and technical expertise.

Zhen He, Ph.D. Associate Professor of Civil and Environmental Engineering
(Principal Investigator)
Department of Civil and Environmental Engineering, Virginia Polytechnic Institute and State University. Blacksburg, VA 24061

Coauthor of chapters 2-8

Zheng Ge, Ph. D.
Department of Civil and Environmental Engineering, Virginia Polytechnic Institute and State University. Blacksburg, VA 24061

Coauthor of chapters 2, 3

Yuan Zhu, M.S., Doctoral Student
MOE Key Laboratory of Wooden Materials Science and Application, Beijing Forestry University. Beijing, 100083, China

Coauthor of chapter 5

Liangpeng Zhuang, Doctoral Student
Department of Sustainable Biomaterials, Virginia Polytechnic Institute and State University. Blacksburg, VA 24061

Coauthor of chapter 5

Yuichiro Otsuka, Ph. D.
Forestry and Forest Products Research Institute. Tsukuba, Ibaraki. 305-8687 Japan

Coauthor of chapter 5

Masaya Nakamura, Ph. D.
Forestry and Forest Products Research Institute. Tsukuba, Ibaraki. 305-8687 Japan
Coauthor of chapter 5

Barry Goodell, Ph. D. Professor of Sustainable Biomaterials
Department of Sustainable Biomaterials, Virginia Polytechnic Institute and State University. Blacksburg, VA 24061
Coauthor of chapter 5

Tomonori Sonoki, Ph. D. Associate Professor of Biochemistry and Molecular Biology
Department of Biochemistry and Molecular Biology, Hirosaki University. Hirosaki, 036-8561. Japan
Coauthor of chapter 5

Graig Rosenberger, Vice President
Veolia Water Solutions and Technologies
Pennsauken, NJ. 08109
Coauthor of chapter 7

Francine Battaglia, Ph. D. Professor of Mechanical Engineering
Department of Mechanical Engineering, Virginia Polytechnic Institute and State University. Blacksburg, VA 24061
Coauthor of chapter 8

Lei Zhao, Doctoral Student
Department of Mechanical Engineering, Virginia Polytechnic Institute and State University. Blacksburg, VA 24061
Coauthor of chapter 8

CHAPTER 1

Introduction

1.1 Wastewater Treatment and Energy Consumption Issue

In 2030, the global population is projected to reach 8.3 billion, and its associated energy demand will increase by 50% (Darton et al. 2014). Safe water supply and proper wastewater treatment are significant issues as well. Proper wastewater treatment and disposal is a key factor for sustainable societal development. In the US, approximately 3-4 % of total electrical energy is consumed by water and wastewater-related industries, and such energy-intensive processes not only cause a threat to non-renewable energy source, but also poses a problem on carbon footprint. Searching for a novel process to treat municipal wastewater with less energy demand seems an option to address this dilemma (Logan et al. 2006a).

1.2 Overview of Membrane Separation

Since the late 1980s, membrane separation has been applied to municipal and industrial wastewater treatment (Judd 2010). Membrane bioreactors have gained a break-through in recent decades. Comparing to conventional activated sludge (CAS) process, membrane bioreactors provides several advantages, including (1) high treatment efficiency, due to high biomass concentration (membrane can accomplish complete liquid/solid separation); (2) high quality of treated effluent; (3) less footprint, due to the absence of secondary clarifier (Judd 2008). Recently, the reduction of membrane cost drove more wastewater treatment plants to install membrane units, in order to enhance its overall treatment performance. It is estimated that pilot-scale MBRs plants have been established in more than 200 countries (Yang et al. 2006).

Unfortunately, several technical difficulties still hinder MBR application. Such disadvantages include: (1) the rapid fouling issue requires aeration or frequent physical and chemical cleaning, which not only enhances treatment capital cost, but also reduces the operational flexibility; (2) construction cost is still unaffordable to the under-developed regions; (3) saline content in membrane effluent is unsuitable for direct potable/agriculture use, and a combined post-treatment (e.g. reverse osmosis) is required for such salinity removal (Melin et al. 2006). Therefore, searching for an alternative to generate high quality effluent, to recover nutrients maximally, and to reduce energy consumption is necessitated.

1.3 Introduction to Bioelectrochemical Systems (BES)

Bioelectrochemical system is a unique process to convert chemical energy of organic waste into electrical energy or hydrogen gas in either microbial fuel cells (MFCs) or microbial electrolysis cells (MECs) configuration (Wang et al. 2015). MFC technology has been used as most typical one among the total BES configurations. Comparing to the conventional activated sludge (CAS) process, MFCs have less or no demand for aeration and produce less sludge due to its anaerobic treatment process (Rabaey and Verstraete 2005). In the anodic compartment of MFCs, organics are bio-degraded and the generated electrons are transferred to a solid electrode through $NADH/NAD^+$, then to the serial cytochrome agents at the outer cell membrane (Logan et al. 2006a). In the cathodic compartment, an electron acceptor, such as oxygen, nitrate or ferricyanide, is supplied to accept produced electrons through an external circuit (Xu et al. 2016).

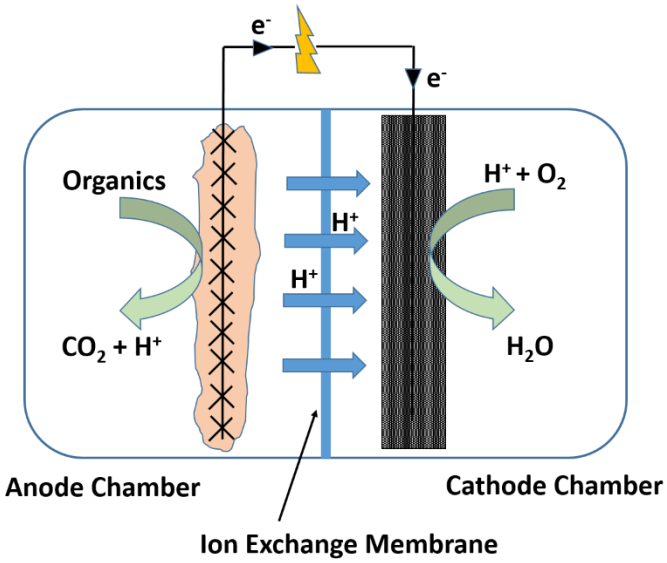

Figure 1.1 Schematic of a two-chamber microbial fuel cell (MFC)

As shown in Table 1.1 (Logan et al. 2006a), a theoretical open circuit voltage (OCV) is about 1.1 V, by assuming sodium acetate is supplied as a carbon source in the anodic chamber and oxygen is used as an electron acceptor in the cathodic chamber. However, a lower potential such as 0.8 V is usually observed and reported, which could be due to the overpotential, electrolyte diffusion resistance and ohmic loss (He and Mansfeld 2009). Comparing to other types of renewable energy such as bio-diesel, which may require several post treatments after production, MFCs can directly convert chemical energy into electrical energy, which not only reduces carbon footprint, but also provides more operational flexibility.

Table 1.1 Standard potentials E_0 and theoretical potentials for typical conditions in MFCs

Electrode	Reaction	E_0 (V)	Conditions	E_{MFC} (V)
Anode	$2\ HCO_3^- + 9\ H^+ + 8\ e^- \rightarrow CH_3COO^- + 4\ H_2O$	0.187	HCO_3^- = 5 mM, CH_3COO^- = 5 mM, pH = 7	-0.296
Cathode	$O_2 + 4\ H^+ + 4\ e^- \rightarrow 2\ H_2O$	1.229	pO_2 = 0.2, pH = 7	0.805
	$O_2 + 2\ H_2O + 4\ e^- \rightarrow 4\ OH^-$	1.229	pO_2 = 0.2, pH = 7	0.805

Note : Sodium acetate is oxidized in anodic chamber and Oxygen is reduced in cathodic chamber

More versatile functions can be accomplished by BES. But in essence, these applications are all due to the fact that electrons are extracted from the anodic chamber, but various reactions may occur in the cathodic chamber with different end-products. For example, microbial electrolysis cell (MEC) can be established by applying an external voltage to generate hydrogen peroxide or gaseous hydrogen evolution within the cathodic chamber (Liu et al. 2005). Or, MFC can be applied as a solution for desalination by inserting a piece of anion exchange membrane (AEM) between the anodic and the cathodic chambers, termed as microbial desalination cells (MDCs) (Cao et al. 2009). More diverse BES applications have been reported in a recent review paper (Li et al. 2014d).

1.4 Membrane Bioelectrochemical Reactors (MBERs)

It is true that BES has gained a lot of attention due to the aforementioned advantages. Unfortunately, several technical bottlenecks exist and require addressing, such as: (1) A long treating period, because previous field test demonstrated organics in the primary effluent can be degraded by 65-70% within 11 hr (Zhang et al. 2013b); (2) Nutrients elements such as phosphorus and nitrogen are not effectively removed from the treatment process (Ge et al. 2013b); (3) Suspended solids in treated effluent is high; (4) Comparing to the conventional energy recovery process, such as anaerobic digestion, BES has marginal energy advantages (Ge et al. 2013c); (5) Construction cost is high due to the use of an ion exchange membrane as a separator and precious metal as catalyst; (6) Scaling-up (over 1 m^3) system has rarely been established.

It is impossible to solve all of these problems simultaneously, but maintaining a high effluent quality should be given a priority consideration. It can be accomplished by combining membrane separation with an MFC system, named as membrane bioelectrochemical reactors (MBERs). MBER is a system that incorporates MFC with MF/UF membranes as a filtration media, which can be installed either inside the anodic chamber or the cathodic compartment. Comparing to conventional aerobic membrane bioreactors (AeMBRs), MBERs have more advantages on energy consumption, due to less aeration requirement and the bio-fouling issue. But comparing to the anaerobic membrane bioreactors (AnMBRs), MBERs can eliminate biogas collection, and enhance nutrients removal. MBERs also have advantages on reducing dissolved methane in the effluent. Hence, it is expected that integrating MFC

with membrane filtration could be an option for next-generation sustainable advanced wastewater treatment.

1.5 Research Objectives

In this study, the overall goal is to explore optimum operation of bench-scale MBERs, including:

- Investigating feasibility of MBER and its associated optimization with minimum fouling control;
- Maximizing overall energy recovery, organics and nutrients removal;
- Developing a mathematical model to help understand and optimize MBER system

The first objective is to search optimum MBER operation with minimal fouling controls. An early study has introduced the concept of MBER by installing a bundle of hollow fiber ultrafiltration membrane in a tubular MFC (Ge et al. 2013b). The MBER has been operated more than 200 days with either defined solution (sodium acetate) or real domestic wastewater (primary effluent). The MBER removed 43-58% of total chemical oxygen demand from the sodium acetate solution and more than 90% organics removal with primary effluent. Periodic backwashing and relaxation could provide a solution for retarding TMP from 0 to 15 kPa more than 40 days under hydraulic retention time (HRT) of 36 h, but higher organic loading rates (either shorten HRT or increasing influent organic strength) could accelerate the membrane fouling issue. Hence, searching for alternative membrane fouling control is a key factor to MBERs operation. Granular activated carbon (GAC) has been used in water or wastewater treatment, due to its higher surface area per unit of volume. But the application of GAC on MFCs has been limited. Fluidizing GAC inside a tubular MBER could provide a solution for alleviating the membrane fouling issue,

due to the constant mechanical contact between GAC and membrane surface area. Moreover, GAC may act as a partial anode electrode, since more conductive surface area from GAC could be favorable for biomass attachment. One more strategy for solving the membrane fouling issue may be gas scrubbing. In a typical MFC configuration, oxygen is usually supplied as electron acceptor within the cathodic compartment. Installing a membrane filtration process within the cathodic compartment can not only provide a post-treatment for anode effluent, but also own a minimum fouling control by taking advantage of constant aeration. Hence, the two abovementioned strategies will be attempted in the present study.

The second objective is to optimize nutrients removal and recovery from MBERs. Nutrients and phosphorus are two critical elements, which can cause serious algae-blooming problems, due to the massive growth of autotrophs. Hence, nutrients removal before discharging pose a significant issue to wastewater treatment facilities. The conventional nitrogen removal process requires high land usage, intensive energy demand and extra carbon source (e.g. methanol). Also, phosphorus removal by chemical precipitation not only requires a strict pH control, but also needs chemical addition, which could increase operational cost for wastewater treatment facilities. Besides disposing such nutrients, searching for a proper way to recycle/reuse them could be another option, due to the more stringent regulation on water discharging and depletion of non-renewable chemical resources. Hence, sustainable nutrients removal will be attempted, and the feasibility of wastewater reclamation and reuse from MBERs will be proved as well.

The third objective is to develop a mathematical model of MBERs, which could be helpful for further understanding and optimization. Given its intrinsic physical, biological and electrochemical factors, an MBER model could consist of two parts: MFC and MBR, which organic matter is a key factor to link these in-series biotic processes. In model formulation, the Nernst-Monod equation is used for biomass growth and electrical generation within the anodic compartment. Conventional activated sludge model integrated with membrane filtration will be used as MBR models. It is expected that findings from the current study could be useful for the next generation MBER models, which includes heterogeneous substrate and microbial distribution within the anodic chamber, and a more dynamic overpotential. Such aspects can be accomplished by a coupled computational fluid dynamics (CFD) with a multi-order Butler-Volmer reaction model, where heterogeneous substrate distribution is simulated by CFD software (ANSYS. Inc.) first, and consequently, using the multi-order Butler-Volmer reaction model to predict electricity generation.

CHAPTER 2

A Fluidized Bed Membrane Bioelectrochemical Reactor for Energy Efficient Wastewater Treatment

(This section has been published as: Li, J., Ge, Z.and He, Z.* (2014) A fluidized bed membrane bioelectrochemical reactor for energy efficient wastewater treatment. **Bioresource Technology**. Vol 167, pp 310-315.)

Abstract

A fluidized bed membrane bioelectrochemical reactor (MBER) was investigated using fluidized granular activated carbon (GAC) as a mean of membrane fouling control. During the 150-day operation, the MBER generated electricity with contaminant removal from either synthetic solution or actual wastewater, as a standalone or a coupled system. It was found that fluidized GAC could significantly reduce transmembrane pressure (TMP), although its function as a part of the anode electrode was minor. When the MBER was linked to a regular microbial fuel cell (MFC) for treating a wastewater from a cheese factory, the MFC acted as a major process for energy recovery and contaminant removal, and the coupled system removed more than 90% of chemical oxygen demand and >80% of suspended solids. The analysis showed that the ratio of energy recovery and consumption was slightly larger than one, indicating that the coupled system could be theoretically energy neutral.

2.1 Introduction

Sustainable wastewater treatment is of great importance to maintain a sustainable societal development, and its key features include high quality of treated effluent and energy-efficient treatment process. Those features can be realized separately using technologies such as membrane bioreactors (MBR) and microbial fuel cells (MFCs). MBR technology

has been applied to treat both municipal and industrial wastewaters. It has several advantages over conventional activated sludge system (Judd 2008); however excessive energy consumption due to aeration and antifouling control is still a hurdle for globally application especially in some energy-shortage areas. MFC technology is an emerging concept and has been intensively studied as an alternative method for energy-efficient wastewater treatment (Wang and Ren 2013). Comparing with conventional activated sludge technology, MFCs have less or no demand for aeration and produce much less sludge due to anaerobic treatment (Rabaey and Verstraete 2005). Research has demonstrated that MFC treatment of domestic wastewater could be energy-neutral (Zhang et al. 2013b).

Integration of MFCs with a membrane filtration process such as MBRs may provide an ideal solution to achieve high-quality effluent, with less energy requirement (than aerobic treatment systems). An early effort used the biofilm formed on the stainless steel as filter materials to achieve low effluent turbidity and high removal of both organic matter and ammonium nitrogen (Wang et al. 2011b, Wang et al. 2012). The use of micro/ultra filtration membranes as filtration media in MFCs was reported in a membrane bioelectrochemical reactor (MBER), in which the commercially available hollow fiber membranes were installed in the anodic chamber of a tubular MFC (Ge et al. 2013b). This MBER system effectively treated both synthetic and domestic wastewater but membrane fouling was a serious issue. To facilitate the application of proper fouling control and minimize its effects on the anode microbial activity, hollow-fiber membranes were installed in the cathode compartment of an MFC with either an aerobic or anoxic cathode

(Li et al. 2014b). In addition to internally installed membrane, MFCs were also directly linked to an MBR (Malaeb et al. 2013).

In a treatment system containing membrane, fouling/scaling is always a great challenge. A new method for fouling control was developed by using fluidized granular activated carbon (GAC) in an anaerobic membrane bioreactor (AnMBR) (Kim et al. 2011). This method allowed little physical or chemical cleaning of membrane module during 120-day operation, and it also had energy benefits for fouling control comparing to conventional MBR. This fluidized AnMBR has been advanced to pilot test that achieved satisfactory performance (Shin et al. 2014). A similar fluidized AnMBR was linked to a single-chamber MFC as a post-treatment for improving effluent quality (Ren et al. 2014). The concept of fluidized particle bed was also applied to prevent inorganic scaling deposit on the surface of cathode electrode in a microbial electrolysis cell (MEC) (Cusick et al. 2014).

Intrigued by the fluidized AnMBR concept, a fluidized bed membrane bioelectrochemical reactor (MBER) was developed here for energy-efficient wastewater treatment. This MBER aimed to take advantage of fluidized GAC as both fouling control media and partial anode electrode. The objectives of this study were: (1) to examine the feasibility of electricity generation and wastewater treatment in this fluidized bed MBER; (2) to investigate membrane fouling affected by the operating conditions; and (3) to formulate a treatment system by linking the MBER to an MFC for treating actual wastewater.

2.2 Materials and Methods

2.2.1 Reactor construction

2.2.1.1 MBER setup

The MBER was constructed as a tubular reactor (45 cm long and 5 cm in diameter) made of cation exchange membrane (CEM- Ultrex CMI 7000, Membrane International, Inc. Glen Rock, NJ, USA) (Fig. 2.1A). The main body of the anode electrode was a piece of carbon cloth supported by stainless steel mesh, which was installed inside the membrane tube (along the interior wall). Ten 38-cm PVDF hollow fiber membranes (15000 Dalton, Litree Purifying Technology Co, China) were installed inside the membrane tube, which was then filled with 230 g of 8 x 30 mesh GAC (Calgon Carbon Corp, Pittsburgh, PA, USA), resulting in an anode liquid volume of 700 mL. The hollow fiber membranes had a pore size of 0.02 μm and the total membrane surface area was 0.021 m^2. Before use, carbon cloth was soaked in acetone solution overnight and heated for 30 min at 450 $^{\circ}$C. The cathode electrode consisted of one layer of carbon cloth (Zoltek Corporation, St. Louis, MO, USA) coated with Pt/C powder (10%, Etek, Somerest, NJ, USA) with a loading rate 0.05 mg Pt cm^{-2}. The cathode electrode wrapped the membrane tube and was exposed in the air for passive oxygen supply as described in the previous studies. The anode and cathode electrodes were connected by using titanium wires to an external resistor of 48 Ω (which was determined by polarization tests for high power output).

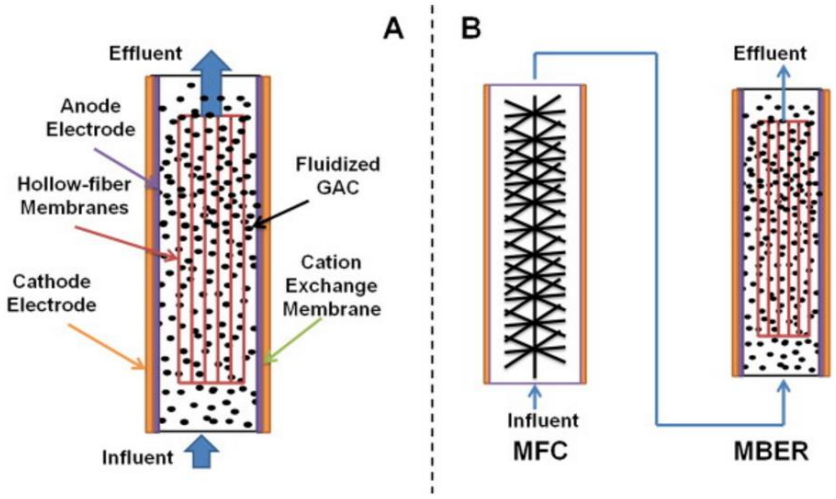

Figure 2.1 The schematic of the system. (A) Individual MBER reactor; (B) The coupled MFC-MBER system

2.2.1.2 MFC construction

A tubular MFC was constructed with a CEM tube (45 cm long and 5 cm diameter), which contained a one-meter long carbon brush folded as an anode electrode (Fig. 2.1B). The anode liquid volume was about 1000 mL. The cathode electrode was a piece of carbon cloth treated and coated with Pt catalyst similarly to that of the MBER. The electrodes were connected to an external circuit using titanium wires.

2.2.2 Operation conditions

2.2.2.1 MBER operation

The MBER anode was inoculated with anaerobic digester sludge from a wastewater treatment facility (South Shore, Oak Creek, WI, USA) and was operated at room temperature of ~20 ºC. The synthetic anode solution contained (per L of tap water): sodium acetate 0.5 g; NH_4Cl 0.15 g; NaCl 0.5 g; $MgSO_4$ 0.015 g; $CaCl_2$ 0.02 g; KH_2PO_4 0.53 g;

K_2HPO_4 1.07 g and 1mL trace element. The anolyte was recirculated at 800 mL min^{-1} unless elsewhere stated. This rate was determined according to a test that examined the height of the fluidized GAC column affected by recirculation rate, and found that 800 mL min^{-1} could fully fluidize the GAC in the MBER. The hollow fiber membranes were operated under an intermittent mode that extracted water for 4 min and then relaxed for 1 min. Tap water was used as a catholyte to rinse the cathode electrode from top to bottom and additional tap water was added to compensate for evaporation. The effects of the anolyte recirculation and hydraulic retention time (HRT) were examined. Organic loading rates varied when adjusting HRT: 0.40 kg COD m^{-3} d^{-1} at 24 h, 0.80 kg COD m^{-3} d^{-1} at 12 h, and 1.31 kg COD m^{-3} d^{-1} at 8 h. The anode of the MBER was acclimated with the seed sludge for about one week with varying the external resistance from 2000 to 10 Ω. After 100-day operation, the tubing for the anode feeding and the influent port of the CEM tube were clogged by GAC due to operating problems, and subsequently a new CEM tube was constructed (while other materials remained same) and used to the end of the study.

2.2.2.2 Integrated MFC+MBER operation

After four-month operation, the fluidized MBER was linked to an MFC to treat an industrial wastewater (Schreiber Foods, Inc., WI, USA). The wastewater collected from the effluent of DAF (dissolved air flotation) unit was first fed into the MFC anode and then the MFC effluent was supplied to the MBER (Fig. 2.1B). The coupled system was operated under an overall HRT 19.6 h (11.6 h in the MFC and 8 h in the MBER). The organic loading rate was about 1.00 kg COD m^{-3} d^{-1}. The anolyte recirculation rates were 200 and 600 ml min^{-1} for the MFC and the MBER, respectively.

2.2.3 Measurements and analysis

The voltage was recorded every 3 min by a digital multimeter (2700, Keithley Instruments, Cleveland, OH). The pH was measured using a benchtop pH meter (Oakton Instruments, Vernon Hills, IL, USA). The concentration of Chemical Oxygen Demand (COD), ammonium, nitrite and nitrate concentration were measured according to the manufacture's procedures (Hach DR/890, Hach Company, Loveland, CO, USA). The trans-membrane pressure (TMP) was manually recorded 3 times daily and the average value was reported in this study. The turbidity was measured using a turbidimeter (DRT 100B, HF Scientific, Inc, Fort Meyers, FL, USA). The polarization testing was performed by a potentionstat (Reference 600, Gamry Instruments, Warminster, PA, USA) at a scanning rate of 0.2 mV s^{-1}. The current and power density was normalized to the anode liquid volume.

The energy performance was evaluated by analyzing energy production and consumption. The estimation of energy consumption (by the pumping system for feeding, recirculation and membrane extraction) was based on power consumption, calculated by the following equation (Kim et al. 2011)

$$P = \frac{Q\gamma E}{1000}$$

where P is power requirement (kW), Q is flowrate ($m^3 s^{-1}$), γ is 9800 (N m^{-3}) and E (m H_2O) is head loss. The energy consumption for membrane filtration was calculated based on an average vacuum pressure of 37 kPa and permeate flow of 0.8 mL min^{-1}. Energy conversion efficiency was assumed as 61.2% from electrical energy to pumping energy (Kim et al. 2011). Energy recovery was calculated by normalizing average operation power to unit

volume of treated wastewater (kWh m^{-3}) or based on the amount of organic contaminants removal (kWh $kgCOD^{-1}$) (Xiao et al. 2014).

2.3 Results and Discussions

2.3.1 Feasibility study of the fluidized bed MBER

The feasibility of the fluidized bed MBER was demonstrated by examining its electricity generation, contaminant removal, and membrane pressure during a 100-day operation. The MBER produced a current density generally varying between 6 and 8 A m^{-3} (Fig. 2.2A). Adjusting HRT and the anolyte recirculation rates did not obviously affect current generation, possibly because substrate distribution was affected by the presence of GAC and the selected recirculation rate could not significant change the distribution situation; the exact reasons warrant further investigation.

The hypothesis that GAC may act as a part of the anode electrode was investigated by compared the MBER with and without GAC. The results of polarization tests showed that the maximum power density of the MBER containing GAC was 1.8 W m^{-3}, 50% higher than that (1.2 W m^{-3}) of the MBER without GAC (Fig. 2.3). Likewise, the MBER with GAC produced a maximum current density of 16.4 A m^{-3}, 53% higher than 10.7 A m^{-3} in the one without GAC. Because the power/current densities were calculated based on the liquid volume and the presence of GAC reduced the liquid volume from 1000 to 700 mL, it is also necessary to compare the absolute power/current output between those two systems. The maximum absolute power production was 1.26 mW with GAC, slightly higher than 1.20 mW in the absence of GAC. The maximum current generation in the MBER with GAC was 11.5 mA, whereas 10.7 mA was produced when no GAC was in the

MBER. The difference in the normalized energy recovery (NER) (Ge et al. 2013a) was more obvious: the MBER with the fluidized GAC recovered 0.0146 kWh m^{-3}, much higher than 0.0095 kWh m^{-3} when GAC was absent; however, the same HRT for those two systems (the MBER with GAC treated less wastewater than the other system) decreased the significance of the difference in NER. Those results do not provide a strong proof that the presence of GAC could greatly improve electricity production and the fluidized GAC could function as a part of the anode electrode, which is different from a recent study using fluidized bed as the anode electrode (Wang et al. 2014b). The possible reason for that difference may be that the liquid velocity of the MBER at 800 mL min^{-1}, about 6.7 mm s^{-1}, may not be the optimal velocity for power output. According to Wang's work, the maximum power density of their MFC reached the highest at 5-6 mm s^{-1} and would become less at either lower or higher velocity. Due to the difference between the present MBER system and their MFC system, it will not be reasonable to use their optimal value to evaluate the present MBER performance; however, their results reveal the relationship between the liquid velocity and electricity generation, which will help to identify the optimal liquid velocity for the MBER. If the future studies can demonstrate the role of the fluidized GAC as a part of the anode electrode, it will make the concept of fluidized bed MBER more attractive and competitive.

The contaminant removal focused on the removal of COD, which was affected by two separate factors, HRT and the anolyte recirculation rate (Fig. 2.2C). At an HRT of 24 h (water flux of 1.38 L m^{-2} h^{-1}) and a recirculation rate of 800 mL min^{-1}, the MBER removed 87.1% of COD. Reducing the HRT to 12 h (water flux of 2.77 L m^{-2} h^{-1}) at a recirculation

rate of 800 mL min^{-1} decreased the COD removal to 56.0%, likely due to the increased COD loading rate at a lower HRT. Stopping the recirculation (0 mL min^{-1}) at the HRT 12 h improved the COD removal to 79.5%; this interesting phenomenon was possibly related to the interaction between fluidized GAC and substrate distribution. However, because of the short testing period for this situation (10 days), it was also possible that the MBER was adapting to the more COD input in the first few days of decreasing the HRT and exhibited improved performance after adaptation. A longer term operation (nearly 70 days) was used to investigate the effect of recirculation at a shorter HRT of 8 h (water flux of 4.17 L m^{-2} h^{-1}). The MBER removed 82.7% of COD in the first nine days after the HRT change at an anolyte recirculation of 800 mL min^{-1}. A lower COD removal was obtained in the following forty days without recirculation. After the recirculation was restarted the MBER removed 91.6% of COD. One can see from the variation of COD removal efficiency that decreasing HRT could instantly decrease the COD removal efficiency because of a higher organic loading rate; however, once the MBER was adapted to the new organic loading rate, the COD removal efficiency could be substantially improved, indicating a strong response and capacity of the MBER for organic variation and removal. Those results also indicate that recirculation is important to COD removal, especially at a higher COD loading rate (shorter HRT) that requires better substrate distribution. The turbidity of the membrane permeate was 1.0±0.7 NTU, within the range of the permeate turbidity from an MBR (typically lower than 1 NTU). It was observed that the microbial growth inside the tubing used to collect the permeate affected the turbidity measurement.

The TMP of the hollow-fiber membranes remained below 30 kPa during the operation, and was influenced by HRT and/or anolyte recirculation rate (Fig. 2.2B). Adjusting HRT will change organic loading rate and water flux through the hollow-fiber membranes, both of which could significantly affect TMP. Increasing organic loading rate at a shorter HRT would bring more organic/inorganic compounds into the reactor and increased the chance of adsorption of those compounds by hollow-fiber membranes, thereby accelerating membrane fouling and increasing TMP. Increasing water flux with a lower HRT will demand a larger pressure difference across hollow-fiber membranes and thus increase TMP. In more details, Decreasing HRT from 24 to 8 h when the recirculation was kept at 800 mL min^{-1} resulted in TMP fluctuation between 5 and 10 kPa. On day 33 (arrow e in Fig. 2.2B), the recirculation was turned off and it was observed that TMP started to increase to above 25 kPa in the following 20 days; when the recirculation was restarted on day 76 (arrow f in Fig. 2.2B), the TMP quickly dropped to 10 kPa. Those results suggest that the recirculation of anolyte and thus fluidized GAC was a key factor to maintain a low TMP and control membrane fouling/scaling, which confirms the findings in the previous study. The fluidized GAC removed the deposits from the surface of hollow-fiber membranes via abrasion, thereby reducing membrane fouling and decreasing TMP. However, it should also be noted that the long-term and/or strong abrasion could damage the membrane. Further decreasing the HRT to 5 h (water flux of 6.67 L m^{-2} h^{-1}) on day 93 (arrow g in Fig. 2.2B) elevated the TMP to 20 kPa, because of a higher water/organic flux.

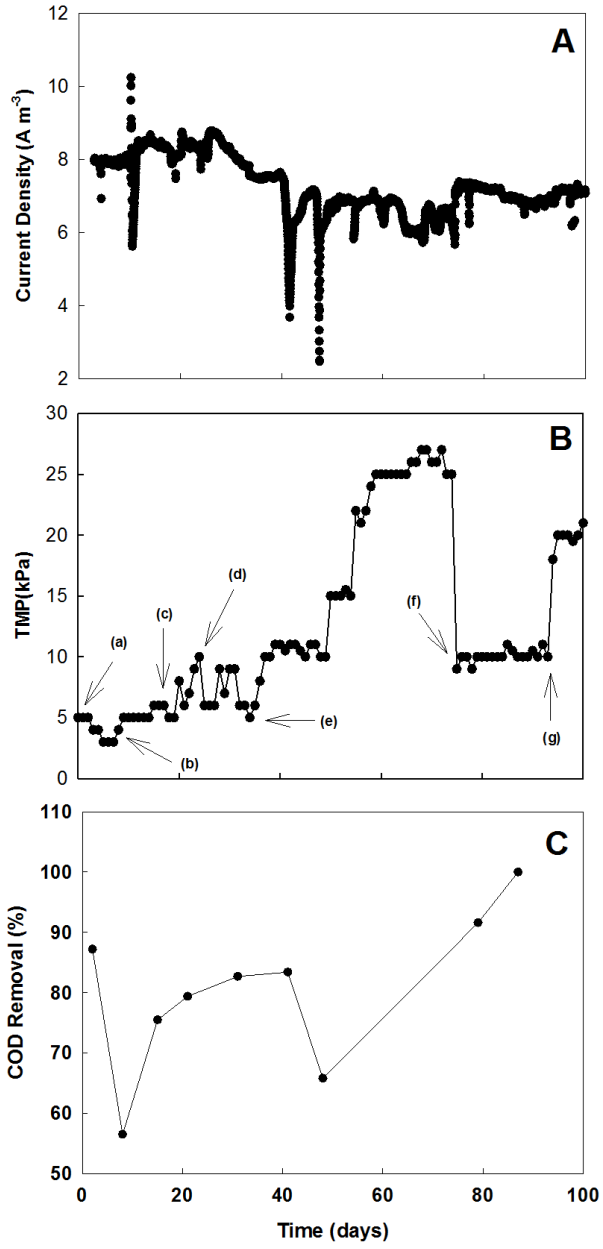

Figure 2.2 The performance of the MBER with synthetic wastewater: (A) Electricity generation; (B) TMP variation; (C) COD removal efficiency

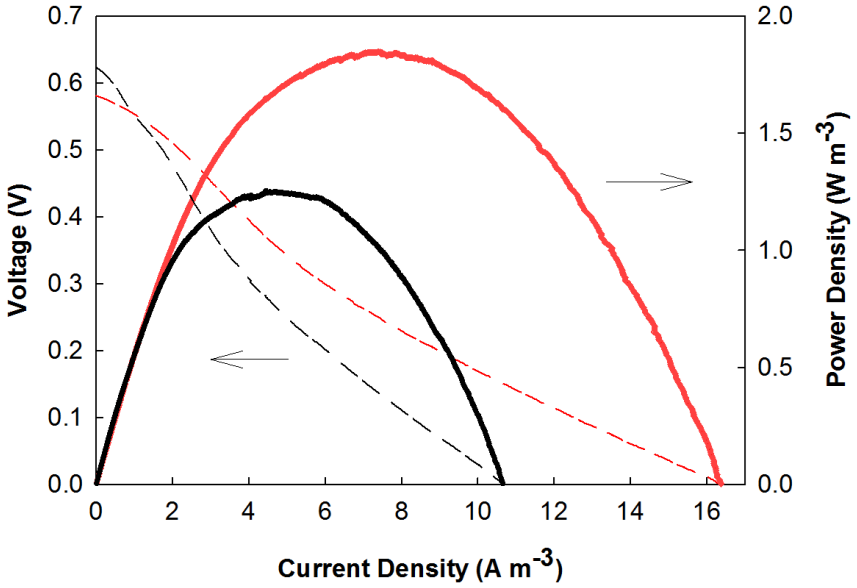

Figure 2.3 The polarization result for the MBERs: with fluidized GAC (red line), and without GAC (black line).

2.3.2 The MFC + MBER system

The MBER was hydraulically connected to an MFC for treating an actual industrial wastewater. This coupled system showed great performance in contaminant removal (Fig. 2.4). The MFC acted as a major removal process, in which the TCOD was reduced from 559±172 mg L^{-1} to 228±34 mg L^{-1} representing removal efficiency of 59.2 %. The MBER further decreased the TCOD to 28±11 mg L^{-1}, thereby achieving a total removal efficiency of 95.0% by the coupled system. The suspended solids, both TSS and VSS, were largely reduced in the MFC, which decreased the TSS and VSS concentrations from 115±142 and 108±148 mg L^{-1} to 23±8 and 13±8 mg L^{-1}, respectively, representing 80.0 and 87.9% of reduction. The final TSS and VSS in the MBER permeate were 6±8 mg L^{-1} and 3±3 mg L^{-1}, respectively. The concentrations of suspended solids in the permeate were higher than expected, possibly because of microbial growth in the tubing that collected water from hollow-fiber membranes. The turbidity of the membrane permeate was 1.6±0.8 NTU. The

coupled system had negligible ammonia and nitrate removal, related to the low concentrations of those compounds (NH_4^+-N, 2±1 mg L^{-1}, and NO_3^--N, 1±0 mg L^{-1}) in the wastewater sample. The nitrite concentration decreased from 26±31 mg L^{-1} to 4±3 mg L^{-1}, likely due to denitrification process occurred in the anodes of the MFC and the MBER. The significant removal of COD and suspend solids by the MFC could help to alleviate the treatment burden on the MBER and thus benefited membrane filtration. During the operation of the coupled system, the TMP of the MBER was around 37 kPa, resulting from the actual wastewater that had a more complex composition than the synthetic solution.

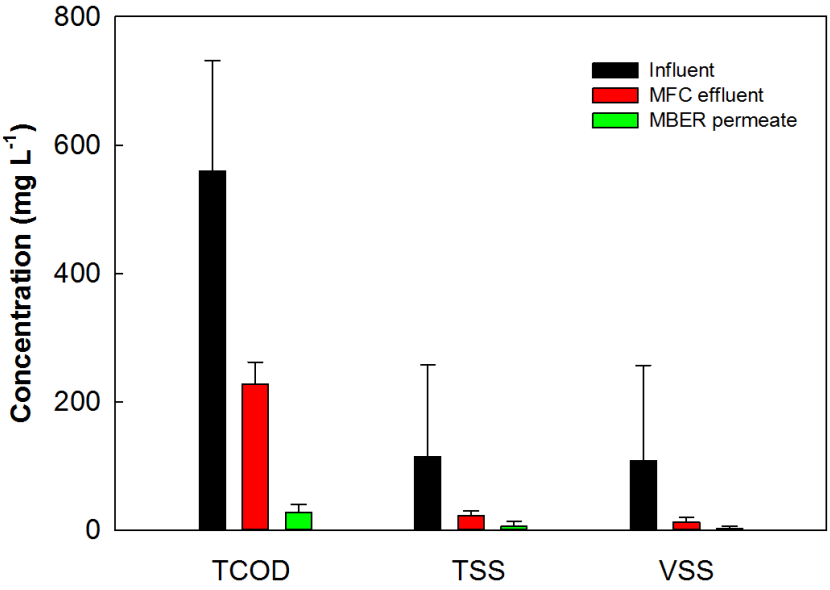

Figure 2.4 The contaminants removal from cheese wastewater by the coupled MFC - MBER system

The coupled system successfully generated electricity and theoretically achieved a slightly positive energy balance. The MFC was a major energy producer in the system, with a current density of 13 A m^{-3} (Fig. 2.5), and energy recovery of 0.036 kWh m^{-3} or 0.109 kWh $kgCOD^{-1}$. The MBER produced a much lower current density of 7 A m^{-3}, and its energy

recovery was lower as well, at 0.011 kWh m^{-3} or 0.060 kWh kgCOD $^{-1}$. The energy performance of the coupled system was summarized in Fig. 2.6, and the energy balance was analyzed by comparing energy production and consumption in both the MFC and the MBER. The total energy recovery per unit of the treated wastewater was 0.047 kWh m^{-3}. Energy was consumed by the pumping system including feeding, recirculation and permeation. Assuming energy conversion efficiency from electrical to pump was 61.2%, the total energy consumption was 0.046 kWh m^{-3}, of which the MFC consumed 0.003 kWh m^{-3} and the MBER used 0.043 kWh m^{-3}. The ratio of energy production/consumption is 1.02, indicating a theoretically neutral energy balance.

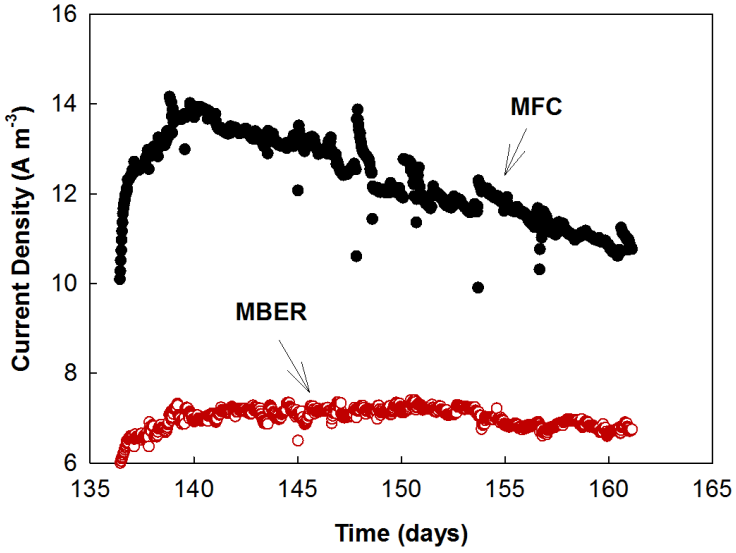

Figure 2.5 The current generation by the individual unit in the couple MFC-MBER system

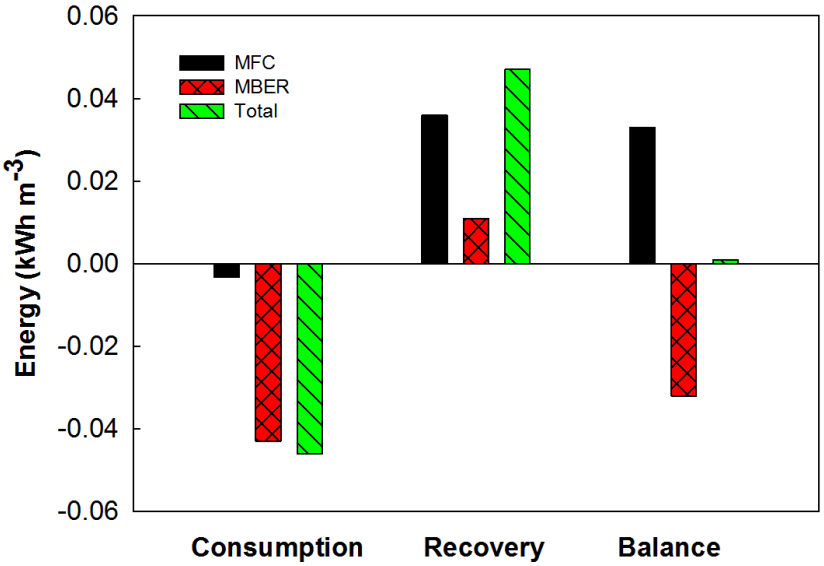

Figure 2.6 The energy analysis of the individual unit and overall coupled MFC-MBER system

The results of both contaminant removal and energy performance demonstrate different role of each unit in this coupled system: the MFC is the major treatment process with most energy recovery, and the MBER functions as post-treatment to improve the effluent quality. The performance of the MFC is critical to the successful operation of the MBER, in the aspects of contaminant removal (to reducing membrane fouling) and energy recovery (to offset energy consumption). More than 90% of energy consumption was due to the MBER operation, especially the anolyte recirculation. Therefore, to make the couple system more energy positive, it is necessary to reduce energy consumption by recirculation through further evaluating fouling condition and recirculation rates.

Despite the successful proof of concept with a bench-scale system in this study, one must also note the challenges and limitations with further development of the coupled system

for practical application. For example, the effect of fluidized GAC on membrane surface properties should be further investigated, because GAC may damage hollow-fiber membranes through long-term abrasion. Proper control of the anolyte recirculation (and thus fluidized GAC bed) is a key factor to minimize the abrasion, with simultaneous effects on fouling control and energy consumption; the interaction among those effects will be critical to the successful operation of the fluidized MBER. The present study had two reactors (MFC+MBER) linked only through the anolyte stream; a practical operation of the coupled system will also need to consider the catholyte, which could be the treated anolyte; in that way, hydraulic coordination between the two reactors will be very important to maintain healthy operation and achieve satisfactory performance. Nutrient removal has not been well addressed in the present study; with aerobic cathodes that receive the treated anolyte, ammonia may be removed via nitrification and this should be further studied for its effects on cathode oxygen reduction and electrode fouling. The credibility of the energy analysis with a bench-scale system must be further verified with stepwise development of the proposed system, because of significant difference between bench- and large-scale systems. However, the energy analysis presented here exhibits the promising advantage of the coupled system, and has important implications for further studies; for example, the results of different role of each reactor in the couple system can guide the development of large-scale treatment systems, and the amount of MFC modules in the coupled system should be more than that of MBER modules, because of MFCs' major function in contaminant removal and energy recovery

2.4 Conclusion

This study has demonstrated a new bioelectrochemical system through incorporating fluidized GAC into an MBER. Membrane fouling was effectively controlled with a low TMP. However, the function of the GAC as a part of the anode electrode was not proved. When coupling this MBER with an MFC, the treatment of actual wastewater was improved compared with a standalone MBER, and the overall energy balance was neutral. The coupled system presents an example of accomplishing low energy consumption and high-quality effluent for wastewater treatment. Those results encourage further research to address several key challenges such as economic feasibility and scaling up.

CHAPTER 3

Advancing Membrane Bioelectrochemical Reactor (MBER) with Hollow Fiber Membranes in the Cathode Compartment

(This section has been published as: Li, J., Ge, Z and He, Z.* (2014) Advancing Membrane Bioelectrochemical Reactor with Hollow Fiber Membranes in Cathode Compartment. **Journal of Chemical Technology and Biotechnology**. Vol 89, pp 1330-1336.)

Abstract

Synergistic cooperation between membrane technology and microbial fuel cells (MFCs) creates a membrane bioelectrochemical reactor (MBER) that can produce electricity directly from organics while maintaining a high-quality effluent. This study aims to advance the MBER concept with hollow-fiber membranes installed in a cathode compartment for alleviating membrane fouling. The MBER achieved 90% removal of the chemical oxygen demand (COD), and 69% removal of the total inorganic nitrogen; the turbidity of the membrane permeate was mostly below 2 NTU. The operation of this MBER theoretically consumed 0.09 kWh/m^3, significantly lower than the energy consumption in membrane bioreactors (MBRs). The energy production in the MBER was 0.011-0.039 kWh/m^3 from the synthetic solution, or 0.032-0.064 kWh/m^3 from the cheese wastewater. The Coulombic efficiency varied between 10 and 30%, affected by the substrate type and loading rates. The MBER with ultrafiltration membranes installed in the cathode greatly improved membrane performance with a constant low trans-membrane pressure (which drives water through membrane) during the testing period, when treating either a synthetic solution or actual wastewater from a cheese plant. The MBER technology has potential advantages in energy consumption/production compared with MBRs, and may offer better handling of operating conditions than AnMBRs.

3.1 Introduction

Proper treatment of wastewater from domestic and industrial sources is critical to maintain a healthy environment for sustainable development of society. Wastewater is treated for removal of organic and inorganic contaminants by using physical, chemical and biological methods. A biological method is a popular approach because of its cost effectiveness, and thus various bioreactors/bio-processes have been developed (Chan et al. 2009). To further improve the quality of the treated effluent and to maintain a high concentration of active biomass, membrane technology is integrated into biological processes to form membrane bioreactors (MBRs) (Judd 2008). MBRs eliminate the use of a secondary clarifier and can directly produce a high-quality effluent. However, the energy consumption in MBRs is still high, estimated at 0.8-1.1 kWh/m^3 (Krzeminski et al. 2012) ; in addition, the energy contents in the organic waste are not effectively recovered, unless an anaerobic MBR (AnMBR) is employed (Smith et al. 2012). There are challenges to apply AnMBRs, such as low temperature, membrane fouling, and dissolved methane in the treated effluent. In general, it is of strong interest to develop a technology that can produce a high-quality effluent while being more energy-efficient than the existing technologies (through both reduced energy consumption and improved energy recovery).

Microbial fuel cells (MFCs) are a promising method for energy-efficient wastewater treatment (Logan et al. 2006b), but have not been commercialized, yet, in spite of intensive studies in the past decade. Direct electricity generation in MFCs avoids the need for biogas collection, processing and treatment as in anaerobic digesters (Morris et al. 2009). The concept of MFCs has been greatly advanced by increased understanding of fundamental issues in materials, reactor structure and operation, microbiology, and electrochemistry.

MFCs do not have a high biological yield (Freguia et al. 2007, Zhang et al. 2013b). , and the attached-growth on electrodes also results in much less biomass in the treated effluent than the suspended-growth treatment such as an activated sludge process. However, the effluent from MFCs still contain a certain amount of suspended solids and the remaining (organic, inorganic and microbial) contaminants, which require further treatment before being discharged. One option for the post-treatment is to use membrane technology such as that in MBRs. Such an integration of membrane technology into MFCs may lead to a new approach that produces a high-quality effluent with less requirement of energy.

A few studies have attempted to accomplish this integration with the use of different membranes. For example, the biofilm grown on the cathode surface was used as a "membrane" to polish the anode effluent in a bioelectrochemical membrane reactor (BMER) (Wang et al. 2011b). The researchers observed great improvement of the effluent quality with such a design, and a significant portion of the organic contents was removed by the aerobic process in the cathode of a BMER. The research team reinforced their BMER by using nylon mesh attached to the biofilm as a filtration material to improve the anode effluent (Wang et al. 2012). A recent study replaced cation exchange membrane with ultrafiltration membrane that has dual functions as both a separator and filtration medium for polishing the effluent; this approach eliminated the cost of ion exchange membrane, but the electricity generation in the MFC was low and the performance of the ultrafiltration membrane requires a long-term investigation (Kim et al. 2013). We have previously integrated commercially available hollow-fiber membranes in the anode compartment of a tubular MFC to form a membrane bioelectrochemical reactor (MBER) (Ge et al. 2013b).

This MBER was capable of treating both the synthetic solution and domestic wastewater. We found that membrane fouling was a key problem for the long-term operation. Because of the anaerobic condition and the biofilm growth in the anode compartment, it was difficult to apply any effective methods to control/reduce fouling in that MBER.

In this study, we have modified the design of the previously-developed MBER and installed hollow-fiber membranes in the cathode compartment. This change has several potential benefits: (1) ultrafiltration membranes are in the catholyte that contains a much lower concentration of organic compounds than the anolyte, and thus microbial growth will be less significant; (2) the cathode reaction is abiotic, and we can apply fouling-control methods such as aeration and chemical cleaning; (3) aeration has dual functions, providing oxygen to the cathode reaction and controlling fouling; and (4) the aerated oxygen in the cathode compartment will not severely affect the anode reaction. Although flowing the anolyte into the cathode compartment may potentially cause a short-circuit issue, a slow flowrate between the two compartment would reduce the chance of this issue and we have not observed it in our previous MFCs with similar flow pattern (Zhang and He 2012b). To investigate its feasibility, we operated this MBER for about 160 days on either a synthetic solution or on actual wastewater (from a cheese factory). We then examined the performance of contaminant removal (organic and nitrogen) and used the trans-membrane pressure to monitor the membrane property. We have also conducted a preliminary analysis of the energy consumption and production in the MBER and compared it with MBRs/AnMBRs.

3.2 Materials and Methods

3.2.1 MBER configuration

The MBER was constructed in a rectangular configuration made of plexiglass; its schematic is shown in Figure 3.1. A cation exchange membrane (CEM- Ultrex CMI7000, Membrane International, Inc, Glen Rock, NJ) was used as a separator between the anode and the cathode compartments. Both the anode and the cathode electrodes were made of carbon cloth (PANEX 30-PW03, Zoltek, Corporation, St Louis, MO), except that the cathode electrode contained Pt (10% Pt on carbon black, Etek, Somerset, NJ, USA) as a catalyst for oxygen reduction. The Pt catalyst was coated onto the cathode electrode by mixing with a Nafion solution and deionized (DI) water to achieve a loading rate of 0.1 mg cm^{-2}, according to a previous study (Xiao et al. 2012). The anode and the cathode electrodes were connected by titanium wires to an external circuit across a resistor box. The anode and cathode liquid volumes were 140 mL and 220 mL, respectively. Twelve 7.5-cm long PVDF hollow-fiber ultrafiltration membranes (150000 Dalton, Litree Purifying

Technology Co, Ltd, China) with a total membrane surface area of 51 cm^2 were installed inside the cathode compartment.

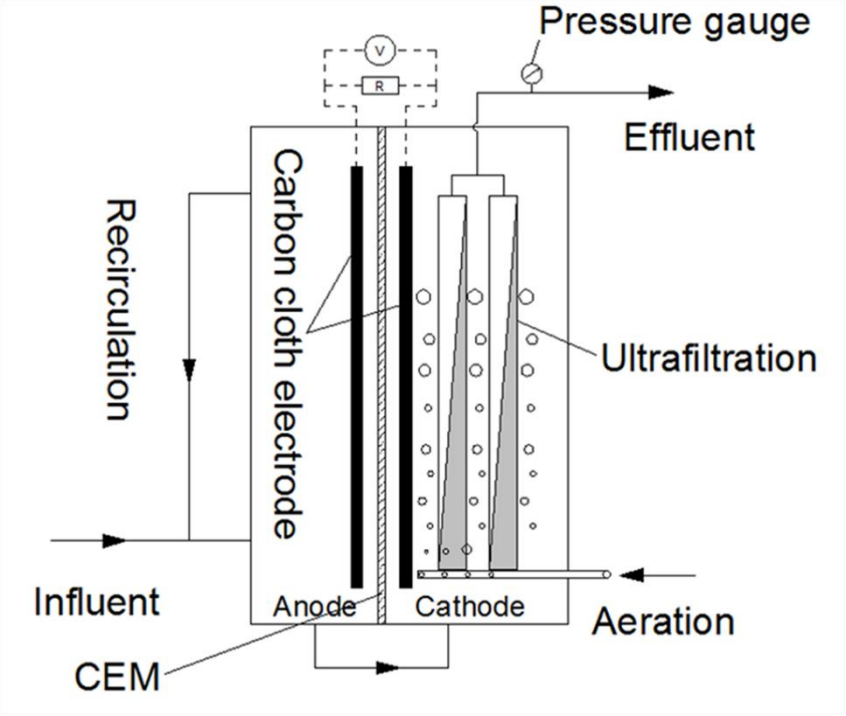

Figure 3.1 Schematic of a membrane bioelectrochemical reactor (MBER)

3.2.2 Operation conditions

The MBER was operated at a room temperature of ~ 22 ^oC. Its anode was inoculated with anaerobic digester sludge (at a volume ratio of 5%) from a local wastewater treatment facility (South Shore, Oak Creek, WI) and fed with either a synthetic solution or with cheese wastewater. The synthetic solution contained (per liter): 1g CH_3COONa; 0.15g NH_4Cl; 0.5g NaCl; 0.015g $MgSO_4$; 0.02g $CaCl_2$; 0.1g $NaHCO_3$; 0.53g KH_2PO_4; 1.07g K_2HPO_4 and 1 mL trace elements (Angenent and Sung 2001). The cheese wastewater was collected from the effluent of DAF (Dissolved Air Flotation) of a wastewater treatment process in a cheese plant (Schreiber Foods, Inc., WI, USA). The MBER was started in a

batch mode for about two weeks and then was switched to a continuous mode. During the batch operation, the anolyte was replaced when the voltage dropped below 10 mV, while tap water was used as the catholyte during the whole batch period. The synthetic solution or cheese wastewater was fed into the anode compartment, whose effluent was transferred into the cathode compartment; the final effluent was extracted from the hollow-fiber membranes. The flow rate of the anode feeding solution was adjusted by a peristaltic pump to achieve different hydraulic retention times (HRT). The cathode compartment was aerated with air at 93 mL min^{-1} unless elsewhere stated.

3.2.3 Measurements and analysis

The MBER voltage was recorded every three minutes by a digital multimeter (2700, Keithley Instrument, Inc, Cleveland, OH). The pH was measured using a benchtop pH meter (Oakton Instruments, Vernon Hills, IL, USA). The concentrations of chemical oxygen demand (COD), ammonium, nitrite, and nitrate were measured using a colorimeter according to the manufacture's procedure (Hach DR/890, Hach Company, Loveland, CO, USA). Turbidity was measured using a turbidimeter (DRT 100B, HF Scientific Inc, Fort Myers, FL, USA). Power density and current density were normalized to the anode liquid volume. Polarization tests were performed by a potentionstat (Reference 600, Gamry Instruments, Warminster, PA, USA) at a scanning rate of 0.2 mV s^{-1}. The trans-membrane Pressure (TMP) was recorded manually three times per day. Coulombic efficiency was calculated based on the ratio of the total charge produced in electricity and the theoretical charge produced from the removed COD, according to a previous study (Ge et al. 2013b):

$$CE=\frac{Q_{out}}{Q_{input}}=\frac{8It}{Fq\Delta COD}$$

where Q_{out} is the produced charge, Q_{input} is the total charge available in the removed organic compounds, I is the average current within time t, F is the Faraday constant, q is the feeding rate, and △COD is the removed COD within time t. The estimation of energy consumption includes the energy utilized by the pumps (feeding, recirculation, and suction) (Kim et al. 2011) , and aeration assuming a saturated dissolved oxygen of 8.7 mg L^{-1} at 22 °C.

3.3 Results and Discussion

3.3.1 MBER performance with synthetic solution

3.3.1.1 Contaminants removal

After the start-up phase, the MBER was continuously operated using a synthetic solution containing acetate as an organic source for about 90 days and the COD concentrations are shown in Figure 3.2A. In the first 23 days, the synthetic solution containing 1 g L^{-1} sodium acetate was supplied to the anode compartment (data not shown). After day 23, the acetate concentration was decreased to 0.5 g/L, and the anode feeding was operated at two HRTs (based on the anode liquid volume) in three stages: 10 h from day 21 to 66, 6 h from day 67 to 80, and 10 h from day 81 to 90. The overall HRTs (based on the total liquid volume of the anode and the cathode) were 26, 15, and 26 h, respectively. In general, the MBER removed more than 90% of COD from the synthetic solution, and the membrane filtrate had a turbidity of ~ 1.0 NTU (Table 3.1). Consistent aeration in the cathode compartment favored the nitrification process and thus enhanced the ammonium removal: the synthetic solution contained 39.3 mg NH_4^+-N /L, which decreased to 21.9 mg NH_4^+-N /L in the anode effluent and further reduced to 6.7 mg NH_4^+-N /L in the membrane filtrate. The decrease in the ammonium concentration in the anode compartment was likely due to microbial synthesis and the movement of ammonium ions across the CEM driving by electricity

generation (Cord-Ruwisch et al. 2011). Meanwhile, the nitrate concentration in the final effluent was 28.5 mg NO_3^--N/L (the synthetic solution did not contain nitrate), suggesting the occurrence of nitrification in the cathode compartment.

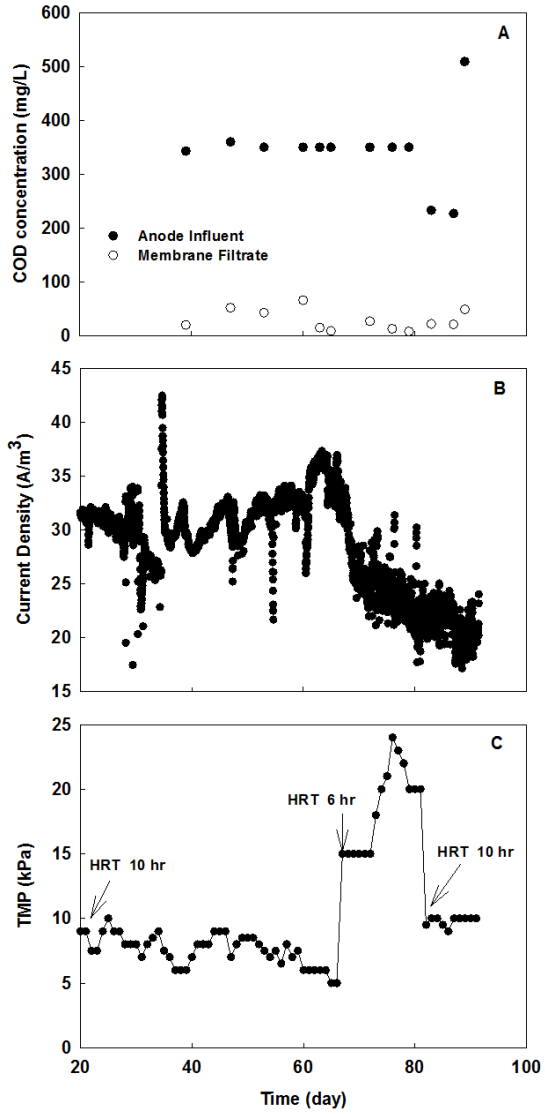

Figure 3.2 Performance of the MBER with synthetic solution: (A) COD concentration; (B) Electricity generation; (C) Membrane TMP

Table 3.1 The summary of MBER performance on synthetic solution

HRT (h)	Organic loading kgCOD m^{-3} d^{-1}	COD removal %	Turbidity (NTU)	CE%	Energy (kWh m^{-3})	Energy (kWh $kgCOD^{-1}$)
10	0.99	90.4±5.9	1.2±0.4	31.2	0.039±0.002	0.117±0.006
6	1.4	95.4±2.8	1.1±0.4	16.4	0.011±0.002	0.042±0.010
10	0.78	90.6±0.2	1.0±0.3	25.7	0.014±0.002	0.058±0.026

3.3.1.2 Electrical Production

During the first 23 days, the external resistance was decreased from 330 to 10 Ω, and a polarization test showed that the maximum power density was 27 W m^{-3} and the internal resistance of the MBER was 22 Ω. Then, the external resistance was set at 22 Ω for the maximum power/energy production. Figure 3.2B shows the current generation from day 20 to 90. The dramatic decrease of current at day 34 resulted from the clogging of the feeding tubing, and current generation restored after the tubing was cleaned. In this stage, the Coulombic efficiency reached 31.2±1.6% at an HRT 10 h, and energy production was 0.039±0.002 kWh/m^3 or 0.117±0.006 kWh/kg COD (Table 3.1). When the HRT was reduced to 6 h at day 67, the current started to decrease from 32.1 to 25.0 A m^{-3}. This decrease was likely due to the oversupply of organic compounds that entered the cathode compartment and affected the cathode reaction by competing for oxygen and stimulating the growth of heterotrophic bacteria that caused biofouling of the cathode electrode. Accordingly, the Coulombic efficiency dropped to 16.4±2.7% and the energy density decreased to 0.011±0.002 kWh m^{-3} or 0.042±0.010 kWh kg COD^{-1} (Table 3.1). The negative effect of oversupplying organics continued even after we switched the HRT back to 10 h: the current kept decreasing to 21.4 A m^{-3}. However, because of less feeding of both the anode solution and the organic compounds at the HRT 10 h, the Coulombic

efficiency increased to 25.7±11.2 % and the energy density slightly increased to 0.014±0.002 kWh m^{-3} or 0.058±0.026 kWh kg COD^{-1} (Table 3.1).

The analyses of the published literature reveal a knowledge gap about energy production in bioelectrochemical systems. MFCs produce an energy density of 0.001- 0.730 kWh m^{-3} or 0.001 – 0.960 kWh kg COD^{-1} when acetate acts as a carbon source. Due to significant differences among different MFC reactors, the ones containing membranes were chosen for a close comparison of energy production between the present and the previous studies. Our previous MBER produced 0.036-0.038 kWh m^{-3} from a synthetic solution at an HRT of 19-27 h (Ge et al. 2013b). A bioelectrochemical membrane reactor (BMER) produced 0.0092 kWh m^{-3} or 0.05 kWh kg COD^{-1} from an acetate solution at an HRT of 2.5 h (Wang et al. 2011b). Another BMER that was submerged in an aeration tank generated an average energy density of 0.006 kWh m^{-3} during 40-day operation (Wang et al. 2012). Therefore, the energy production in the present MBER was in the range of energy production in bioelectrochemical systems, and the HRT 10 h resulted in more energy production than those prior membrane-based systems.

3.3.1.3 Membrane performance

The trans-membrane pressure (TMP) is a key parameter to evaluate the property of ultrafiltration membranes, and the suggested operating TMP by membrane manufacturer for the hollow-fiber membranes used in this study is below 30 kPa. The TMP remained below 10 kPa at the HRT 10 h (day 20-67) (Figure 3.2C). Upon reducing HRT to 6 h, the TMP jumped to 15 kPa because of a higher flux rate, and then further increased to 24 kPa

at day 76. When the HRT was changed back to 10 h, the TMP also returned to around 10 kPa. During the operation with the synthetic solution, we did not apply any physical or chemical cleaning to the hollow-fiber membranes. The low TMP of the present MBER is a significant improvement compared with our previous MBER that suffered from a high operating TMP (Ge et al. 2013b). This improvement likely benefited from the cathode installment of hollow-fiber membranes with less microbial contamination due to a lower organic concentration.

3.3.2 MBER performance with cheese wastewater

3.3.2.1 Contaminants removal

The anode feeding solution was switched to wastewater from a cheese plant on day 93, and the COD concentrations are shown in Figure 3.3A. The MBER was first operated without any recirculation of the anolyte for about 37 days and at an HRT of 24 h. During this stage, the MBER removed about 90% of the total COD, in which the anode degraded 73.3% of the TCOD and the cathode further decreased 16.6% (Figure 3.4A). In the 96% reduction in total suspended solid (TSS) by the MBER, the anode removed about 78%. The ammonium concentration decreased from 7.4±3.1 mg NH_4^+-N L^{-1} in the feeding solution to 2.8±0.8 mg NH_4^+-N L^{-1} in the membrane filtrate, mostly due to nitrification in the cathode compartment; the MBER also reduced the nitrite concentration from 16.9±13.2 to 1.0±0.7 mg NO_2^--N L^{-1} (Figure 3.4B). The membrane filtrate contained a nitrate content of 1.5±1.2 mg NO_3^--N L^{-1}, slightly higher than 0.7±0.4 mg L^{-1} in the feeding solution, likely due to nitrification in the cathode compartment.

On day 130, the recirculation of the anolyte was conducted at a rate of 40 mL min^{-1}, and the MBER was operated at two different HRTs, 24 h briefly from day 130 to 137 and HRT 18 h from day 138 to 165. The performance of the MBER under those conditions is summarized in Table 3.2. The COD removal was 91% at an HRT 24 h, and decreasing the HRT to 18 h also decreased the COD removal to 85% (the removal in the anode was 78%). The organic loading rate at the HRT 18 h was lower than that at 10 h, because of a different organic concentration in the cheese wastewater that was sampled at different times. The MBER decreased the TSS concentration by 89% and reduced the nitrite concentration from 9.6 to 1.5 mg NO_2^--N L^{-1}.

Unlike municipal wastewater or synthetic solutions, cheese wastewater contains a higher concentration of nitrite than ammonium, which results from food processing. Nitrite is known to be toxic to aquatic life (Alonso and Camargo 2006, Palachek and Tomasso 1984) , and its concentration must be reduced to an appropriate level before discharging the wastewater. The present MBER system removed 84-94% of the influent nitrite. In the presence of oxygen (via aeration), bioelectrochemical denitrification with the cathode electrode as an electron donor (Zhang and He 2012a) would be less possible. Therefore, nitrite removal in the cathode compartment was mainly due to nitrification (to nitrate). The overall nitrite removal in the MBER occurred in two places, heterotrophic denitrification using organic compounds as electron donors (Knowles 1982) in the anode compartment (61.7% reduction), and nitrification in the cathode compartment (28.2% reduction) (Figure 3.4B). The decreased nitrate concentration in the membrane permeate compared with that in the cathode compartment was likely due to denitrification with the remaining organic

compounds in the permeate as electron donors by microbes growing inside the pump tubing that collected water from the hollow-fiber membranes (water samples for chemical analysis were collected at the other end of this tubing). The microbial growth inside the tubing also resulted in a higher turbidity (e.g., > 2.0 NTU in some cases).

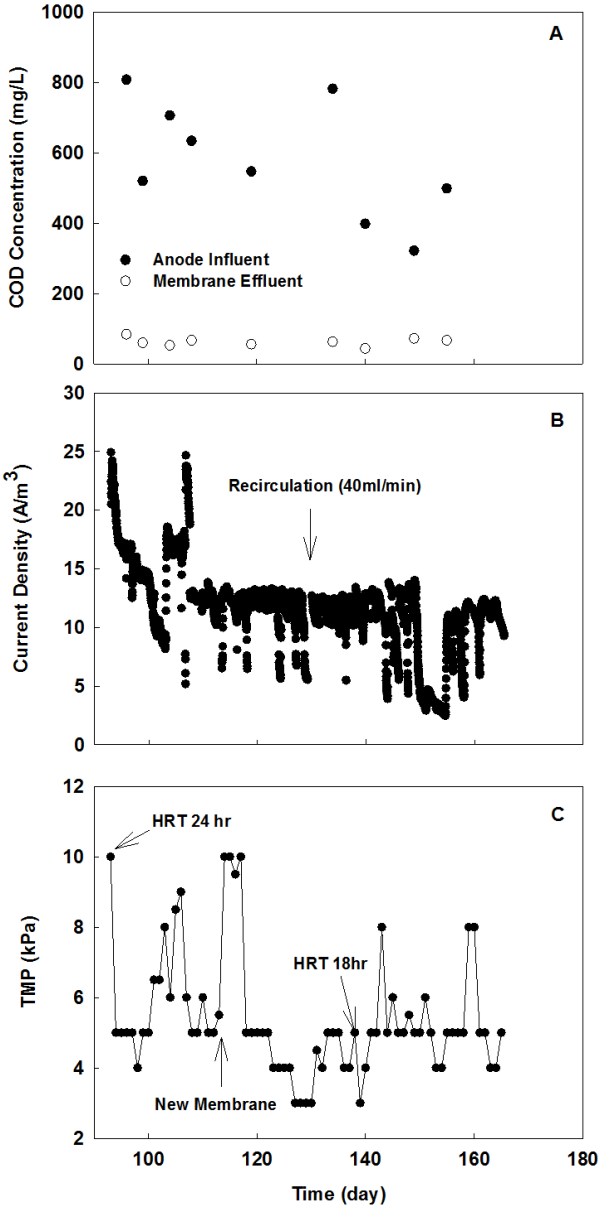

Figure 3.3 Performance of the MBER with cheese wastewater; (A) COD concentration; (B) Electricity generation; (C) Membrane TMP

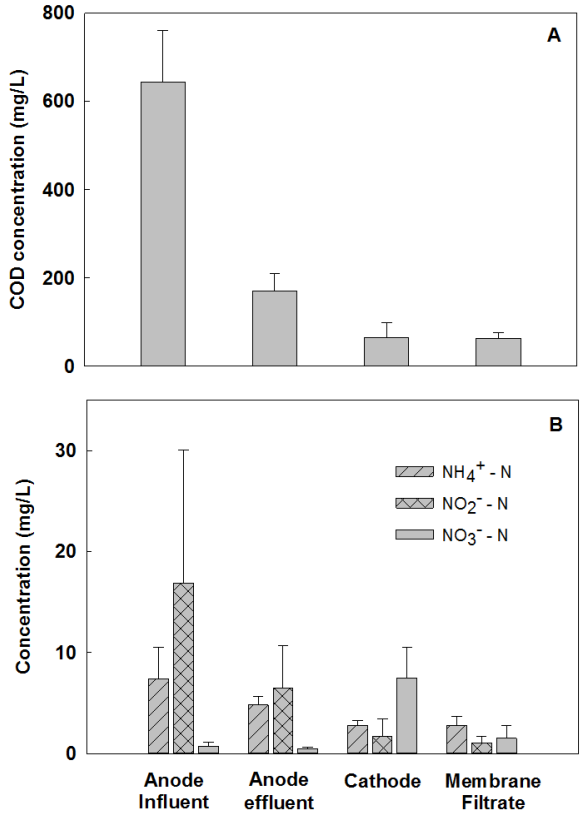

Figure 3.4 Contaminants removal from cheese wastewater in different compartments (A) COD concentration; (B) Nitrogen concentration

Table 3.2 The performance of MBER with cheese wastewater

HRT (h)	Organic loading kgCOD m^{-3} d^{-1}	COD removal %	Turbidity (NTU)	CE%	Energy (kWh m^{-3})	Energy (kWh $kgCOD^{-1}$)
24	0.64	90.0±1.5	2.4±1.4	22	0.04±0.032	0.088±0.071
24*	0.78	91.9±0.0	1.7±0.0	11.5	0.064±0.000	0.089±0.000
18*	0.54	84.4±0.0	1.8±1.3	13.1	0.032±0.024	0.085±0.064

* with anolyte recirculation at 40 mL min^{-1}

3.3.2.2 Electrical generation

The current generation from cheese wastewater is shown in Figure 3.3B. The energy production from the cheese wastewater was 0.040±0.032 kWh m^{-3} or 0.088±0.071 kWh kg

COD^{-1} without anolyte recirculation; the Coulombic efficiency was 22.0±4.6% (Table 3.2). With recirculation, the energy density was improved to 0.064 kWh m^{-3} or 0.089 kWh kg COD^{-1} at HRT 24 h, while the Coulombic efficiency decreased to 11.5%, likely due to a higher organic loading rate and more COD removal. When the HRT was changed to 18 h, the energy density decreased to 0.032±0.024 kWh m^{-3} or 0.085±0.064 kWh $kgCOD^{-1}$, because of lower organic input with a different wastewater sample from that of HRT 24 h. Those results did not demonstrate an obvious advantage of the anolyte recirculation, which is different from the previous findings (Pham et al. 2008, Zhang et al. 2010). A few factors could have contributed to this result. First, the recirculation rate that was applied here was not high enough: the prior studies observed an improved performance with a high recirculation rate that was 4-12 times (Zhang et al. 2010) or 100-270 times (Pham et al. 2008) of the anode liquid volume per minute, while this study had less than 0.3 times of the anode liquid volume per minute; the tradeoff between energy input for a higher recirculation rate and benefits from improved system performance is not clear at this moment. Second, the design of the anode chamber might not facilitate a good mixing via anolyte recirculation (even at a higher rate): the narrow anode chamber containing the carbon cloth electrode did not have any spacers for liquid distribution; we expect to improve this design by using either a tubular configuration or installing appropriate spacers in the future study.

3.3.2.3 Membrane performance

The TMP was maintained constantly under 10 kPa during the treatment of the cheese wastewater (Figure 3.3 C). On day 113, improper operation of chemical cleaning (the only

cleaning during the whole operation of the MBER occurred; membranes soaked in the pH-12 solution containing 400 ppm NaOH and 50 ppm NaOCl) caused membrane breakage, and subsequently new hollow-fiber membranes were installed and used until the end of the project. The TMP when using the cheese wastewater was lower than that with the synthetic solution for two reasons: a longer HRT reduced water flux, and increased aeration from 93 to 200 mL/min applied on day 109 helped to remove the deposit on the surface of membranes.

3.4 Perspectives

The present study demonstrates the improvement of the MBER system in both energy production and membrane fouling control, compared with our previous MBER (Ge et al. 2013b). The integration of ultrafiltration membranes within an MFC also exhibits advantages in nitrogen removal, energy recovery, and effluent quality, compared with an aerobic treatment such as an activated sludge process. However, to understand the benefits of the MBER technology, we need to evaluate it by comparing it with the existing membrane-based treatment technologies; a precise comparison, especially about capital investment and operating expense, is not possible at this time because of the early stage of MBER development.

The potential advantage of MBERs compared with MBRs is mainly in energy (Table 3.3). MBRs are based on aerobic degradation and rely on aeration for fouling control; thus, energy consumption is significant and estimated at 0.8-1.1 kWh m^{-3}; in addition, energy is not well recovered from the organic contents in MBRs. Unlike MBRs, MBERs use anaerobic processes to remove a large amount of COD; the MBERs' ultrafiltration

membranes are in a solution (catholyte) containing a low concentration of COD and thus require less aeration for fouling control. In this study, the MBER was estimated to consume 0.09 kWh m^{-3} (including pumping and aeration), and produced 0.032-0.065 kWh m^{-3} from the cheese wastewater, thereby resulting in a negative energy balance. Some of the prior studies have achieved positive energy balances (Ge et al. 2013b, Wang et al. 2013), which benefited from the elimination of recirculation and/or aeration. Aeration may not be completely eliminated in the present MBER because of the need for nitrification in the cathode compartment, but the aeration can certainly be optimized for reducing its intensity and thus the energy requirement. Although the energy balance in the MBER is still negative, the overall energy requirement in MBERs is much lower than that in MBRs.

When comparing MBERs with AnMBRs, the former needs partial oxygen supply and recovers less energy, and thus does not have an obvious energy advantage over AnMBRs (Ge et al. 2013c). The energy consumption in AnMBRs is 0.03-3.57 kWh/m^3, and the energy production via biogas is estimated to be 1.47-1.67 kWh/m^3 (Martin et al. 2011). Although the estimated energy consumption in the present MBER is generally lower than in many reported AnMBRs, we believe the present MBERs will have higher energy requirements than AnMBRs because of the partial aeration. On the other hand, the MBER achieved a good COD removal efficiency, which is at the high end of the range of the COD removal by AnMBRs (Table 3.3). Nitrogen removal has become a key challenge for AnMBRs and nitrogen removal in an AnMBR requires addition of electron donors such as hydrogen gas (Rezania et al. 2007). The present MBER was capable of removing nitrogen compounds through both nitrification and (heterotrophic and bioelectrochemical)

denitrification without external electron donors. Moreover, the dissolved methane in the treated effluent becomes a serious problem for using anaerobic technology to treat low-strength wastewater, because it causes a loss of energy contents and a release of greenhouse gas to the atmosphere (Souza et al. 2011). Although the dissolved methane was not examined in the present study, the previous work on MFCs treating domestic wastewater showed that the MFC effluent contained little dissolved methane (Zhang et al. 2013b). It is also believed that MFCs can handle temperature fluctuation better than anaerobic treatment.

To further develop MBER system, we must also understand several challenges. First, the rates of contaminant removal need to be further improved. Although the MBER achieves good removal efficiencies, its HRT is generally longer than that of MBRs; reducing HRT while maintaining a good efficiency of contaminant removal can reduce the reactor size and thus lower the capital investment. Second, energy production should be increased. An energy-neutral process is a goal of the MBER treatment, and to achieve this goal, more electric energy should be recovered from organic compounds through optimizing the reactor configuration and operation. Third, nitrogen removal, especially the removal of nitrate, should be further improved through either incorporating additional treatment or taking advantage of the denitrification process in the anode compartment. Fourth, membrane performance requires further examination with actual wastewater under non-laboratory conditions. Last but not least, like other bioelectrochemical systems, the MBER also faces great challenges in system scaling up and the high costs associated with the materials (membranes and electrodes).

Table 3.3 Comparison between MBER with cheese wastewater with other membrane bioreactors

	MBER	MBR	AnMBR
Aeration requirement	Partial	Yes	No
COD removal %	84-92%	91-97%	56-99%
Total nitrogen removal %	69%	36-80%	N/A
Effluent turbidity (NTU)	2	<1.0	<1.0
Energy consumption (kWh m^{-3})	0.09	0.8-1.1	0.03-3.57
Energy production (kWh m^{-3})	0.03-0.07	N/A	1.47-1.67

3.5 Conclusion

This study has advanced the MBER concept with improved performance through installing ultrafiltration membranes in its cathode compartment. The MBER achieved effective removal of both organic and nitrogen compounds from either a synthetic solution or cheese wastewater. The system maintained a low TMP for a long period of time. The MBER exhibited a treatment performance comparable to other membrane bioreactors, with potential advantages in energy consumption and recovery over MBRs, and better nitrogen removal (no need of external electron donors) and lower dissolved methane than AnMBRs. Further development of MBERs must address the challenges such as system scaling up and capital cost.

CHAPTER 4

Optimizing the Performance of a Membrane Bioelectrochemical Reactor Using Anion Exchange Membrane for Wastewater Treatment

(This section has been published as: Li, J.and He, Z.* (2015) Optimizing the Performance of a Membrane Bioelectrochemical Reactor using Anion Exchange Membrane for Wastewater Treatment. **Environmental Science: Water Research and Technology**. Vol 1, pp 355-362.)

Abstract

Membrane bioelectrochemical reactor (MBER) is a system integrating ultrafiltration membranes into microbial fuel cells (MFCs) for energy-efficient wastewater treatment. To improve nitrogen removal, an MBER based on anion exchange membrane (AEM), the MBER-A, was investigated for treating synthetic solution or actual wastewater during a 200-day operation. The MBER-A significantly improved the removal of total nitrogen to 56.9% with the synthetic solution, compared with 7.6% achieved in the MBER containing cation exchange membrane (MBER-C). This was mainly due to the removal of nitrate through both nitrate migration across AEM and heterotrophic denitrification in the anode. The final filtrate from MBER-A contains 11.9 mg L^{-1} nitrate-nitrogen, 6.0 mg L^{-1} nitrite-nitrogen, and less than 1 mg L^{-1} ammonia-nitrogen. The MBER-A achieved 91.3±6.4% of COD removal, resulting in a COD concentration of 21.6±17.8 mg L^{-1} in its membrane filtrate. The transmembrane pressure (TMP) remained below 10 kPa during the period of synthetic solution. The actual wastewater (primary effluent) led to the decrease in both COD and nitrogen removal, likely due to complex composition of organic compounds and low electricity generation. The MBER-A decreased the COD concentration by 84.5±14.4% and total nitrogen concentration by 48.4±1.9%. The ammonia-nitrogen concentration

remained at 0.3 mg L^{-1} in the final filtrate. The energy consumption by the MBER-A could be significantly decreased through reducing the strength of the anolyte recirculation rate. Those results encourage further investigation and development of the MBER technology for energy efficient removal of organic and nitrogen compounds from wastewater.

4.1 Introduction

There has been a great demand for sustainable wastewater treatment because of increased energy expense and high water quality for direct discharge or reuse. In general, sustainable wastewater treatment requires minimal input of energy and resource for treatment and maximal recovery of valuable resources such as energy and high-quality water, thereby decreasing carbon and water footprint of the treatment process. Those tasks can be accomplished through either optimizing the existing treatment systems or developing new technologies. Among the new technologies/concepts, membrane bioreactors (MBRs) and bioelectrochemical systems (BES) are of strong interests because of their advantages in producing high-quality water and energy efficient treatment. MBRs use ultra/micro-filtration membranes to achieve separation of water and biomass, eliminating the sedimentation processes; BES takes advantages of microbial interaction with a solid electron acceptor/donor to achieve the production of bioelectricity from organic contaminants. More details about MBR or BES can be found in various review publications (Judd 2008, Li et al. 2014c, Logan et al. 2006b, Meng et al. 2009). Research found that there is a strong synergy between MBR and BES, and proper integration of the two can complement each other with achieving low energy treatment and high-quality effluent.

Several efforts have been made to integrate membrane modules with BES to form a new treatment technology. The early studies used biofilm attached on stainless steel mesh as a

filter material to achieve low effluent turbidity and high removal of both organic compounds and ammonia removal (Wang et al. 2011b, Wang et al. 2012). Theoretical analysis indicated that such a system with biofilm-membrane could recover net energy from wastewater (Wang et al. 2013). The commercially available ultra-filtration hollow fiber membranes were installed in the anode chamber of a microbial fuel cell (MFC) system to form a membrane bioelectrochemical reactor (MBER) (Ge et al. 2013b). It was found that hollow fiber membranes can be rapidly fouled in the presence of a large amount of microorganisms, and to alleviate fouling issues, fluidized granular activated carbon (GAC) was applied to the anode of the MBER (Li et al. 2014a). However, having hollow fiber membranes in the anode created challenges for membrane cleaning; to solve this problem, the MBER was modified with hollow fiber membranes installed in its cathode chamber with aeration (Li et al. 2014b). The linkage between MBR and BES was also accomplished through external connection, for example, a two stage MFC-anaerobic fluidized bed MBR (MFC-AFMBR) was demonstrated to produce high quality effluent using AFMBR as a post treatment process of the MFC (Ren et al. 2014).

The integrated MBR-BES system can achieve good removal of organic contaminants with low energy consumption. However, because of its anaerobic characteristic, nitrogen removal has not been well addressed in an anaerobic MBR (Smith et al. 2012). BES, on the other hand, can accomplish the removal of nitrogen through multiple approaches, including ammonia recovery, bioelectrochemical denitrification and/or heterotrophic denitrification (Kelly and He 2014). A proper design of the integrated system may accomplish the removal of nitrogen with help of aeration. In this study, an MBER

containing anion exchange membrane (AEM) as a separator between the anode and the cathode was developed and investigated for enhancing nitrogen removal (Figure 4.1). The hypothesized path of nitrogen compounds in this system is that, ammonium remains in the effluent of the anode after organic compounds are greatly reduced and electrons are generated; the anode effluent is then supplied to the cathode as a catholyte, where aeration is provided to convert ammonium into nitrate via nitrification; in the presence of AEM and driven by electricity generation, nitrate ions move back to the anode across the AEM and are reduced to nitrogen gas with organic compounds as electron donors via heterotrophic denitrification.

To examine this hypothesis, a tubular MBER was built with AEM and compared with the one containing cation exchange membrane (CEM). The specific objectives of this study include: (1) to examine whether the removal of inorganic nitrogen can be enhanced with the use of AEM in the MBER fed with either synthetic or municipal wastewater; (2) to investigate the membrane fouling and the removal of organic compounds with either synthetic or actual municipal wastewater under different operation modes; and (3) to analyze energy consumption of the MBER system treating wastewater.

4.2 Materials and Methods

4.2.1 MBER setup

The proposed MBER system was constructed as a tubular reactor (38 cm long and 5 cm in diameter) made of anion exchange membrane (AEM-Ultrex AMI 7001, Membrane International. Inc, Glen Rock, New Jersey, USA). A carbon brush was installed in the anodic chamber as an anode electrode, resulting in an anode liquid volume of 750 mL.

Before use, carbon brush was soaked in acetone solution overnight and then heated for 30 min at 450 °C. The cathode electrode was one piece of carbon cloth (Zoltek Corporation, St. Louis, MO, USA) coated with Pt/C powder (10% Etek, Somerest, NJ, USA) with a loading rate 0.2 mg Pt cm^{-2}. The cathode electrode wrapped the membrane tube. The MBER was put in a 2-L container that acted as a cathode compartment, and the aeration with air was supplied from bottom of the container. Thirteen 35-cm PVDF hollow fiber membranes (15,000 Dalton, Litree Purifying Technology Co. China) were glued by epoxy as a bundle and installed in the cathode compartment. The anode and cathode electrodes were connected by using titanium wire to an external resistor. As a control, an identical MBER was constructed with cation exchange membrane (CEM-Ultrex CMI 7000, Membrane International Inc. Glen Rock, NJ, USA). Two MBER systems were recognized as the MBER-A (AEM) and the MBER-C (CEM), respectively, and operated in parallel.

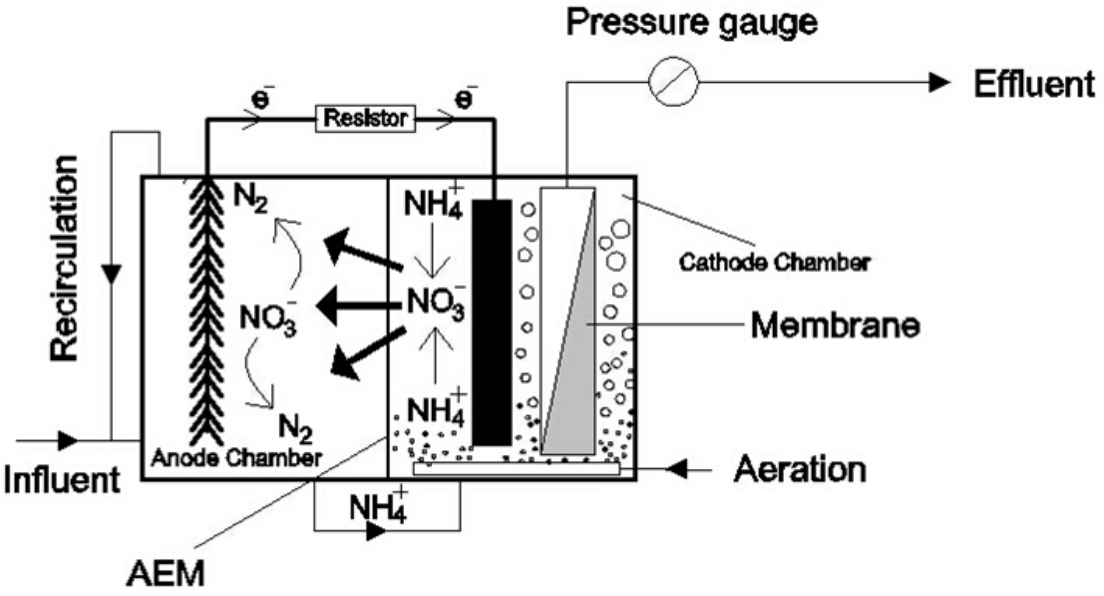

Figure 4.1 Schematic of a membrane bioelectrochemical reactor

4.2.2 Operation conditions

The MBER anodes were inoculated with anaerobic sludge from the Peppers Ferry Wastewater Treatment Plant (Radford, VA, USA) and were operated at room temperature. The synthetic solution contains (per L of tap water): sodium acetate 0.2 g; NH_4Cl 0.15 g; NaCl 0.5 g; $MgSO_4$ 0.015 g; $CaCl_2$ 0.02 g; KH_2PO_4 0.53 g; K_2HPO_4 1.07 g and 1mL trace elements. Municipal wastewater used in this study was the effluent from the primary clarifier at the Peppers Ferry. The anolyte was recirculated at 250 mL min^{-1} unless otherwise noted, and there was no recirculation applied to the catholyte. The MBER was operated in a hydraulic full loop mode, in which wastewater was first fed into the anode compartment and then the anode effluent flowed into the cathode compartment. The final permeate was extracted from the hollow fiber membranes. The flow rate was controlled by peristaltic pumps to achieve the desired hydraulic retention time (HRT).

4.2.3 Measurements and analysis

The voltage was recorded every 5 min by a digital multimeter (2700, Keithley Instruments, Cleveland, OH). The current and power density was normalized to the anode liquid volume. The pH was measured using a benchtop pH meter (Oakton Instruments, Vernon Hills, IL, USA). The conductivity was measured by a benchtop conductivity meter (Mettler-Toledo, Columbus, OH, USA). The concentration of chemical oxygen demand (COD), ammonium, nitrite and nitrate were measured according to the manufacturer's procedure (Hach DR/890, Hach Company, Loveland, CO, USA). Transmembrane pressure (TMP) was recorded manually and the average value was reported in this study. Turbidity was measured using a turbidimeter (DRT 100B, HF Scientific, Inc, Fort Meyers, FL, USA). Energy consumption by the MBER came from two parts, pumping system and aeration.

The estimation of energy consumption by the pumping system (for feeding, recirculating and membrane extraction) was calculated by the following equation (Kim et al. 2011): The energy by aeration was estimated according to a previous study (Zhang et al. 2013a). The data of energy consumption were expressed based on the volume of treated wastewater (kWh m^{-3}), the removed organics (kWh $kgCOD^{-1}$) (Xiao et al. 2014), and the removed nitrogen (kWh kg N^{-1}) .

4.3 Results and Discussion

4.3.1 MBER fed with Synthetic Solution

4.3.1.1 Electricity generation

The MBER systems were fed with synthetic solution until day 62. Electricity was generated in both systems (at external resistance of 10 ohm) at 20.6±3.0 A m^{-3} in the MBER-A and 27.2±4.6 A m^{-3} in the MBER-C (Figure 4.2 A). The MBER-C produced more current than the MBER-A (p<0.05), likely because of denitrification consuming organic compounds in the anode of the MBER-A. On average, the MBER-A produced 4.9 mA current less than the MBER-C, and the concentration of nitrate-nitrogen in the MBER-A membrane permeate was 6.8 mg L^{-1} lower than that from the MBER-C (Figure 4.3). Assuming that the decreased nitrate concentration was exclusively due to nitrate migration into the anode and denitrification in the anode (while neglecting new biomass synthesis etc.), the difference in nitrate concentration in the membrane permeate between the two MBERs could be equivalent to 5.2 mA, if 1 mole of nitrate ions was assumed to consume 5 mole of electrons from organics for denitrification. Thus, this theoretical analysis indicates that the lower current generation in the MBER-A was related to organic consumption by denitrification in the anode. Coulombic efficiency of the MBER-A was 47.7%, which is

12% lower than the MBER-C (p<0.05), indicating that part of electrons were sacrificed to other processes such as denitrification in the MBER-A.

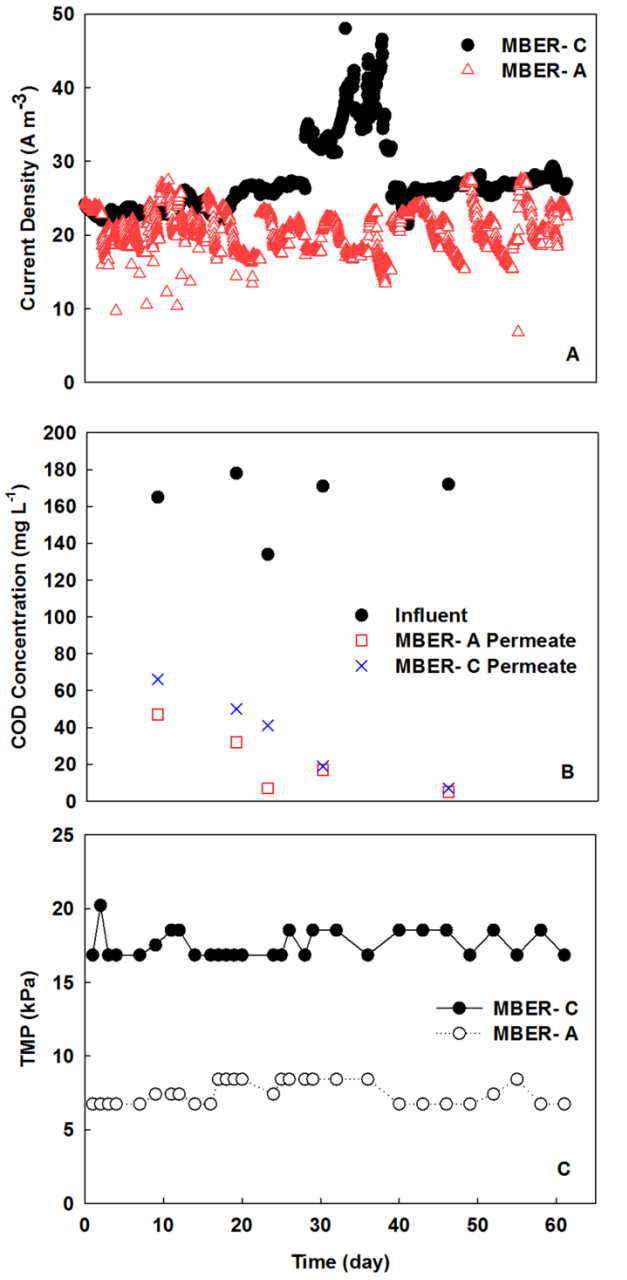

Figure 4.2 The performance of MBER-A and MBER-C fed with synthetic solution: (A) Current density; (B) COD concentration; (C) Transmembrane pressure (TMP)

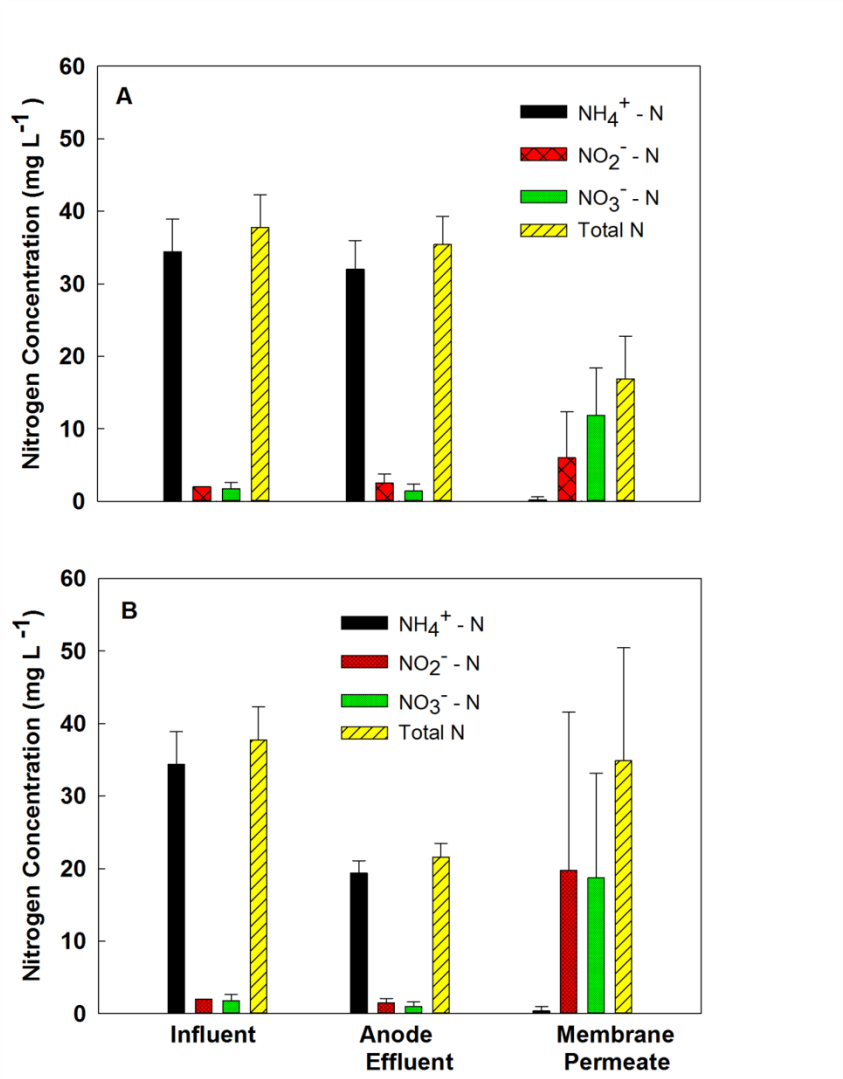

Figure 4.3 The removal of nitrogen in MBER-A (A) and MBER-C (B)

4.3.1.2 Removal of Organics and Nitrogen

The removal efficiencies of both organic and nutrients pollutants are the key parameters to evaluate system performance. At an anodic HRT of 9.3 h (total HRT 21.7 h for the whole system including the cathode) and an anodic recirculation rate of 250 mL min^{-1}, the anodes removed 84.5±12.9 and 74.5±20.1% of soluble COD in the MBER A and the MBER-C, respectively, and the final COD concentrations in the membrane permeate were 21.6±17.8

(MBER-A) and 36.6±23.7 mg L^{-1} (MBER-C) (Figure 4.2 B). Although both systems achieved more than 99% removal of ammonium nitrogen because of nitrification in the aerobic cathode, the removal efficiency of total inorganic nitrogen (ammonia + nitrite + nitrate) was significantly different. The MBER-A removed 56.9% of total inorganic nitrogen, while the MBER-C removed only 7.6% (Figure 4.3). The difference was mainly due to nitrate and nitrite remained in the final effluent: there was 18.7 mg L^{-1} of nitrate-nitrogen and 19.8 mg L^{-1} of nitrite-nitrogen in the MBER-C membrane permeate, much higher than 11.9 mg L^{-1} of nitrate-nitrogen and 6.0 mg L^{-1} of nitrite-nitrogen in the MBER-A membrane permeate (Figure 4.3). Those results have demonstrated that the use of AEM in an MBER can significantly improve the removal efficiency of total inorganic nitrogen.

4.3.1.3 Membrane Performance

Membrane fouling is a key factor that affects the operation of membrane-based treatment system, and transmembrane pressure (TMP) is usually used to monitor membrane fouling. The operating TMP of the hollow-fiber membranes used in this study is below 35 kPa, as suggested by the membrane manufacturer. Fed with synthetic solution, both MBERs maintained a low TMP, less than 10 kPa in the MBER-A and varying between 15 and 20 kPa in the MBER-A (Figure 4.2 C). There was no physical or chemical cleaning applied to those MBERs during this period. The low TMP could be resulted from two aspects: (1) the anode removed most organic compounds and low remaining organics resulted in low microbial contamination of the hollow-fiber membranes; and (2) aeration in the cathode might alleviate membrane fouling.

4.3.2 MBER fed with Primary Effluent (actual wastewater)

Because the MBER-A demonstrated superior performance in improved nitrogen removal, the following sections report the performance of the MBER-A only fed with actual wastewater (primary effluent) from day 62 to 200.

4.3.2.1 Electricity Generation

With feeding the actual wastewater, the MBER-A generated much lower current than that with the synthetic solution, likely because of low organic concentration and complex organic compounds in the wastewater. On day 75, the HRT was decreased to 6 h (arrow a, Figure 4.4 A) for increasing the organic loading, which resulted in higher current generation. However, the current generation still remained low at only 3.3±1.9 A m^{-3}, which might be related to microbial community: during the period of synthetic solution, acetate was the only organic compound and thus microbial community could be dominated by the species that degraded acetate and there could lack microorganisms for degrading complex substrates. Thus, on day 109, the MBER-A was reinoculated with anaerobic sludge and HRT was adjusted to 15 h, which led to obvious improvement in current generation (arrow b, Figure 4.4 A). After two-week reinoculation and adaptation period, anaerobic sludge was removed from the feeding solution (wastewater) on day 123 and the MBER-A was still operated at HRT 15 h. The current of the MBER-A decreased to 4.0 A m^{-3} after inoculum was excluded in the feeding solution, indicating that organic supply could still be a major reason for decreased current generation. The MBER-A produced current density of 3.5±2.1 A m^{-3} at HRT 15 h in the following 42 days, followed by a series of changes in HRT to 10 h on day 165 (arrow c, Figure 4 A) and 5 h on day 187 (arrow d, Figure 4.4 A). On day 195, 200 mg glucose per liter was added into the feeding solution to

increase organic supply (arrow e, Figure 4.4 A). Unfortunately, we did not observe substantial improvement in current generation with this addition, possibly because of short operating period under this condition.

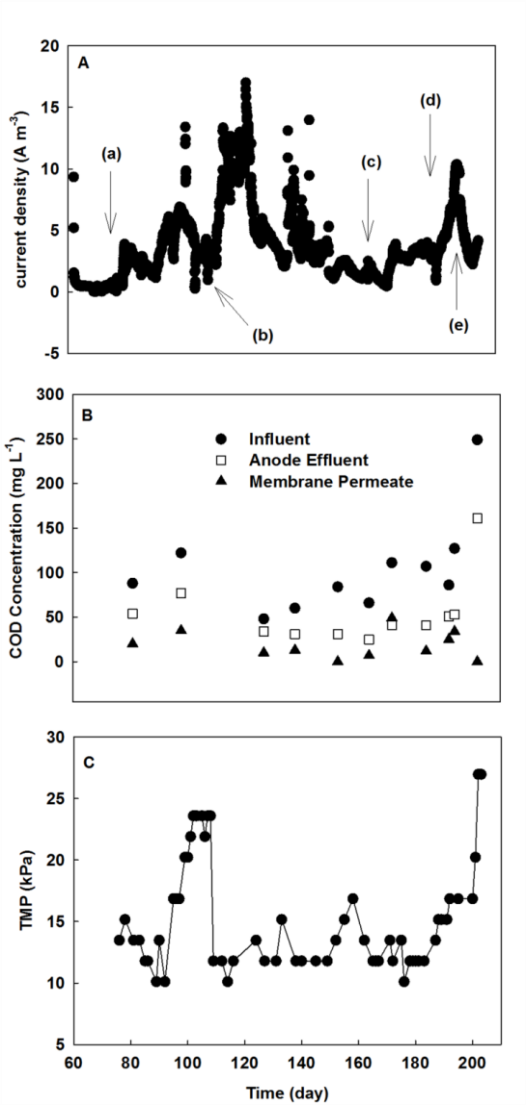

Figure 4.4 The performance of the MBER-A fed with actual wastewater (primary effluent): (A) Current generation at 10 ohms; (B)COD concentration; (C) Transmembrane pressure (TMP)

4.3.2.2 Removal of Organics and Nitrogen

In general, the MBER-A exhibited lower COD removal efficiency with wastewater, affected by HRT, compared with that of the synthetic solution (Figure 4.4 B). At HRT 6 h, the anode removed 21.6±0.0 % COD and the whole system achieved 66.5±15.3% COD removal. When the HRT increased to 15 h, the COD removal efficiency increased to 43.1±19.5 and 84.5±14.4% in its anode and the whole system, respectively. Decreasing HRT to 10 and 5 h did not obviously change the overall COD removal, but affected the COD removal in the anode (55.0±12.7 and 41.9±15.8 % under those two HRTs, respectively). The COD removal efficiency was also related to the COD concentration in the primary effluent, which varied from time to time during those tests. It should be noted that with additional 200 mg L^{-1} glucose in the wastewater, the COD removal rate of the MBER-A actually improved from 0.41 to 1.33 kg m^{-3} d^{-1}, indicating that the MBER-A had capacity for higher organic loading.

The removal of total inorganic nitrogen also became lower with actual wastewater, although the ammonia-nitrogen concentration remained low at 1.0 mg L^{-1} in the membrane filtrate. The decreased removal of total inorganic nitrogen was mainly due to the accumulation of nitrate. At HRT 6 h, the concentrations of nitrate- and nitrite-nitrogen in the membrane filtrate were 15.2 and 2.0 mg L^{-1}, respectively. Increasing HRT to 15 h improved the removal of nitrate and decreased its final concentration to 10.0 mg L^{-1}. On the other hand, decreasing HRT to 10 and 5 h reduced total nitrogen removal rate, resulting in the final total nitrate-nitrogen concentration of 11.5 and 22.0 mg L^{-1} (Figure 4.5). Low current generation was a major factor that decreased migration of nitrate ions from the

cathode into the anode, and thus less nitrate ions were removed via heterotrophic denitrification in the anode.

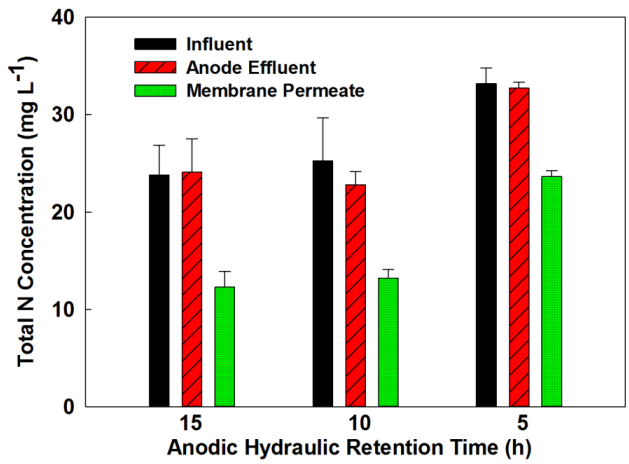

Figure 4.5 The effects of the anolyte HRT on the nitrogen concentration in the MBER-A

4.3.2.3 Membrane Performance

The TMP of the hollow-fiber membranes varied between 10 and 15 kPa TMP for most of the time with actual wastewater (Figure 4.4 C). The complex composition of actual wastewater was related to the increase in TMP, compared with the synthetic solution. A significant increase in the TMP from 10 to 24 kPa occurred on day 92, likely because of more serious membrane fouling that was caused by complex composition of wastewater and/or the growth of heterotrophic bacteria. Extending the HRT from 6 to 15 h decreased the TMP to 12 kPa, benefited from a reduced organic loading and a lower water flux. From day 198 to 203 when additional glucose was added as a supplemental substrate, the TMP increased from 16 to 28 kPa, confirming the previous finding that carbohydrates can accelerate membrane fouling because of increased amount of flocs formed by extracellular polymeric substances (EPSs) (Zuriaga-Agustí et al. 2013).

4.3.3 Energy Consumption

Energy consumption is a key parameter to evaluate the MBER system. When the MBER-A was fed with the synthetic solution, it was estimated that the system would consume 0.12 kWh to treat 1 m^3 wastewater or 0.86 kWh energy to remove 1 kg COD. Further analysis shows that the anolyte recirculation was the major consumer with 55% of total energy consumption used to drive the recirculation pump. The remaining energy consumption was mostly by aeration in the cathode; and the energy requirement by feeding and extracting water was very minor. The MBER-A produced 0.03 kWh m^{-3} or 0.20 kWh $kgCOD^{-1}$ energy from synthetic solution. The final energy balance (considering both energy consumption and production) showed that the MBER-A would consume 0.09 kWh m^{-3} or 0.66 kWh kg COD^{-1}. For each kg total nitrogen removal, the MBER-A would consume 4.40 kWh.

To further understand the effect of the anolyte recirculation on energy consumption, we have investigated the energy requirement by the MBER-A at three different recirculation rates, 50, 150, and 250 mL min^{-1}; the external resistance was fixed at 1 ohm, the HRT was 5 h for those tests, and actual wastewater was used as an anode substrate. The use of 1 ohm was because that with actual wastewater, the energy production was very low (0.05 kWh kg COD^{-1} at 150 ohm, which was close to the internal resistance of the MBER). The results clearly show that a lower recirculation rate would result in much less energy consumption. The total energy consumption at 50 mL min^{-1} was 0.02 kWh m^{-3} or 0.25 kWh kg COD^{-1}, less than 40% of the ones at 250 mL min^{-1} (0.05 kWh m^{-3} or 0.57 kWh kg COD^{-1}) (Figure 4.6). The energy demand for nitrogen removal was 3.0 kWh kg N^{-1} at 50 mL min^{-1}, much lower than 12.6 kWh kg N^{-1} at 250 mL min^{-1}. Varying the anolyte recirculation rate did not significantly affect the anode COD removal efficiency, which was 41.6±25.3% at 50 mL

min^{-1} or 39.9±7.5% at 250 mL min^{-1}; in addition, the total nitrogen concentration in the final membrane filtrate was 21.9 mg L^{-1} at 50 mL min^{-1} or 19.5 mg L^{-1} at 250 mL min^{-1}. Those results of contaminant removal and energy consumption at different anolyte recirculation rates suggest that the energy consumption by the MBER could be decreased by optimizing the operating condition without negative influence on the treatment performance.

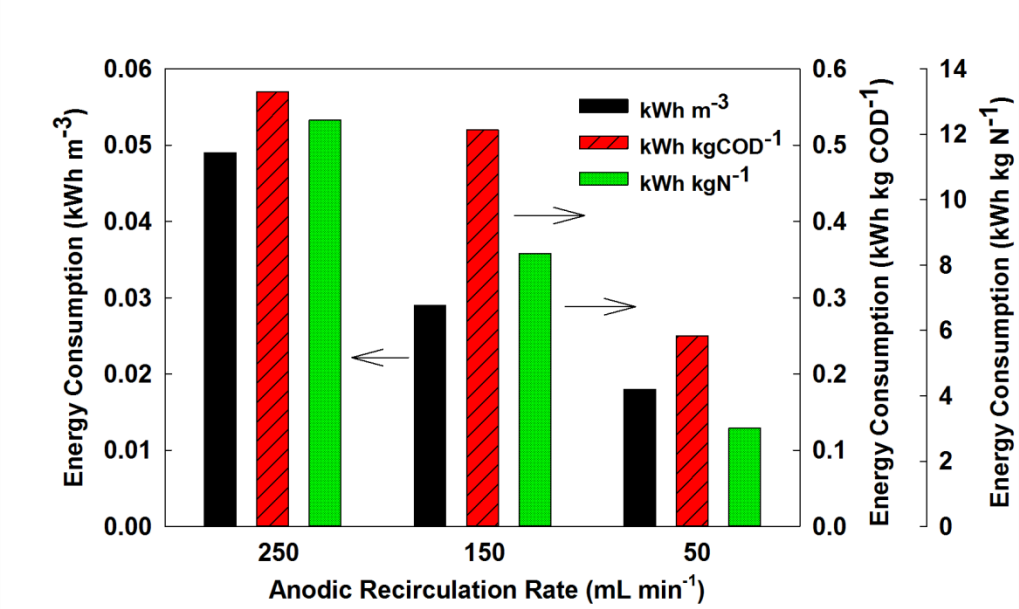

Figure 4.6 Energy consumption by the MBER-A per volume of wastewater treated, per COD removed, or per kg nitrogen removed at different anolyte recirculation rate

4.3.4 Perspectives of the MBER technology

The developed MBER possesses a certain advantages compared with the existing technologies. Its energy consumption is much lower than MBRs. Unlike MBRs, MBER is an integrated system to combine anaerobic process in the anode chamber and aerobic process in the cathode chamber. With anaerobic treatment, the organic input to the aerobic process (the cathode) is low, resulting in less requirement of aeration energy, low

production of aerobic sludge, and low membrane fouling. However, compared with AnMBRs, the MBERs do not have obvious energy advantage, because of much lower energy recovery (although AnMBRs also have significant challenges in recovering methane that is largely dissolved in the membrane filtrate (Liu et al. 2014)). The main advantage of the MBERs lies in nitrogen removal through an integrated aerobic and anaerobic processes involving electricity generation. In addition, the MBERs can be operated at lower temperature than AnMBRs, thereby saving a large amount of energy associated with heating.

There are some challenges that must be addressed in future development of the MBER technology. First, nitrogen removal efficiency needs to be further improved; because nitrate removal is the bottleneck of the total nitrogen removal, nitrate migration across the AEM or bioelectrochemical denitrification in the cathode should be further investigated. One possible approach for promoting nitrate migration is to apply a small external voltage to increase current generation (Ge et al. 2014). Second, the energy consumption needs to be minimized by controlling aeration intensity and electrolyte recirculation, with simultaneous evaluation of the effects of those control strategies on the MBER performance (e.g., removal of contaminants and membrane fouling). Third, a strategy for system scaling up should be developed to transform laboratory results into a practical technology.

4.4 Conclusions

This study has demonstrated the improved removal of total nitrogen by using anion exchange membrane in a membrane bioelectrochemical reactor. The present design

promoted nitrate migration/removal, and maintained a low membrane fouling due to the removal of organic compounds in the anode. The MBER system effectively removed organic and nitrogen compounds from both synthetic solution and actual wastewater (primary effluent). Energy consumption could be reduced by decreasing the intensity of the anolyte recirculation. Further investigation needs to further improve nitrate removal, decrease energy consumption, and develop a proper strategy for system scaling up.

CHAPTER 5

A Novel Approach to Recycle Bacterial Culture Waste for Fermentation Reuse via a Microbial Fuel Cell – Membrane Bioreactor System

(This section has been published as: Li, J., Zhu, Y., Zhuang, L., Otsuka, Y., Nakamura, M., Goodell, B., Sonoki, T. and He, Z.* (2015) A novel approach to recycle bacterial culture waste for fermentation reuse via a microbial fuel cell-membrane bioreactor system. **Bioprocess and Biosystem Engineering**. Vol 38, pp 1795-1802.)

Abstract

Biochemical production processes require pure water and nutrient resources for culture media preparation, but aqueous waste is generated after the target products are extracted. In this study, culture waste (including cells) produced from a lab-scale fermenter were fed into a Microbial Fuel Cell-Membrane Bioreactor (MFC-MBR) and electrical energy was generated via the interaction between the microbial consortia and the solid electrode in the MFC. High quality treated wastewater was reclaimed in this process which was reused as a solvent and a nutrient source in subsequent fermentations. Polarization testing showed that the MFC produced a maximum current density of 37.53 A m^{-3} with a maximum power density of 5.49 W m^{-3}. The MFC was able to generate 0.04 kWh of energy per cubic meter of culture waste treated. Separate lab-scale fermenters containing pure cultures of an engineered *Pseudomonas* spp. were used to generate 2-pyrone-4,6-dicarboxylic acid (PDC) as a high value platform chemical. When the MFC-MBR treated wastewater was used for the fermenter culture medium, a specific bacterial growth rate of 1.00±0.05 h^{-1} was obtained with a PDC production rate of 708.11±64.70 mg PDC L^{-1} h^{-1}. Comparable values for controls using pure water were 0.95±0.06 h^{-1} and 621.01±22.09 mg PDC L^{-1} h^{-1} ($P>0.05$), respectively. The results provide insight on a new technique for more sustainable bio-material production while at the same time generating energy, and suggest that recycled

treated wastewater can be used as a solvent and a nutrient source for the fermentation production of high value platform chemicals.

5.1 Introduction

Fermentation is a biological process that permits the biosynthesis of energy-rich compounds such as carbohydrates, acids, gases, alcohols and other biochemicals. Typical fermentation products include lactic acid, succinic acid, hydrogen, ethanol and butanol (Nozzi et al. 2014, Rosa et al. 2014, Wang et al. 2014a, Yan et al. 2014), with more complex platform chemicals for polymer production now being produced via engineered organisms. Biosynthesis of almost all of these biofuels and biochemicals requires strict culture conditions (temperature, pH, nutrients balance, etc.). However, after the target products have been extracted - typically through salt precipitation, organic solvation, and/or evaporation - the microorganisms and culture media must be disposed of, generating large amounts of waste. The demand for clean water and nutrients increases the costs of biosynthesized platform chemical production, and the generated waste causes environmental problems as well.

Considerable research has focused on improvement of target compound yields in fermentation processes (Arimi et al. 2015, Passanha et al. 2014, Sato et al. 2015, Sonoki et al. 2014, Xu and Xu 2014, Yadav et al. 2014), but to the best of our knowledge, no studies have focused on the reuse of water and chemicals for culture media preparation and resulting platform chemical production. Water scarcity problems have become a global issue and according to the United Nations, around 1.2 billion people are living with physical water scarcity while another 1.6 billion people are facing an economic water

shortage situation (Ang et al. 2015). It is also desirable to limit nutrient and metal element usage relative to pending shortages of natural resources such as cobalt, nickel and phosphorus (Nges et al. 2015). Development of a process for sustainable biochemical production with minimal input of chemicals and pure water would therefore be desirable and this drove our interest in exploring methods for reclaiming and reusing treated wastewater as a potential solution for sustainable product development.

Typical water recycling involves processes such as groundwater recharge or industrial re-use (Asano and Cotruvo 2004, Matos et al. 2014, Mohsen and Jaber 2003), but for broader recycling efforts, treatment processes are the key to efficient wastewater reuse. Anaerobic digestion is an ideal process for the treatment of high concentration waste streams; however, several technical obstacles still remain relative to the application of this method including temperature control and regulation of dissolved methane (Smith et al. 2012). Microbial fuel cell (MFC) treatment is considered an alternative to anaerobic treatment, which offers a potential solution for wastewater treatment in an energy-neutral manner. In MFCs, microorganisms convert chemical energy stored in biodegradable materials into electrical energy. A more detailed description of MFCs can be found in a recent review article (Li et al. 2014c) but few studies have focused on the reuse of MFC effluent to achieve zero liquid discharge (ZLD). Borole (Borole 2011) suggested that a bioelectrochemical system (such as MFC/MEC) could potentially improve energy efficiency and enable water recycling in bio-refineries; however, no data was presented and 'real-case' study on wastewater reclamation for fermentation based on MFC technology has not yet been reported.

Herein, we investigated an integrated system that couples a MFC with a membrane bioreactor (MBR). We explored whether spent fermentation media could be treated using a combined MFC-MBR system, and assessed whether the treated water could then be used as make-up water for additional fermentation runs. The treated wastewater (recycled effluent, RE) was tested for use both as a potential solvent and as a chemical source for fermentation (Figure 5.1) in the production of a high-value 2-pyrone-4,6-dicarboxylic acid (PDC) platform chemical monomer which has previously been reported to be produced by an engineered *Pseudomonas putida* bacterium. The two primary objectives of this work were to: (1) to examine the treatment of bacterial culture waste and generation of electrical energy via a coupled MFC-MBR system; and (2) to investigate bacterial growth coupled with the biosynthetic production of a high value PDC monomer via the use of recycled effluent (RE)-based culture medium.

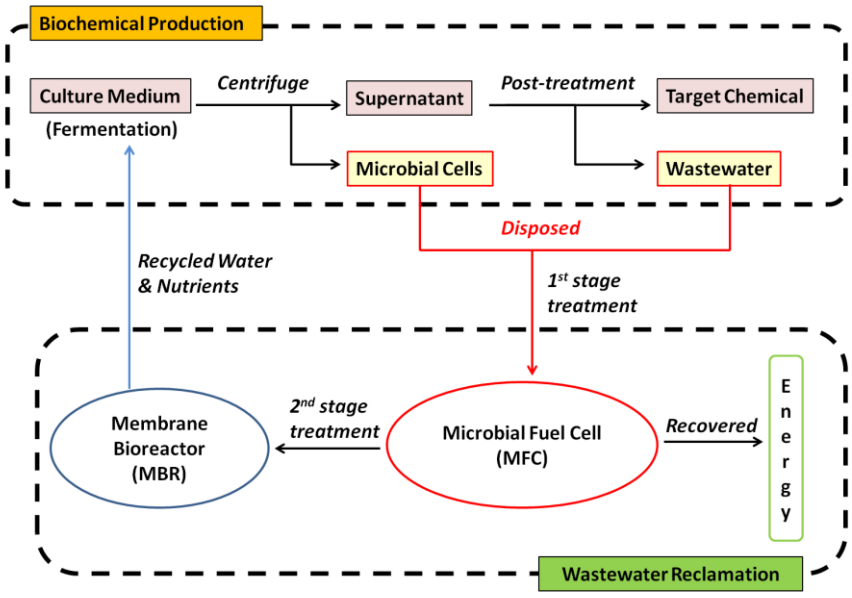

Figure 5.1 Overall schematic of the integrated MFC-MBER system with biochemical production

5.2 Materials and Methods

5.2.1 Bacterial strains and culture media

Pseudomonas putida PpY1100 and *P. putida* PpY1100/pDVZ21X were used in this study (Otsuka et al. 2006). The plasmid pDVZ21X encodes for vanillate demethylase, protocatechuate-4,5-dioxygenase and 4-carboxy-2-hydroxymuconate-6-semialdehyde dehydrogenase that are essential for the production of PDC from vanillic acid (VA) and other aromatic compounds, including waste crude lignin. Both strains were routinely maintained on LB agar plates containing nalidixic acid (Nal, 20 mg L^{-1}), and additional Kanamycin (Km, 50 mg L^{-1}) was added when *P. putida* PpY1100/pDVZ21X was cultured on the plates. The modified W medium consisted (per liter) of 6.025 g $(NH_4)_2SO_4$, 3.875 g KH_2PO_4, 16.607 g $Na_2HPO_4 \cdot 7H_2O$, 2.9 g yeast extract, 200.0 mg $MgSO_4 \cdot 7H_2O$, 19.0 mg $FeSO_4 \cdot 7H_2O$, 21.5 mg MgO, 4.0 mg $CaCO_3$, 2.9 mg $ZnSO_4 \cdot 7H_2O$, 2.2 mg $MnSO_4 \cdot 4H_2O$, 0.5 mg $CuSO_4 \cdot 5H_2O$, 0.6 mg $CoSO_4 \cdot 7H_2O$, 0.1 mg H_3BO_4, and 0.1 mL concentrated HCl, was used to culture both strains in liquid medium (Yano and Nishi 1980).

5.2.2 Culture condition

Culture waste from *P. putida* PpY1100 was generated as follows: The PpY1100 strain was used to inoculate 10 mL of the modified W medium containing 20 mg L^{-1} Nal and 10 g L^{-1} glucose, and shake-incubated at 30 ^oC for 16 h. Ten mL of the pre-culture was used to inoculate modified W medium containing (per liter) 20 mg L^{-1} Nal and 15 g L^{-1} glucose, and cultured for 7 h at 30^oC with constant aeration and 700 rpm agitation. The glucose concentration in the culture was measured using a Glucose C-II Test Wako (Wako Pure Chemical Industries, Ltd., Osaka, Japan). Culture waste was then collected and fed into the MFC-MBR.

5.2.3 Fermentation using recycled effluent

New culture medium was prepared using either pure water or RE (RE-A, RE-B & RE-C – Table 5.1) from the MFC-MBR treatments. For fermentation using RE water, pre-cultured *P. putida* PpY1100 was inoculated in each RE-based culture medium as discussed in section 5.2.2, to obtain growth profiles. The recycled effluent from batch A was tested to replace pure water for the culture media preparation, which was named as RE-A. The recycled effluent from batch B was tested to minimize both macro-and-micronutrients addition for culture media preparation, which was named as RE-B1 and RE-B2, respectively. The PDC-producing bacterium, *P. putida* PpY1100/pDVZ21X, was also used to assess PDC production. The organism was inoculated into 10 mL of modified W medium containing 20 mg L^{-1} Nal, 50 mg L^{-1} Kanamycin (Km) and 10 g L^{-1} glucose and shake-incubated at 30^{o} C for 16 h. The medium for preculture was prepared using deionized water throughout this work. The preculture (50 µL) was inoculated into 50 mL of modified W medium containing 20 mg L^{-1} Nal, 50 mg L^{-1} Km and 10 g L^{-1} glucose in a baffled shake-culture flask. The recycled effluents from batch B and C (see section 5.2.4) were used as solvent for the culture media preparation as a parallel to the control experiment that used deionized (DI) water. The recycled effluent from batch C test was divided into three sub-tests, which were named as RE-C, RE-C (1:2) and RE-C (1:2r), respectively. The "1:2" meant that the recycled effluent was diluted to 1:2 before chemical addition, and "r" indicated that a reduced amount of chemicals were added into culture media. After inoculation the flask was shake-cultured at 30^{o} C and 500 µl of VA (100 g L^{-1}, pH 7) was added to the culture at 6 h after the inoculation and then collected 500 µL of the culture at 0, 0.5 and 1 h after the addition of VA. Each collected culture was centrifuged (15,000xg,

5 min) and the supernatant was acidified to pH 2 with H_3PO_4 and filtrated with 0.45µm filter.

5.2.4 MFC & MBR setup

The MFC system was constructed as a tubular reactor (100 cm long and 4 cm in diameter) made of cation exchange membrane (CEM-Ultrex CMI 7000, Membrane International, Inc., Glen Rock, NJ, USA). A one-meter long carbon brush electrode was installed inside the anode chamber resulting in a net anodic liquid volume of 1400 mL. Before use, the carbon anode was soaked in acetone overnight and heated for 30 min at 450º C. The cathode electrode was one piece of carbon cloth (Zoltek Corporation, St. Louis, MO, USA) coated with activated carbon at a loading rate of 5 mg cm^{-2}. The completed MFC consisted of the CEM tube, wrapped within the finished cathode electrode. The anode and cathode electrodes were connected to a 10-ohm external resistor using titanium wire. The MFC was set up in a 4.5-L cylindrical container that acted as a cathode compartment (with the anode encapsulated within that), and the 4.5-L container was subsequently aerated with air to oxygenate the cathode.

The MBR system was developed as a submerged hollow-fiber ultrafiltration membrane system. Due to the high concentration of media solutes, we employed an obsolescent MFC (net anode volume at 250 mL) operated in an open circuit mode as a supplemental anaerobic treatment system before the MBR (Figure 5.2), to lessen the membrane fouling problem. Three 30-cm polyvinylidene fluoride (PVDF) hollow fiber ultrafiltration membranes (15,000 Dalton, Litree Purify Technology, Co. China) were glued together as

a membrane bundle and installed inside the MBR, which was aerated by an aquarium pump. The MBR liquid volume was maintained at approximately 1.1 L.

5.2.5 MFC & MBR operation

The MFC was initially inoculated with anaerobic sludge from the Peppers Ferry Wastewater Treatment Plant (Radford, VA. USA) and was connected to the MBR system in series (Figure 5.2). During the start-up period, a defined solution was fed into the MFC containing (per L of DI water) sodium acetate 0.2 g; NH_4Cl 0.15 g; NaCl 0.5 g; $MgSO_4$ 0.015 g; $CaCl_2$ 0.02 g; KH_2PO_4 0.53 g; K_2HPO_4 1.07 g and 1mL trace elements. A 10 mM phosphorus buffer solution was used as a catholyte solution in the MFC. After start-up, the defined media solution was gradually switched to the waste stream inoculum, by diluting the stream with DI water at ratios of 20, 10, 4, and 2 times stepwise at one week intervals. After the acclimation process with the diluted waste, the raw culture waste (no dilution) was fed to the MFC-MBR system using three different batch mode delivery methods designated as: (A) where the waste stream was fed at 0.4 mL min^{-1}, resulting in a total hydraulic retention time (HRT) for both MFC and MBR of 4.8 d; (B) the system was operated under the same conditions as the batch A except that 0.1 mole L^{-1} sodium bicarbonate was added as a buffering reagent; and (C) the waste feed rate was reduced to 0.12 mL min^{-1} with a total HRT (MFC+MBR) of 15.9 d and with 0.1 mole L^{-1} sodium bicarbonate as a buffering reagent. Correspondingly, the effluent collected from those batches was designated: RE-A, RE-B and RE-C, respectively. Recirculation was applied to the anolyte of the MFC at 80 mL min^{-1}.

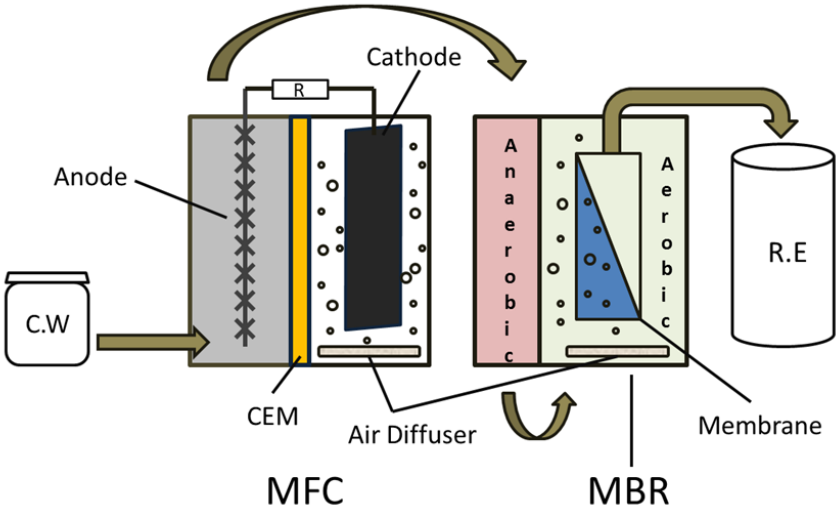

Figure 5.2 Schematic of a Microbial Fuel Cell-Membrane Bioreactor (MFC-MBR) system

Table 5.1 Characteristics of the recycled effluent from MFC-MBER system

Sample #	TCOD (mg L^{-1})	Conductivity (mS cm^{-1})	NH_4^+-N (mg L^{-1})	Total P (mg L^{-1})
Control	16000	18.84	1583	3070
RE-B	40	14.78	510	N/A
RE-C	188	15.08	350	2380

"Control" indicates the culture medium was prepared using pure water and the complete complement of chemicals and nutrients as outlined in the procedures.

5.2.6 Measurements and analysis

Fermentation: Bacterial growth in the fermenters (Section 5.2.3) was monitored at 600 nm with a Nanodrop 2000 (Thermo Fisher Scientific, Wilmington, DE). PDC production was quantified using high performance liquid chromatography (HPLC, Shimadzu LC-10A, Kyoto, Japan) equipped with a Inertsil-ODS-3 column (reverse phase, 4.6 mm in diameter, 250 mm in length, 0.5 µm particle size) run at 40^{o} C using a mobile phase gradient (Solvent A: 10 mM H_3PO_4. Solvent B: acetonitorile introduced 5 min after injection and ramped

from 10 to 50% over 10m). The mobile phase flow rate was 1.0 mL min^{-1} and the detection wavelength was 280 nm.

MFC/MBR analysis: The voltage of the MFC (Section 5.2.5) was recorded every 5 min by a digital multimeter (2700, Keithley Instruments, Cleveland, OH) and the current and power density was normalized to the anode liquid volume. The pH was measured using a benchtop pH meter (Oakton Instruments, Vernon Hills, IL, US). Conductivity was measured using a benchtop conductivity meter (Mettler-Toledo, Columbus, OH, USA). The concentration of chemical oxygen demand (COD), ammonium, nitrite, nitrate and phosphorus were measured according to the manufacturer's procedure (DR/890, Hach Company, Loveland, CO, USA). Transmembrane pressure (TMP) was recorded manually and the average value was reported. Turbidity was measured using a turbidimeter (DRT 100B, HF Scientific, Inc, Fort Meyers, FL, USA).

5.3 Results and Discussions

5.3.1 MFC Electrical Generation

The MFC internal resistance was about 10 ohms and its maximum power density reached as high as 5.49 W m^{-3} when fed with an acetate solution (Figure 5.3). Given these values, the MFC was operated under an external resistance of 10 ohms to ensure maximum power output when the culture waste was treated. Unexpectedly, a high COD concentration of 9000 mg L^{-1} in the raw culture waste did not result in high power output from the MFC. In batch A, a low power density of only 0.16±0.04 W m^{-3} was obtained but this increased to 0.48±0.15 W m^{-3} in the batch B tests; a significant improvement ($P<0.05$). This enhancement was likely due to the buffering effect caused by the addition of 0.1 M sodium

bicarbonate. These results demonstrated that low pH (4.4) culture waste inhibited anodic activity and thus electricity generation, and as a consequence, pH buffering in larger scale systems would be necessary. The exact reason for low electricity generation was not clear at this moment, and it could be related to the complex composition of culture wastes, recalcitrant compounds, and low pH. Those warrant further investigation and improvement of electricity generation in MFCs.

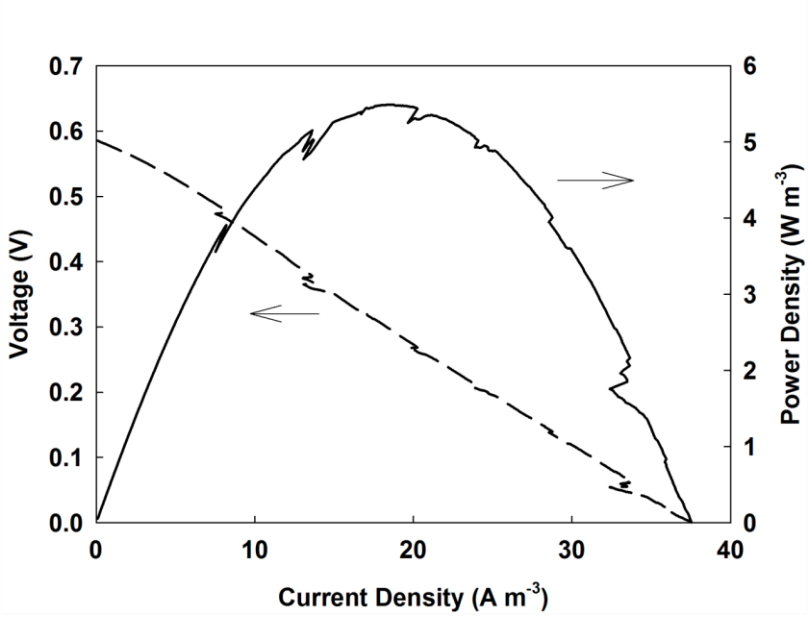

Figure 5.3 The polarization results for the MFC. The solid line represents power density and the dashed line is for voltage

5.3.2 Reuse of the MBR effluent for bacterial growth

The purpose for use of the MFC-MBR system in this work was not only to decrease the concentration of contaminants in the culture waste and recover electrical energy via the oxidation of organic compounds, but also to polish the wastewater for reuse by fermentation. *P. putida* PpY1100 is a KT2440-derivative strain that has previously been used for production of a variety of platform chemicals (Sun et al. 2007, Vardon et al. 2015). A growth profile was obtained (Figure 5.4) for this strain when 500 mL of the RE-A treated

wastewater collected from the MBR after 24 h and was used as a replacement for water in the culture medium. Specific bacterial growth rates (OD600) were 0.79 h^{-1} from the control (pure water based), vs. 0.64 h^{-1} from the RE-A based medium. These results suggest that undiluted RE can potentially be used for bacterial culture preparation with limited inhibitory effects.

In addition to using RE to replace water in the media, we also investigated whether ion concentration in the system would be modified by the MFC-MBR treatment. Chemical analysis showed that RE-B contained some residual macro-nutrient elements (Table 5.1). Therefore, two modifications of the RE-B based culture media were developed for test; RE-B1 and RE-B2. In RE-B1, a small amount of nitrogen (as ammonium sulfate) was added, and metals were also added to bring their concentrations to the same level as in the original media (Table 5.1 and Table 5.2) prepared with water (termed as the Control media). No phosphorus was added to RE-B1. In RE-B2, no metals were added, but the same amounts of other nutrients were used as in the control (Table 5.1 and Table 5.2). The PpY1100 strain in both RE-B1 and RE-B2 had a similar growth profile to the control (Figure 5.4). The specific growth rate (OD600) of RE-B1 was approximately 0.69 h^{-1}, lower than that of the control (0.79 h^{-1}). However, the specific growth rate in the RE-B2 culture was 0.57 h^{-1}, or 28% lower than that for growth in the control media. This suggests that the low growth rate may be due to insufficient residual metals in the recycled effluent. Metals, such as Mg, Fe, Zn etc., have important roles in maintaining a wide variety of normal cellular activities, although the required amount of each metal element may be very small. These metals are used for biomass synthesis during both culturing by the bacterial consortia in the MFC-MBR treatment, and the residual metals in the RE-B would be

therefore be insufficient to maintain normal bacterial growth in the fermenter. With metal supplementation however, these results suggest that the RE from the MFC-MBR can be reused as a pure water replacement for culture medium preparation to ensure normal bacterial growth with limited inhibition.

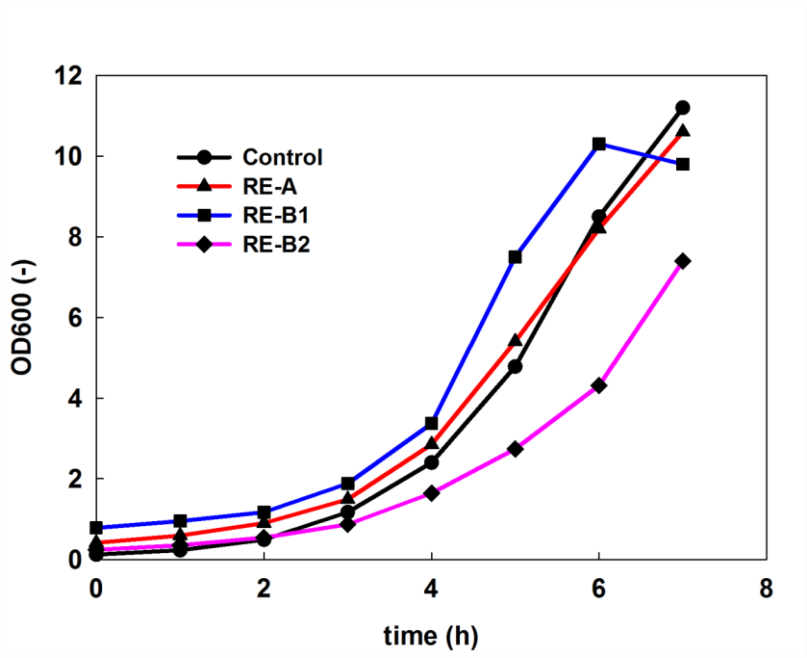

Figure 5.4 The growth profiles of P. putida PpY1100 in the RE-based culture media.

Table 5.2 Specific growth rates of P. putida PpY1100/pVDZ21X and PDC production rates with RE-based cultures

	Specific Growth Rate (h^{-1})	PDC Production Rate (mg PDC L^{-1} h^{-1})
Control	0.95±0.06	621.01±22.09
RE-B	0.82±0.03	N/A
RE-C	0.75±0.11	293.19±37.82
RE-C (1:2)	1.00±0.05	708.11±64.70
RE-C (1:2r)	0.97±0.05	508.79±78.88

RE-C (1:2) indicates the recycled effluent (RE) from batch C was diluted 1:2 with pure water before adding chemicals; RE-C (1:2r) indicates the recycled effluent (RE) from batch C was diluted 1:2 with pure water before adding a reduced amount of chemicals.

5.3.3 Effects of the extended HRT on the MFC-MBR operation

The batch C treated effluent, with an extended total HRT of 15.2 d was used to examine both power generation and energy recovery, with energy recovery expressed as kWh m^{-3} (Ge et al. 2013a). Extending HRT did not improve power output, which was only 0.20±0.07 W m^{-3} in batch C. However, increasing HRT enhanced energy recovery to 0.04±0.01 kWh m^{-3}, which was significantly greater than the 0.01±0.00 kWh m^{-3} observed for batch A ($P<0.05$), and close to the energy recovery obtained in from batch B (0.03±0.01 kWh m^{-3}, $P>0.05$). This result suggests that there may not be an obvious energy recovery advantage when HRT is increased, possibly due to the accumulation of aromatic compounds that may have inhibitory effects on normal cellular activity (discussed further below).

Increasing HRT also did not obviously improve organic removal in the MBR recycled effluent. In RE-C, a residual COD (188 mg L^{-1}) was greater than the 40 mg L^{-1} for RE-B (Table 5.1); however, the ammonium nitrogen concentration (350 mg L^{-1}) in the RE-C, was lower in RE-B (510 mg L^{-1}). The reduced ammonium accumulation in RE-C may potentially have been caused by three possible mechanisms: (1) In the MFC, more positively charged ammonium ions could potentially have migrated to the cathode compartment given the electrical potential field generated during the elongated retention time (Kelly and He 2014); (2) more nitrification could potentially occur in the MBR with increasing HRT. However, a low nitrate nitrogen level (1.4 mg L^{-1} data not shown) was observed across the membrane indicating that denitrification occurred inside the MBR compartment, resulting in a higher pH 8.4 in RE-C than in RE-B (pH 7.8); and (3) Constant aeration inside the MBR may have removed ammonia through air stripping (Qin and He 2014). The total phosphorus content was 2380 mg L^{-1} in RE-C, indicating that a theoretical

amount of 690 mg L^{-1} total phosphorus would be required to make up the gap between RE-C and the control.

5.3.4 Effects of RE on biochemical production

The effect of RE on bacterial growth and biosynthesis of PDC were assessed initially using RE-B culture media. The specific growth rate for the *Sphingobium* sp. SYK-6, PDC-producing strain of 0.82±0.03 h^{-1}, was significantly lower than the control culture (0.95±0.06 h^{-1}, $P<0.05$). A similar growth rate of 0.75±0.11 h^{-1} was measured in the RE-C based culture medium with a PDC production rate of 293.19±37.82 mg L^{-1} h^{-1} which was significantly lower ($P<0.05$) than the PDC production (621.01±22.09 mg L^{-1} h^{-1}) in the control culture. We speculate that the low specific bacterial growth rate and PDC production rate were likely due to two possible reasons: (1) the addition of nutrients in both undiluted RE-B and the RE-C may have led to an excessive salt level that exhibited an unfavorable effect on bacterial growth; and (2) the RE contained some unidentified inhibitors which could potentially affect bacterial growth and biochemical production simultaneously. HPLC analysis of RE-C showed a single peak with absorbance maxima at 254 and 280 nm, indicating that aromatic compounds may be present in the recycled effluent. Aromatic compounds may have been generated in the treatment process as we did not observe similar peaks in the raw culture waste. Certain aromatic compounds are known to be detrimental to normal cellular activity.

To address such inhibitory effects, we tested a RE dilution before reuse. Two types of the RE-C based culture media were prepared as follows: RE-C(1:2) was diluted 1:2 with pure water before adding the required nutrients; RE-C(1:2r) was diluted 1:2 with pure water

before adding a reduced level of nutrients to the culture medium (Table 5.2). It was observed that using a 1:2 dilution was enough to offset the inhibitory effects of RE-C on bacterial growth and PDC production. In RE-C(1:2), the specific bacterial growth rate was 1.00±0.05 h^{-1} and PDC production rate was 708.11±64.70 mg L^{-1} h^{-1}, which were not significantly different from 0.95±0.06 h^{-1} and 621.01±22.09 mg L^{-1} h^{-1} obtained in the control culture ($P>0.05$) (Figure 5.5, Table 5.2). In the RE-C (1:2r), a specific bacterial growth rate of 0.97±0.05, similar to that of the control ($P>0.05$), was obtained. However, when RE-C(1:2r) was used, the PDC production rate dropped to 508.79±70.88 mg $L^{-1}h^{-1}$ ($P<0.05$). These results indicate that the use of a 1:2 dilution ratio is adequate to permit the reuse of treated water from culture waste in new culture medium; however, complete nutrient levels comparable to controls must be added. The results further suggest that inhibitory factors for bacterial growth and PDC production may be different, but separation of these effects will require further investigation in future work.

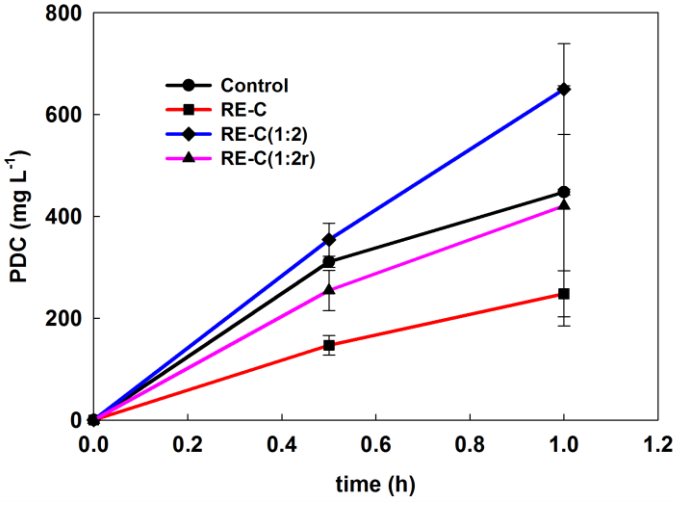

Figure 5.5 Initial PDC production in RE-based culture media.

It is well known that processes such as reverse osmosis (RO), can be used to polish water for secondary treated urban wastewater reuse (Bunani et al. 2015). However, the extensive energy requirements for RO treatment and the vulnerability of RO units to membrane fouling make RO treatment an expensive option. Therefore, the 2:1 dilution of RE offers a more affordable alternative for treatment of spent culture medium.

5.3.5 Outlook

In this work, we demonstrate the potential for reclaiming and reusing wastewater from spent culture media through the use of a MFC-MBR system. Although a 2 times dilution was effective for preparation of new culture media, the inhibitory compounds associated with the recycled effluent must be identified. Polymeric absorbents such as styrene-divinylbenzene (Amberlight®) can potentially be used as a low cost method for phenolic compound removal. Also, although high salt levels did not appear to be a problem, potential desalination methods could be applied to reduce sample salinity (e.g., electrodialysis, reverse osmosis, and microbial desalination cell) if this were required. This research represents a preliminary study demonstrating proof of concept, and more tests should be conducted to validate the reproducibility of the system's performance. Energy recovery should also be further optimized, for example through the use of multiple-stage MFC systems prior to the membrane bioreactor polishing process. Finally, a comprehensive assessment of the treatment and recycling system should be conducted to evaluate tradeoffs between costs (construction and operation) and benefits (recovery of energy, water and nutrients).

5.4 Conclusions

This paper presents a preliminary study on the re-use of water from spent culture media through treatment with an MFC-MBR system. Results demonstrate that treated wastewater can successfully be used to prepare new culture media for fermentation and associated platform chemical production. Under an appropriate reuse strategy (such as 1:2 dilution); both bacterial growth rate and PDC production were comparable to that obtained in control cultures using fresh water for media make up. The synergistic processes examined in this research offer a potential solution for minimizing environmental problems with wastewater treatment while also generating limited amounts of electrical energy. Benefits also include reduced carbon emissions and enhanced waste management, while also providing methodology that supports sustainable fermentation by conserving the use of fresh water in the production of new biosynthesized platform chemicals.

CHAPTER 6

Development of a Dynamic Mathematical Model for Membrane Bioelectrochemical Reactors with Different Configurations

(This section has been published as: Li, J. and He, Z.* (2015) Development of a Dynamic Mathematic Model for Membrane Bioelectrochemical Reactors with Different Configurations. **Environmental Science and Pollution Research**. Vol 23, pp 3897-3906.)

Abstract

Membrane bioelectrochemical reactors (MBERs) integrate membrane filtration into bioelectrochemical systems for sustainable wastewater treatment and recovery of bioenergy and other resource. Mathematical models for MBERs will advance the understanding of this technology towards further development. In the present study, a mathematical model was implemented for predicting current generation, membrane fouling and organic removal within MBERs. The relative root-mean-square error was used to examine the model fit to the experimental data. It was found that a constant to determine how fast the internal resistance responds to the change of the anodophillic microorganism concentration could have a dominant impact on current generation. Hydraulic cross flow exhibited a minor effect on membrane fouling unless it was reduced below 0.5 m s^{-1}. This MBER model encourages further optimization and eventually can be used to guide MBER development.

6.1 Introduction

Integrating filtration membranes into bioelectrochemical systems such as microbial fuel cells (MFCs) represents a new approach for sustainable wastewater treatment and has attracted great interest (Yuan and He 2015). In MFCs, bioenergy in wastewater is extracted through the interaction between microbes and electrodes in the anodic compartment and

the produced electrons are transferred to cathode electrode through an external circuit (Logan et al. 2006b). Comparing with the conventional activated sludge (CAS) process, MFC technology requires less energy input, yields less sludge and produces useful bio-electricity (Rabaey and Verstraete 2005, Zhang et al. 2013b). Combining a membrane separation process with MFCs helps to achieve high quality effluent, and the combined system is called membrane bioelectrochemical reactors (MBERs) or bioelectrochemical membrane reactors (BEMRs).

MBERs have been demonstrated feasible and advanced in several aspects including configurations, nutrient removal, and energy balance. Early studies applied biofilm grown on stainless steel mesh as a membrane-like filtration process to achieve high removal of both organics and ammonia (Wang et al. 2011b, Wang et al. 2012). Commercial hollow-fiber ultrafiltration membranes were installed in the anodic compartment of a tubular MFC, forming an MBER, but membrane fouling reduced water flux and required frequent membrane cleaning (Ge et al. 2013b). To alleviate fouling issue, MBERs were modified, such as a fluidized-bed MBER with granular activated carbon (GAC) in the anodic chamber, or hollow fiber membrane being installed in the cathodic chamber with constant aeration (Li et al. 2014a, b). Nitrogen removal could be improved by using an anion exchange membrane (AEM) as a separator (Li and He 2015b). Membrane bioreactors (MBRs) can be linked to MFCs for achieving treatment of wastewater or reuse of media for fermentation (Li et al. 2015). Two staged microbial fuel cell-anaerobic fluidized bed membrane bioreactor generated a high quality effluent with the MBR as an external post-treatment of the MFC (Ren et al. 2014). High quality effluent, more energy advantage and

minimal operation maintenance offers the MBER related technology as an alternative to the conventional membrane bioreactors (MBRs), but its performance (eg. electrical generation/membrane fouling) warrants further optimization before large scale commercialization.

Given its intrinsic physical, biological and electrochemical factors, developing a mathematical model will be helpful for further understanding of MBER systems. An MBER model consists of two parts, MFCs and MBR, linked by some key factors such as organic loading rates (OLR), aeration intensity and reactor configuration. The available MFC/MEC models are based on Nernst-Monod type of equations to calculate substrate consumption and bacteria growth in the anodic compartment, but the mass transfer equations vary depending on the spatial distribution of substrates and microbial activities (Marcus et al. 2007, Picioreanu et al. 2007, Ping et al. 2014, Pinto et al. 2010). The existing MBR models are derived from activated sludge model (ASM) with a physical membrane filtration process (Ng and Kim 2007). Biomass kinetic models and membrane fouling models are major components to describe the MBR process (Diez et al. 2014, Zuthi et al. 2015). Development of MBER models will need to synergistically integrate MFC models with MBR models. In this study, a dynamic MBER model was developed for the first time. The model was validated and examined with the data from three different MBERs reported previously: an MBER with ultrafiltration membranes in its cathodic compartment, an MBER with improved nitrogen removal, and an MBER with fluidized GAC. It is expected that findings from current study can be helpful for next generation MBER model

development, which includes heterogeneous substrate and microbial distribution inside anodic compartment, and dynamic cathode overpotential.

6.2 Methods

6.2.1 MBER systems

The data of three MBER systems published previously were used to examine and validate the developed model, and the schematics of the three MBER systems are shown in Figure 6.1. The first MBER, MBER-1, was a cubic reactor containing cation exchange membrane (CEM) as a separator and hollow-fiber membranes installed in its cathodic compartment; the synthetic organic solution was treated in the anode and the effluent flew through the cathode (Li et al. 2014b). The second MBER, MBER-2, was a tubular reactor containing AEM as a separator and operated similarly to the MBER-1; it was designed to enhance nitrogen removal via heterotrophic denitrification in the anode (with nitrate movement across AEM) and bioelectrochemical denitrification in the cathode (Li and He 2015b). The third MBER, MBER-3, was a tubular reactor with hollow-fiber membranes installed in its anodic compartment; fluidized GAC was applied for fouling control (Li et al. 2014a).

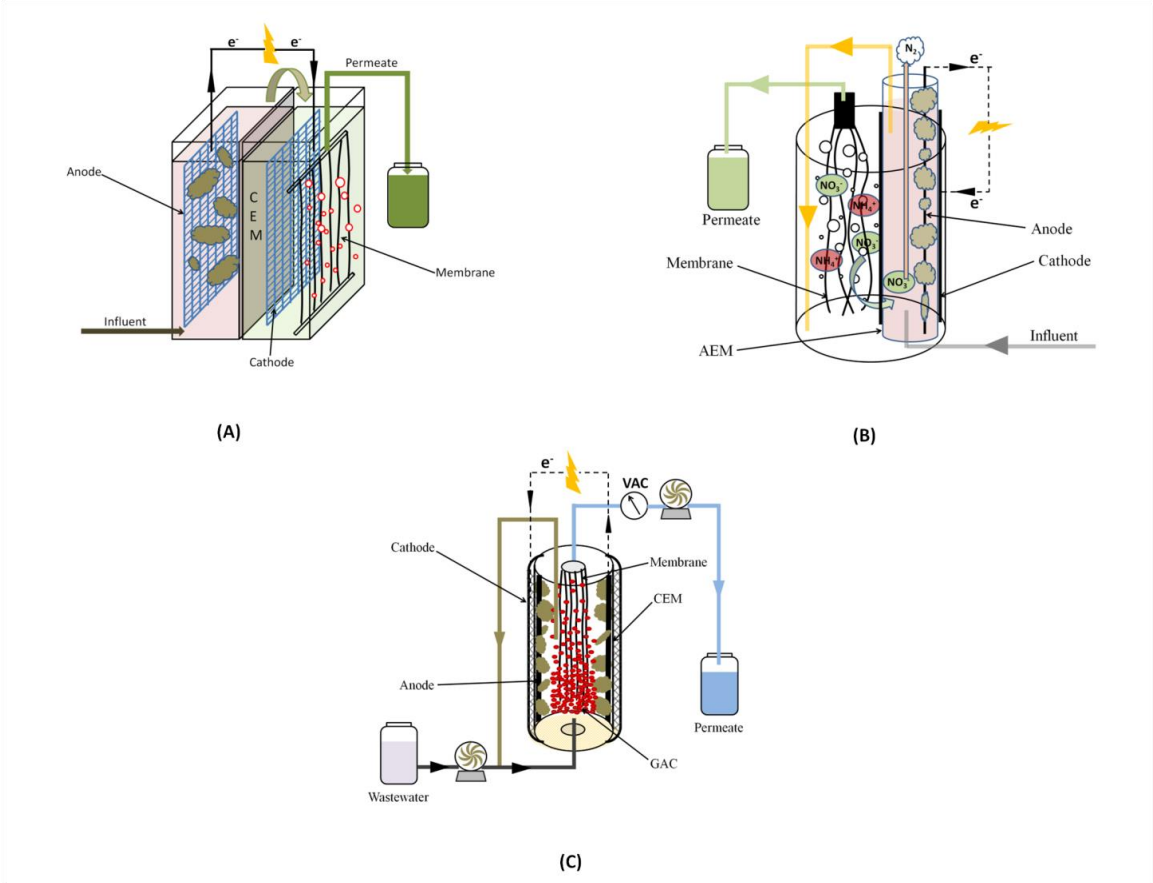

Figure 6.1 Schematics of the previously developed membrane bioelectrochemical reactors (MBERs): (A) MBER-1, hollo-fiber membranes installed in the cathode; (B) MBER-2, enhanced nitrogen removal with AEM; (C) MBER-3, fluidized GAC in the anode

6.2.2 Model formulations

6.2.2.1 Mass Balance for substrate, Microorganisms, and Electron Mediators in the Anode

The mass balance is established by applying multiplicative Monod kinetics for microbial growth (Pinto et al. 2010). An intracellular redox mediator is assumed to be generated by anodophillic bacteria to aid transfer of the electrons which were produced from substrate degradation. To simplify the process of model formulation, a well mixing condition is assumed in both chambers, and ordinary differential equation (ODE) is used to calculate

the concentration of substrate, anodophillic and methanogenic microorganism in the anode compartment.

The mass balance for the substrate is shown in eq 6.1:

$$\frac{dS}{dt} = D_{anode} * (S_{in} - S) - k_{s,a,\max} * \frac{S}{K_a + S} * \frac{M_{ox}}{K_M + M_{ox}} * C_a - k_{s,m,\max} * \frac{S}{S + K_m} * C_m \qquad (6.1)$$

Where S is the concentration of substrate (mg-S L^{-1}); S_{in} is concentration of influent substrate (mg-S L^{-1}); C_a and C_m are the concentrations of anodophillic and methanogenic microorganism (mg-C L^{-1}), respectively; $k_{s,a,max}$ and $k_{s,m,max}$ are the maximum substrate consumption rates by anodophillic and methanogenic microorganisms (mg-S mg-a $^{-1}$ day^{-1}), respectively; M_{ox} is the oxidized fraction per anodophillic microorganism (mg-M mg-a^{-1}); K_a, K_m and K_M are the half-saturation concentration for the anodophillic microorganisms, methanogenic microorganisms, and the redox mediator (mg-S L^{-1} , mg-S L^{-1} and mg-M mg-a^{-1}), respectively. $D_{anode} = \frac{Q_{in}}{V_{anode}}$, where D_{anode} is the dilution rate (day^{-1}), Q_{in} is the influent flow rate of the substrate (L day^{-1}), and V_{anode} is the volume of the anode compartment (L).

It is assumed that the growth of anodophillic bacteria is limited by both substrate concentration and the oxidized form of the mediator; whereas the growth of methanogenic microorganism is limited only by the substrate concentration.

The concentration of anodophillic or methanogenic microorganisms is calculated by the differential equations:

$$\frac{dC_a}{dt} = k_a * C_a - k_{d,a} * C_a - D_{anode} * \frac{1 + tanh(k_{a,x} * (C_a + C_m - C_{a,\max}))}{2} * C_a \qquad (6.2)$$

$$\frac{dC_m}{dt} = k_m * C_m - k_{d,m} * C_m - D_{anode} * \frac{1 + tanh(k_{m,x} * (C_a + C_m - C_{m.,\max}))}{2} * C_m \quad (6.3)$$

where $k_{d,a}$ and $k_{d,m}$ are decay rates of the microorganisms (day^{-1}); $k_{a,x}$ and $k_{m,x}$ are the steepness factors for anodophillic microorganisms (L mg-a $^{-1}$) and methanogenic microorganisms (L mg-m $^{-1}$) for the biofilm retention; $C_{a,max}$ and $C_{m,max}$ are the maximum attainable concentration for anodophillic microorganisms (mg-a L^{-1}) and methanogenic microorganisms (mg-m L^{-1}); k_a and k_m are the growth rates of microorganisms (day^{-1}) calculated by eq. 6.4 and 6.5:

$$k_a = k_{a,\max} * \frac{S}{K_a + S} * \frac{M_{ox}}{K_M + M_{ox}} \quad (6.4)$$

$$k_m = k_{m,\max} * \frac{S}{K_m + S} \quad (6.5)$$

Where $k_{a,max}$ and $k_{m,max}$ are the maximum microorganism growth rates (day $^{-1}$)

The intercellular materials balance for the oxidized mediator can be described as follows:

$$\frac{dM_{ox}}{dt} = -Y_M * k_{s,a} + \frac{\gamma * I}{V_{anode} * C_a * n_e * F} \quad (6.6)$$

$$M_{total} = M_{ox} + M_{red} \quad (6.7)$$

where M_{total} is the total mediator fraction per microorganisms (mg-M mg-a^{-1}); M_{red} is the reduced mediator fraction per microorganisms (mg-M mg-a^{-1}); Y_m is the mediator yield (mg-M mg-S^{-1}); γ is the mediator molar mass (mg-M mole-M^{-1}); I is the current through the circuit of an MBER (A); F is the Faraday constant (A day mole^{-1}); and n_e is number of electrons transferred per mole of mediator (mole -e mole-M^{-1}).

6.2.2.2 Electrical generation

The overall cell voltage in an MBER is modeled by the following equation:

$$I * R_{ext} = V_{oc} - OP_{anode} - OP_{cathode} - OP_{conc} - I * R_{\text{int}} \quad (6.8)$$

Where R_{ext} is the external resistance (Ω); V_{oc} is the open circuit voltage (V); OP_{anode} is the anode overpotential (V); $OP_{cathode}$ is the cathode overpotential (V); OP_{conc} is the concentration overpotential; R_{int} is the internal resistance (Ω).

Usually, R_{int} includes mass transfer resistance, ohmic resistance, and activation resistance. In present study, the internal resistance was calculated as follows:

$$R_{\text{int}} = R_{\min} + (R_{\max} - R_{\min)} * e^{-k_r * C_a} \quad (6.9)$$

Where R_{min} and R_{max} are the minimum and maximum internal resistance (Ω), and k_r is the constant that determines how fast the internal resistance respond to the change in microorganism concentration C_a (L mg-a^{-1}).

The open circuit voltage was calculated as:

$$V_{oc} = V_{\min} + (V_{\max} - V_{\min}) * e^{-1/(k_r * C_a)} \quad (6.10)$$

Where V_{min} and V_{max} are the lowest and highest observed V_{oc} values (V).

The concentration overpotential is assumed to be associated with electron mediators and could be modeled as follows:

$$OP_{conc} = \frac{R * T}{F} * \ln \frac{M_{total}}{M_{red}} \quad (6.11)$$

It is noteworthy that the anode overpotential and cathode overpotential have been neglected, due to the sufficient buffer solution in both chambers. Hence, the current generation equation is simplified to be as follows:

$$I = \frac{V_{oc} - OP_{conc}}{R_{ext} + R_{\text{int}}} \tag{6.12}$$

6.2.2.3 Membrane fouling

6.2.2.3.1 Membrane simulation of MBER-1

Due to the similarity of system configuration, sMBR models are used for membrane performance prediction. Being as a stand-alone technology, sMBR models include aeration, cake formation, filtration, fouling, physical and bioprocess description. The total membrane fouling is represented by combining cake layer resistance (R_{cake}), intrinsic resistance (R_m) and resistance which is caused by total resistance disturbance ($\delta_{R)}$. However, the formation of cake layer is usually responsible for membrane fouling issue (Khan et al. 2009).

$$R_{total} = R_m + R_{cake} + \delta_R \approx R_{cake} \tag{6.13}$$

where the cake layer resistance is calculated by:

$$R_{cake} = \rho * (\frac{m + m_0}{A}) \tag{6.14}$$

where ρ is the specific cake layer resistance (m g^{-1}); m_0 is the initial cake mass (g); A is the area of the membrane surface and m is the current cake mass (g).

The calculation of the transmembrane pressure is expressed as follow:

$$\Delta P = Q_{out} * \eta * R_{total} \tag{6.15}$$

where ΔP is the trans-membrane pressure (Pa); η is the water apparent viscosity (Pa.S); Q_{out} is effluent rate ($m^3\ day^{-1}$).

The change of the cake layer mass can be expressed:

$$\frac{dm}{dt} = Q_{out} * X - J_{air} * \mu_{air} * m \tag{6.16}$$

$$\mu_{air} = \beta * \frac{m}{K_{air} + m} \tag{6.17}$$

where X is the concentration of the suspended solids ($g\ m^{-3}$); J_{air} is the air crossflow ($m^3\ m^{-2}\ day^{-1}$); β is the linked to the resistance of the cake to detachment (m^{-1}); K_{air} is the half saturation coefficient of air flow (g).

The biological activity is described involving one biomass growing on a limited substrate.

$$\frac{dS}{dt} = -\frac{1}{Y} * \mu(S) * X + \frac{Q_{in}}{V} * (S_{in} - S) \tag{6.18}$$

$$\mu(S) = \mu(S)_{\max} * \frac{S}{K_s + S} \tag{6.19}$$

$$\frac{dX}{dt} = (\mu(S) - \frac{Q_W}{V}) * X + \frac{Q_{in}}{V} * X_{in} - \frac{Q_{out}}{V} * X + \frac{J_{air}}{V} * \mu * m \tag{6.20}$$

where Y is yield coefficient of the substrate consumption; $\mu(S)$ is the microbial growth rate (day^{-1}); $\mu(S)_{max}$ is the maximum microbial growth rate (day^{-1}); Q_{in} is the inflow rate ($m^3\ day^{-1}$); V is the volume of the cathode chamber (m^3); S_{in} is the substrate concentration in the influent flow; S is the substrate concentration ($g\ m^{-3}$); K_s is the half saturation of substrate ($g\ m^{-3}$); Q_w is the waste flux ($m^3\ day^{-1}$); and X_{in} is the solid concentration in the influent ($g\ m^{-3}$).

The parameter β represents the ease (or difficulty) of detaching the cake from the membrane using an air crossflow.

$$\frac{d\beta}{dt} = \gamma * \beta \tag{6.21}$$

6.2.2.3.2 Membrane simulation for the fluidized-bed MBER-3

A previous study was used to develop and predict membrane fouling problem in the fluidized MBER system (Liu et al. 2003). The membrane fouling rate under various hydrodynamic conditions has been estimated.

The filtration resistance is calculated as an indicator for membrane fouling status:

$$R = 3.6 * 10^{9} * \frac{\Delta P}{\eta * J} \tag{6.22}$$

Where R is the filtration resistance (m^{-1}), J is filtration flux (L m^{-2} h^{-1}), ΔP was the transmembrane pressure (Pa). The η is approximately expressed by the viscosity of tap water and is calculated as follows:

$$\eta = 1.6003 * e^{-0.021*T} \tag{6.23}$$

Where T is the temperature of water.

It is assumed that the membrane filtration resistance increases with time during the filtration, and the increasing rate of resistance K is obtained as a slope of the straight line to the changing course of the measured resistance.

The increase rate of resistance K is calculated as follows:

$$K = f * U_{Lr}^{c} * J^{d} * X^{e} \tag{6.24}$$

where f , c, d and e were constants. X is the concentration of suspended solids in mixed liquor (g L^{-1}); J is filtration flux (L m^{-2} h^{-1}); U_{Lr} is the cross flow velocity on the membrane surface (m s^{-1}).

6.2.2.4 Nitrogen removal from the MBER-2

Nitrogen can be removed from an MBER by either ionic migration or diffusion due to the concentration gradient. To quantify the total nitrogen concentration in the membrane permeate:

$$\frac{dC_{TN}}{dt} = (C_{TN,in} - C_{TN}) * D_{cathode} - \alpha * \frac{I}{F * V_{cathode}} - \beta * C_{TN} \quad (6.25)$$

where $C_{TN,in}$ and C_{TN} are the total nitrogen concentration in the anode effluent and membrane filtrate, respectively (mole-N L^{-1}); $D_{cathode}$ is the dilution rate (day^{-1}) in the cathode compartment that is quantified by the ration of effluent rate (Q_{out}) over the volume of the cathode compartment($V_{cathode}$); α is the fraction of produced electrons for total nitrogen removal; I is the current produced (A); F is the Faraday constant; β is the diffusion coefficient for concentration gradient (day^{-1}).

6.2.3 Parameter estimation

The information about the estimated parameters can be found in Table 6.1-6.5. The parameters obtained are further re-estimated from additional experimental data. The genetic algorithm routine in MATLAB is used for parameter estimation to minimize the relative root-mean-square error (RMSE) between the predicted value and the experimental data. The RMSE is calculated as follows:

$$RMSE = \frac{\sqrt{\frac{\sum_{i=1}^{N}(y_m - y_e)^2}{N}}}{\max(y_e)} \quad (6.26)$$

where N is the total number sampling time points in the simulation; y_m and y_e represents model predicted values and experimental data at t_i, respectively. The maximum value of experimental data was used to normalize the error in equation 6.26. A smaller RMSE indicates that model has a good fit to experimental data. It is also worthy to note that MATLAB function ODE 23 is applied to solve all of differential equation in our study.

6.3 Results and Discussion

6.3.1 Model performance with the MBER-1 data

The developed model was examined with the data of the MBER-1 that was operated under a hydraulic full loop mode and the flow rate of its anode feeding was adjusted at 0.23, 0.39 and 0.23 mL min^{-1} on day 20, 66 and 78, respectively, resulting in an anodic HRT of 10, 6 and 10 h. The model output of current value shows a general agreement with the experimental measurement, but some underestimation and overestimation can be seen (Figure 6.2 A). The RMSE indicated that the mean error for the current generation was within 15.2% of their maximum value during first 46 days. Such a discrepancy can be from the mismatch at the early period: the current simulation was started from day 20 of the MBER operation, and a sharp decrease in the modeled current occurred in a short period of time afterward. The initial anodophillic bacteria concentration was estimated as 345.3 mg L^{-1}, and the lagging time of bacteria growth resulted in a temporary drop of current generation; when the anodophillic bacteria concentration reached a steady state, a stable current generation was achieved as a result. The simulated current generation increased by

0.5 mA from day 66, as a response to enhanced organic loading rate, but overestimation can be observed and the RMSE for the current generation was 20.8%. The formulated model has a high sensitivity to the change of organic loading rate, but the experiment did not respond correspondingly, possibly related to the fact that a large amount of organic compounds was consumed by microorganisms rather than anodophillic bacteria. The predicted current generation was below 4 mA after the feeding flowrate was changed back to 0.23 mL min^{-1} on day 78 with slight overestimation and a RMSE of 18.4%.

The predicted TMP profile had a very good fit to the experimental data (Figure 6.2 B), and the relative RMSE was 11.3% when the system was operated at an anodic HRT of 10 h from day 20 to 66. The simulated TMP experienced a dynamic process, in which it started from 5 kPa on day 20, increased to a peak value of 8 kPa on day 40, and then dropped back to 5 kPa. The underestimation of the TMP during the starting period was likely related to the formation of membrane fouling. The arch shape of the TMP change can be explained from eq 6.16, in which the first term represents the attachment of total suspended solids on the membrane surface depending on the effluent rate, and the second term in the equation represents cake detachment proportional to the air cross flow. The eq 6.16 indicates that the change of cake layer mass is proportional to the instantaneous cake layer mass, with a factorial of 2. Hence, the change of cake layer mass follows a parabolic shape and "archy" shape is a portion of the parabola. The change of TMP was less obvious in the experimental measurements due to the method of TMP recording (data were recorded manually three times a day, and the average value was used for analysis). The developed model was further evaluated and validated for TMP by changing the feeding rate to 0.39 mL min^{-1} on day 66

and then to 0.23 mL min^{-1} on day 78 in a step-wise way. The model prediction for TMP generally followed the trend of experimental data, and the simulated TMP increased from 14 to 25 kPa before the anode feeding rate was changed back to 0.23 mL min^{-1}. During this period, a linearized change of TMP indicates that the enhanced water flux played a dominant role for cake layer accumulation on the membrane surface, and cake mass detachment from air crossflow became a marginal effect due to a higher vacuum pressure after water flux adjustment. The change of cake layer mass is proportional to water flux by a factorial of 1, resulting in a linearized TMP change. The simulated TMP dropped back to 10 kPa along with reduced water flux after the anolyte was fed at 0.23 mL min^{-1} again on day 78; it is worth noting that the TMP began to increase from an initial TMP of 10 kPa, higher than 5 kPa on day 20, likely because of irreversible fouling. The model gave a fairly good prediction on TMP variation with a low RMSE of 5.4% during the final period.

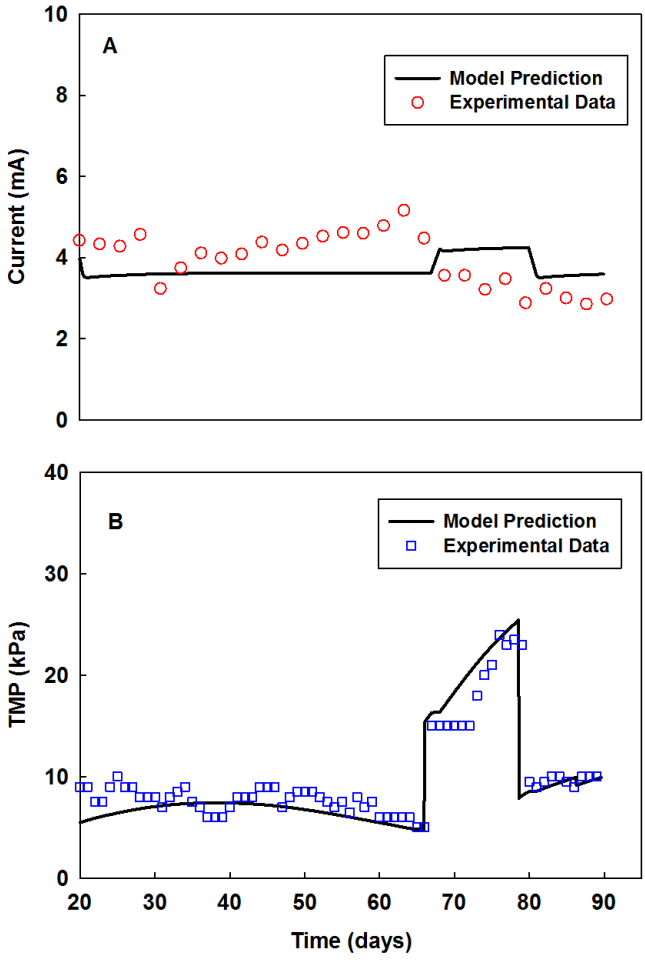

Figure 6.2 Experimental data and model simulation of the MBER-1 (A) current generation; (B) TMP change

Table 6.1 Parameters of the MBER-1 for electrical performance

Parameters	*Description*	*Value*	*Units*
F	Faraday constant	96,485	C mol^{-1}
R	Ideal gas constant	8.314	J K^{-1} mol^{-1}
T	Temperature	298.15	K
Y	Yield of anodophillic	10.5	mg-M mg-S^{-1}
Y_{CH4}	Methane Yield	0.3	mL CH_4 mg-S^{-1}
$q_{max,a}$	Maximum anodophillic reaction rate	2.32	mg-S mg-x^{-1} d^{-1}
$q_{max,m}$	Maximum methanogenic reaction rate	8.2	mg-S mg-x^{-1} d^{-1}
$\mu_{max,\,a}$	Maximum anodophillic growth rate	0.797	d^{-1}
$\mu_{max,\,m}$	Maximum methanogenic growth rate	0.1	d^{-1}
$K_{s,a}$	Half-rate constant of anodophillic	20	mg-S L^{-1}
$K_{s,m}$	Half-rate constant of methanogens	80	mg-S L^{-1}
m	Electrons transfer per mol of mediator	2	mol^{-1} mol mediator $^{-1}$
γ	Mediator molar mass	663,400	mg-M mol $mediator^{-1}$
M_{total}	Mediator fraction	0.05	mg-M mg-x^{-1}
K_M	Mediator half rate constant	0.01	mg-M L^{-1}
$K_{d,a}$	Decay rate of anodophillic microorganism	$0.02*\mu_{max,a}$	d^{-1}
$K_{d,m}$	Decay rate of methanogenic microorganism	$0.02*\mu_{max,m}$	d^{-1}
$X_{max,a}$	Anodophillic biofilm space limitation	512.5	mg-x L^{-1}
$X_{max,m}$	Methanogenic biofilm space limitation	525	mg-x L^{-1}
K_x	Steepness Factor	0.04	L mg-x^{-1}
R_{min}	Minimum internal resistance	31	Ω
R_{max}	Maximum internal resistance	2000	Ω
E_{min}	Minimum open circuit potential	0.1	V
E_{max}	Maximum open circuit potential	0.7	V
K_R	steepness factor correction coefficient	0.0818	L mg-x^{-1}

Table 6.2 Parameters of the MBER-1 for membrane performance

Parameters	*Description*	*Value*	*Units*
η	Water apparent viscosity	0.00089	Pa.S
A	Membrane surface area	0.0051	m^{-2}
ρ	Specific cake resistance	100000000	$m\ g^{-1}$
γ	Coefficient of β	0.05	
Y	Yield coefficient of the substrate consumption	1.4	$mg\text{-}Mmg\text{-}S^{-1}$
$\mu_{s,max}$	Maximum growth rate	0.09	d^{-1}
J_{air}	Air crossflow	80	$m^3\ m^{-2}\ d^{-1}$
K_s	Half saturation of substrate	10	$g\ m^{-3}$
K_{air}	Half saturation of airflow	$4.6*10^{-5}$	$g\ m^{-3}$
β	Resistance of detachable cake by air crossflow	0.01	m^{-1}
Q	Inflow	0.000336	$m^3\ d^{-1}$
V	Volume of cathodic compartment	0.00022	m^3

6.3.2 Model performance with the MBER-2 data

The MBER-2 was a modified MBER-1 with AEM as a separator for enhancing nitrogen removal through nitrate migration driven by electricity generation and denitrification. Thus, nitrogen was a new parameter for the model to include. This MBER was fed with an anolyte at 1.34 mL min^{-1} in a hydraulic full loop mode until day 60. The developed model gave good prediction on current generation from a synthetic solution with slight overestimation and a low RMSE of 10.7% (Figure 6.3 A). The using of carbon brush and enhanced separator area resulted in an improved electrical performance (compared to the MBER-1). The substrate consumption in the anodic chamber was also simulated (Figure 6.3 B), and the simulated results suggest that the MBER-2 almost reached a steady state in 40 days with a low concentration of residual COD. It should be noted that the measurement was taken once a week, and future studies to improve the developed model will require more frequent measurement. Cake mass accumulation endured a dynamic process, in

which a peak TMP value of 10 kPa was obtained on day 30 and it dropped back to 5 kPa on day 60 (Figure 6.3 C), due to the low suspended solids and organic content from the anolyte. The simulated concentration of total nitrogen concentration in membrane permeate exhibited a satisfactory agreement with the experimental measurement (Figure 6.3D), and the mean error for the total nitrogen concentration was within 6.5% of their maximum values. Eq 6.25 indicates that the concentration-gradient driven diffusion from the cathodic to the anodic compartment, and the ion migration driven by ionic current and charge balance, which is described by the Faraday's law, are two major mechanisms for nitrogen removal. Compared to ion migration effect, ion diffusion from concentration gradient played a minor role for nitrogen removal. A coefficient α (0.13) was applied to modify on ion migration, which indicates about 13% of generated electrons was used for driving negative charged nitrate ions into the anodic compartment and other negative charged ions such as chlorine and sulfate may use the rest of electrons.

The MBER-2 was also operated by feeding actual wastewater, a primary effluent from a local wastewater treatment plant, at 1.25 mL min^{-1}, resulting in anodic HRT of 10 h, and the data obtained from actual wastewater were also used for model validation. In general, the developed model can well predict TMP and total nitrogen (Figure 6.4 C and D), with low RMSE of 8.6 and 9.7%, respectively. The current predication (Figure 6.4 A) has a high RMSE of 24.8%, mainly because of the fluctuating current generation with actual wastewater. It should be noted that the conductivity of the primary effluent was below 1 mS cm^{-1}, much lower than 3.3 mS cm^{-1} of the synthetic solution; therefore, the parameter R_{min} was re-designated as 300 Ω for model fitting. The COD consumption in the anodic

compartment was predicted with underestimation, with simulated COD concentration about 10 mg L^{-1} higher than the experimental measurement (Figure 6.4 B). The new R_{min} might be responsible for this discrepancy, but this warrants further investigation.

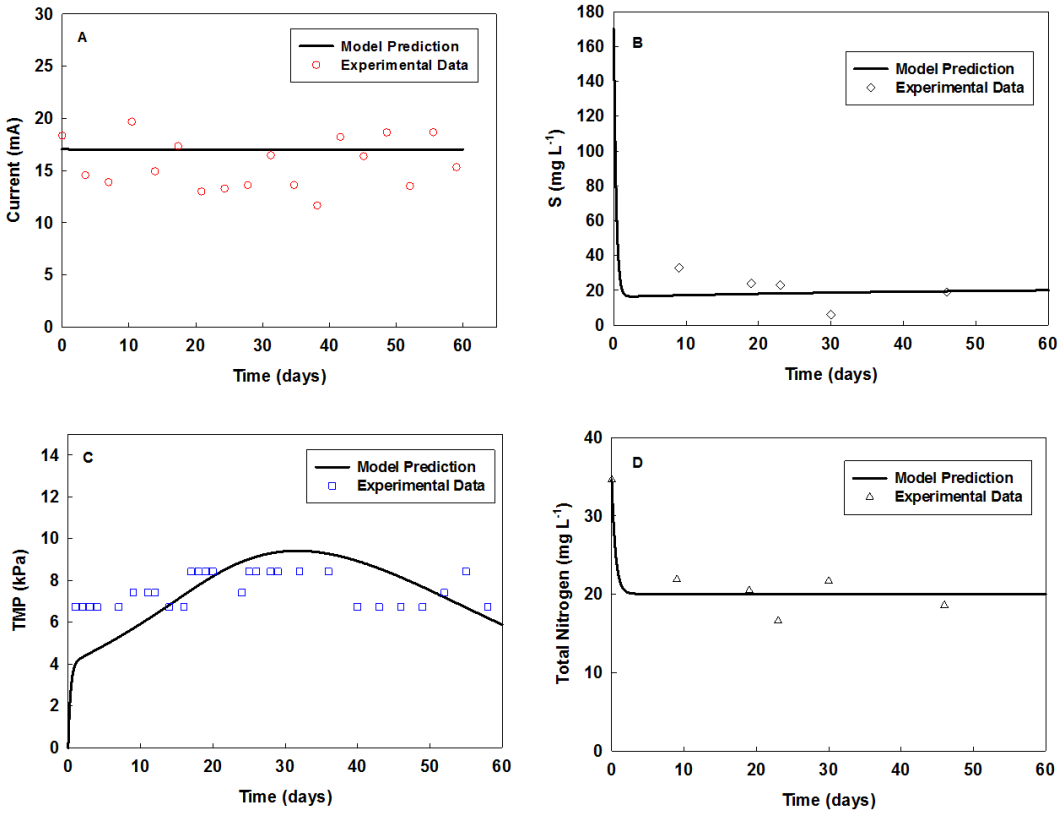

Figure 6.3 Experimental data and model simulation of the MBER-2 fed with a synthetic solution: (A) Current generation; (B) Substrate concentration in the anode effluent; (C) TMP change; (D) Total nitrogen concentration in membrane permeate

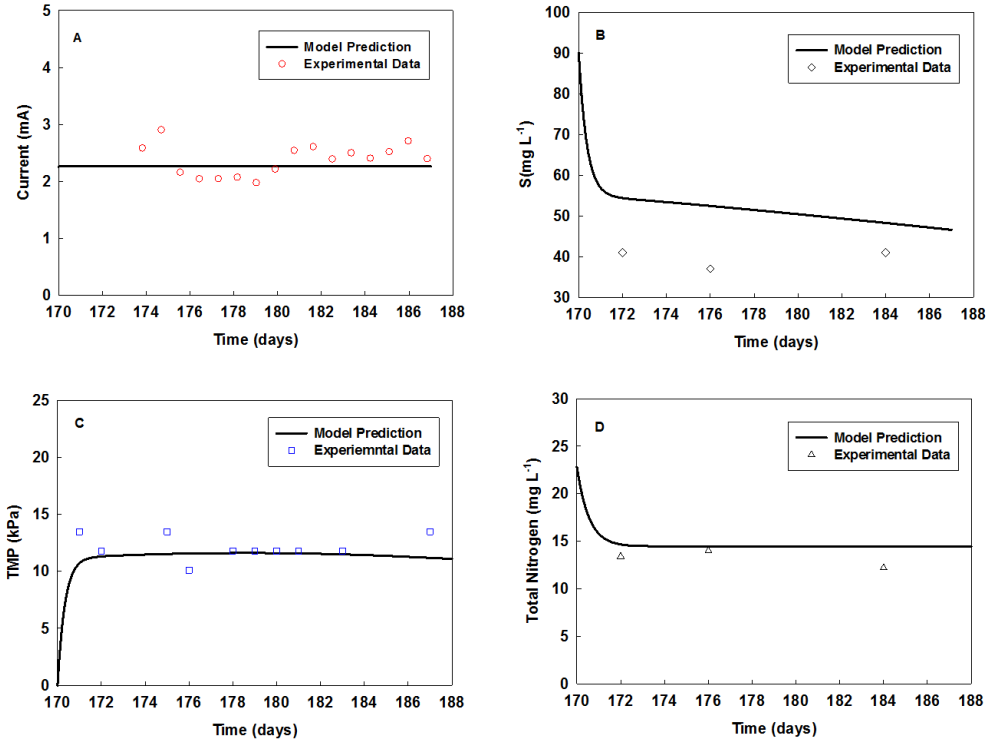

Figure 6.4 Experimental data and model simulation of the MBER-2 fed with actual wastewater (primary effluent): (A) Current generation; (B) Substrate concentration in anode effluent; (C) TMP change; (D) Total nitrogen in membrane permeate

Table 6.3 Parameters of the MBER-2 for electrical performance

Parameters	*Description*	*Value*	*Units*
F	Faraday constant	96,485	C mol^{-1}
R	Ideal gas constant	8.314	J K^{-1} mol^{-1}
T	Temperature	298.15	K
Y	Yield of anodophillic	17.1	mg-M $mg\text{-}S^{-1}$
Y_{CH4}	Methane Yield	0.3	mL CH_4 $mg\text{-}S^{-1}$
$q_{max,a}$	Maximum anodophillic reaction rate	5.32	mg-S $mg\text{-}x^{-1}$ d^{-1}
$q_{max,m}$	Maximum methanogenic reaction rate	8.2	mg-S $mg\text{-}x^{-1}$ d^{-1}
$\mu_{max,\ a}$	Maximum anodophillic growth rate	0.797	d^{-1}
$\mu_{max,\ m}$	Maximum methanogenic growth rate	0.1	d^{-1}
$K_{s,a}$	Half-rate constant of anodophillic	20	mg-S L^{-1}
$K_{s,m}$	Half-rate constant of methanogens	80	mg-S L^{-1}
m	Electrons transfer per mol of mediator	2	mol^{-1} mol mediator $^{-1}$
γ	Mediator molar mass	663,400	mg-M mol $mediator^{-1}$
M_{total}	Mediator fraction	0.05	mg-M $mg\text{-}x^{-1}$
K_M	Mediator half rate constant	0.01	mg-M L^{-1}
$K_{d,a}$	Decay rate of anodophillic microorganism	$0.02*\mu_{max,a}$	d^{-1}
$K_{d,m}$	Decay rate of methanogenic microorganism	$0.02*\mu_{max,m}$	d^{-1}
$X_{max,a}$	Anodophillic biofilm space limitation	512.5	mg-x L^{-1}
$X_{max,m}$	Methanogenic biofilm space limitation	525	mg-x L^{-1}
K_x	Steepness Factor	0.04	L $mg\text{-}x^{-1}$
R_{min}	Minimum internal resistance	31	Ω
R_{max}	Maximum internal resistance	2000	Ω
E_{min}	Minimum open circuit potential	0.1	V
E_{max}	Maximum open circuit potential	0.7	V
K_R	Steepness factor correction coefficient	0.0818	L $mg\text{-}x^{-1}$

Table 6.4 Parameters of the MBER-2 for membrane and nutrients removal performances

Parameters	*Description*	*Value*	*Units*
η	Water apparent viscosity	0.00089	Pa S
A	Membrane surface area	0.0261	m^{-2}
ρ	Specific cake resistance	100000000	$m\ g^{-1}$
γ	Coefficient of β	0.05	
Y	Yield coefficient of the substrate consumption	1.2	mg-M $mg\text{-}S^{-1}$
$\mu_{s,max}$	Maximum growth rate	0.12	d^{-1}
J_{air}	Air crossflow	120	$m^3\ m^{-2}\ d^{-1}$
K_s	Half saturation of substrate	10	$g\ m^{-3}$
K_{air}	Half saturation of airflow	$4.6*10^{-5}$	$g\ m^{-3}$
β	Resistance of detachable cake by air crossflow	0.01	m^{-1}
Q	Inflow	0.0019	$m^3\ d^{-1}$
V	Volume of cathodic compartment	0.001	m^3
D_n	Diffusion coefficient for nitrate ions through AEM	0.0293	d^{-1}
α_n	Fraction of electrons for nitrate ions migration	0.13	

6.3.3 Model performance with the MBER-3 data

The MBER-3 was a fluidized bed system with GAC as media. The fluidized GAC was affected by the anolyte recirculation, and thus recirculation strategy was examined. The developed model showed a satisfactory agreement of current prediction with the experimental measurement and its RMSE was within 8.8% of their maximum value (Figure 6.5 A). The slight overestimation of current between day 10 and 43 was related to the assumption that a homogeneous condition for substrate and biomass distribution is always valid, even though the absence of recirculation flow may retard substrate transfer to electrode surface. A significant mismatch with a high RMSE of 55.7% was observed on day 63 when the anodic HRT was changed to 5 h. Such a discrepancy was likely related to several factors: the stacked GAC in the anodic chamber may have offset the effect of the enhanced flowrate of feeding solution; the electrochemically-active biofilm on the electrode surface may require longer time for acclimating to new hydraulic condition;

and/or the enhanced organics could be consumed by the non-electrochemically-active microorganism on the GAC surface (which could be dominate in a mixed culture system).

The model gave a very good prediction for TMP change with a low RMSE of 9.0% (Figure 6.5 B). The change of filtration resistance (R) correlates to water flux (J) and hydraulic cross flow (U_{Lr}), which has been shown in eq. 6.23 and 6.25. The change of membrane resistance rate (K) is proportional to water flux by a factorial of 0.38 and to hydraulic cross flow inversely by a factorial of 1.1. The increase of TMP has been expressed in a linearized way after the recirculation flow was stopped, and the effect of U_{Lr} can be neglected due to the extremely low cross-flow on membrane surface. Therefore, since day 10, TMP has been increasing along with a slope, mainly determined by water flux. Water flux might have a minor effect after the recirculation flow was re-started, due to the quantitative relationship between J and U_{Lr}. Hence, filtration resistance is determined by hydraulic cross flow in an inverse relationship, and a low TMP can be seen between day 43 to 63. The model prediction of TMP was also validated after the MBER system was fed at 2.33 mL min^{-1} on day 63, and based on the model results, hydraulic cross-flow still could have played a dominant role for membrane fouling control.

The effects of multiple factors were studied focusing on water flux (J) and hydraulic cross flow on membrane surface (U_{Lr}), where these two parameters are changed simultaneously for evaluating filtration resistance change (Figure 6.6). The simulation results show that a higher water flux can be compensated by increasing the recirculation rate. It is demonstrated that for a fixed water flux, the change of membrane resistance K decreases

upon the increase of hydraulic cross flow at 0.0005 m s^{-1}, corresponding to 630 mL min^{-1} recirculation flow in this MBER. The membrane has a minor fouling issue (or it requires a long time for noticeable fouling) when a recirculation flow rate is higher than 630 mL min^{-1}. However, for a fixed recirculation flow rate lower than 630 mL min^{-1}, the change of filtration resistance increases upon the increase of water flux. Therefore, controlling recirculation flow rate at 630 mL min^{-1} can be an optimum operation method to minimize membrane fouling issue, thereby extending membrane's lifetime and reducing energy consumption, in the absence of aeration and chemical cleaning.

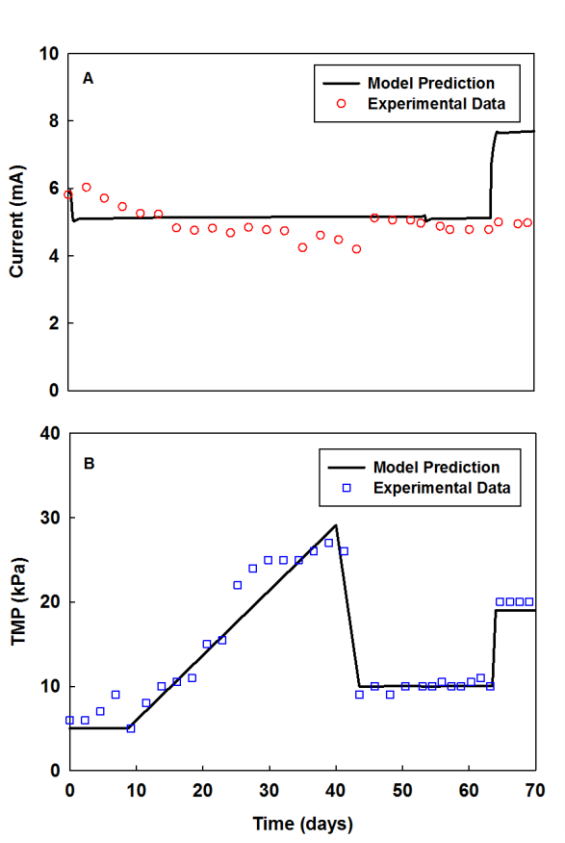

Figure 6.5 Experimental data and simulation results of the MBER-3 (A) Current generation; (B) TMP change.

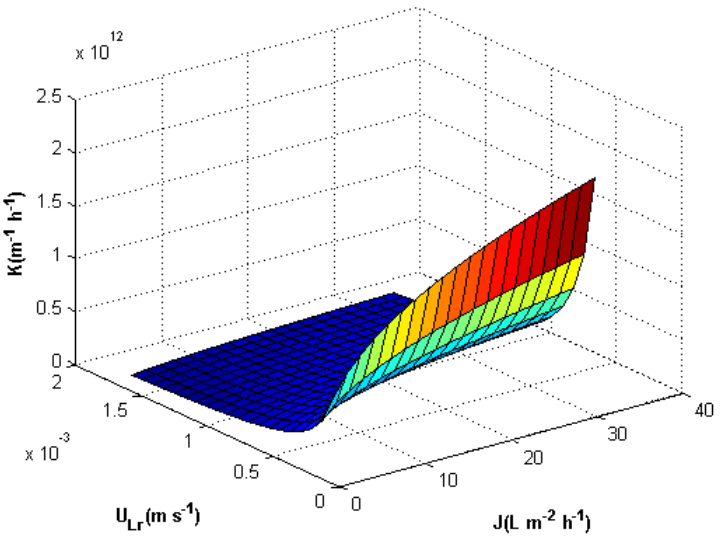

Figure 6.6 Model simulation of the effects of multiple factors including membrane filtration resistance (K), cross-flow velocity (U_{lr}) and water flux (J)

Table 6.5 Parameters of the MBER-3 for electrical and membrane performance

Parameters	*Description*	*Value*	*Units*
F	Faraday constant	96,485	C mol^{-1}
R	Ideal gas constant	8.314	J K^{-1} mol^{-1}
T	Temperature	298.15	K
Y	Yield of anodophillic	2.04	mg-M mg-S^{-1}
Y_{CH4}	Methane Yield	0.3	mL CH_4 mg-S^{-1}
$q_{max,a}$	Maximum anodophillic reaction rate	6.32	mg-S mg-x^{-1} d^{-1}
$q_{max,m}$	Maximum methanogenic reaction rate	8.2	mg-S mg-x^{-1} d^{-1}
$\mu_{max,\ a}$	Maximum anodophillic growth rate	0.797	d^{-1}
$\mu_{max,\ m}$	Maximum methanogenic growth rate	0.1	d^{-1}
$K_{s,a}$	Half-rate constant of anodophillic	20	mg-S L^{-1}
$K_{s,m}$	Half-rate constant of methanogens	80	mg-S L^{-1}
m	Electrons transfer per mol of mediator	2	mol^{-1} mol mediator $^{-1}$
γ	Mediator molar mass	663,400	mg-M mol mediator^{-1}
M_{total}	Mediator fraction	0.05	mg-M mg-x^{-1}
K_M	Mediator half rate constant	0.01	mg-M L^{-1}
$K_{d,a}$	Decay rate of anodophillic microorganism	0.02*$\mu_{max,a}$	d^{-1}
$K_{d,m}$	Decay rate of methanogenic microorganism	0.02*$\mu_{max,m}$	d^{-1}
$X_{max,a}$	Anodophillic biofilm space limitation	512.5	mg-x L-1
$X_{max,m}$	Methanogenic biofilm space limitation	525	mg-x L^{-1}
K_x	Steepness Factor	0.04	L mg-x^{-1}
R_{min}	Minimum internal resistance	31	Ω
R_{max}	Maximum internal resistance	2000	Ω
E_{min}	Minimum open circuit potential	0.1	V
E_{max}	Maximum open circuit potential	0.7	V
K_R	steepness factor correction coefficient	0.0818	L mg-x^{-1}
J	Water flux	4.2	L m^{-2} h^{-1}
f	Constant in eq. 25	89330000	
U_{Lr}	Hydraulic crossflow on membrane surface	0.000634	m s^{-1}
c	Constant in eq. 25	-1.1	
d	Constant in eq. 25	0.376	
e	Constant in eq. 25	0.532	
X	Suspended solids concentration in the mixed liquor	200	mg L^{-1}

6.3.4 Perspectives

This work represents the first attempt to model membrane bioelectrochemical systems and the developed model can effectively predict the key parameters of an MBER such as

current generation, substrate consumption and TMP. However, limitations still exist in the current model. For example, the present model is based on the assumption that a homogeneous condition has been well established within an MBER; although this assumption simplifies simulation and calculation procedures, such an ideal condition cannot be easily obtained with real operation. In addition, the model assumes that the overpotential of both anode and cathode electrodes are kept constant in a low range, which may not always be the case because the residual organics from the anode chamber can act as a source of organics for the microbial simulation in the cathode and as a result the overpotential will vary. Furthermore, other factors such as nitrogen consumption due to the microbial synthesis have not been accounted for total nitrogen simulation. Future studies will optimize and advance this MBER model from several aspects: (1) complex substrates and substrate gradient, and heterogeneous spatial distribution of microorganism will be considered; (2) dynamic variation of electrode overpotential will be included; (3) other biological processes such as denitrification should be included for the organic consumption; and (4) the model will be used to guide the system scaling up for developing large-scale MBER system for treating actual wastewater.

6.4 Conclusions

A dynamic mathematical model has been developed and used to simulate/predict the key parameters of the MBER systems, such as current generation, substrate consumption, membrane fouling, and nitrogen removal. It was adjusted to successfully model three different types of MBER systems with distinct features such as nitrogen removal and fluidized GAC. The model gave a satisfactory agreement with experimental data, but some

under/over estimation was observed. The results of this work encourages further optimization of this MBER model through including more dynamic factors and ultimately the model can guide the development of large-scale MBER systems for actual wastewater treatment.

CHAPTER 7

Integrated Experimental Investigation and Mathematical Modeling of a Membrane Bioelectrochemical Reactor with an External Membrane Module

(This section has been published as: Li, J. Rosenberger, G and He, Z.* (2015) Integrated Experimental Investigation and Mathematical Modeling of a Membrane Bioelectrochemical Reactor with an External Membrane Module. **Chemical Engineering Journal.** Vol 287, pp 321-328.)

Abstract

Membrane bioelectrochemical reactors (MBER) integrate membrane filtration module into microbial fuel cells (MFCs) to achieve simultaneous wastewater treatment, bioenergy production, and high-quality effluent. Previous MBERs usually have membrane modules as a part of the MFC reactors that creates challenges for membrane cleaning. In this study, an MBER with an external membrane module was investigated through both experiments and mathematical modeling. This MBER produced a current density of 7.1±0.5 A m^{-3} with an anolyte recirculation of 90 mL min^{-1}; reducing the anolyte recirculation rate had a negligible effect on MBER's electrical performance but resulted in a positive energy balance of 0.003±0.002 kWh m^{-3}. Periodic backwashing (1 min-backwashing/15 min-operation) was demonstrated as an effective method for fouling control. A mathematical model was developed and validated using the experimental data. The model could predict the influence of key parameters such as influent organic concentration and anolyte flow rate on the current generation, and identify the maximum organic loading rate for current generation. Those results encourage further investigation and development of this MBER towards system scaling up.

7.1 Introduction

Membrane bioelectrochemical reactors (MBERs) are a newly emerged technology for sustainable wastewater treatment and resource recovery (Yuan and He 2015). An MBER is a combination of bioelectrochemical system (BES), such as microbial fuel cells (MFCs), with membrane separation. Thus, the technology inherits the advantages of both BES and membrane treatment (e.g., membrane bioreactors), and can directly generate electricity and produce a high-quality effluent. MBERs have been demonstrated in various studies. For example, biofilm was formed on the stainless steel mesh as a filtration material to achieve high organics and nutrient removal (Wang et al. 2011b, Wang et al. 2012). Commercial ultrafiltration hollow fiber membrane was integrated into a tubular MFC, either in the anode or the cathode (Ge et al. 2013b, Li et al. 2014b, Li and He 2015b). The MBER operation can generate energy and require low energy input, thereby creating an energy neutral treatment system. It was estimated that net electricity could be recovered from treating a low-strength synthetic wastewater after eliminating aeration process in the cathode chamber of an MBER (Wang et al. 2013). Increasing organic loading rate by decreasing hydraulic retention time (HRT) can also diminish the gap between energy consumption and production because of more energy production (Ge et al. 2013b).

Membrane fouling poses a great challenge to MBER operation, especially when membranes are integrated with BES in an internal configuration. It was reported that foulants could accumulate on the membrane surface rapidly when the membrane was installed in the anodic compartment of an MBER, and severe fouling occurred in two weeks with a rapid TMP increase from 0 to 50 kPa (Ge et al. 2013b). Coating polydopamine on membrane surface to increase hydrophobicity (Kim et al. 2014b) or lowering particle zeta

potential to increase electro-repulsion force (Tian et al. 2015) have been demonstrated to control membrane fouling effectively, but a long-term operation should be examined on membrane fouling. Fluidized bed granular activated carbon (GAC) was applied in the anodic compartment of an MBER to reduce transmembrane pressure (Li et al. 2014a), but the high pumping load due to the high recirculation and clogging issue after long-term abrasion of GAC could cause maintenance issues and high energy demand.

Periodic cleaning of membranes using physical and chemical methods is necessary to maintain a functioning membrane module, but with an internal membrane installation, *in situ* cleaning becomes very difficult because of potential effects on biological and electrochemical reactions. Thus, external linkage between BES and membrane module may provide a flexible system in which the membrane module can be cleaned/replaced without affecting the BES. Such a linkage was reported in two recent studies. In one study, an air-cathode MFC was connected to an anaerobic fluidized membrane bioreactor (AFMBR), forming a two-staged MFC-AFMBR (Ren et al. 2014). This system achieved the removal of more than 90% total COD and almost 100% total suspended solids; biogas production in the AFMBR may compensate for energy consumption by the system. The other study used an MFC-MBR system to treat the waste from a fermentation process that helped recycle the water and nutrients back to the fermentation process (Li et al. 2015). The challenge of those systems is that the external membrane module involves biological reactions that have high requirement for operation and maintenance; in addition, the collection of methane (and dissolved methane in the effluent) in the AFMBR (Ren et al.

2014) and aeration in the MBR (Li et al. 2015) may limit their application. In contrast, an abiotic membrane module could be easier to manage.

Given much interest in MBERs and in light of the above mentioned issues of managing membrane module, an MBER system consisting of an MFC and an abiotic membrane module was developed and investigated through an integrated approach of experimental investigation and mathematical modeling. The membrane module was linked to the MFC through a unique approach to take advantage of the catholyte dripping from the MFC (Figure 7.1). This type of tubular MFCs with dripping catholyte has been extensively demonstrated in previous studies including a long-term operated system with actual wastewater in a wastewater treatment plant (Ge et al. 2013c, Ge and He 2015, Yuan et al. 2015, Zhang et al. 2010, Zhang et al. 2013b). A dynamic mathematical model for MBER has been recently developed (Li and He 2015a) and is applied with proper modification for further understanding of the present MBER. The objectives of this study were: (1) to demonstrate feasibility of this MBER in an energy-neutral operation; (2) to maintain low membrane fouling with an enhanced flexibility; and (3) to apply a mathematical model to predict MBER performance affected by organic loading rate (OLR).

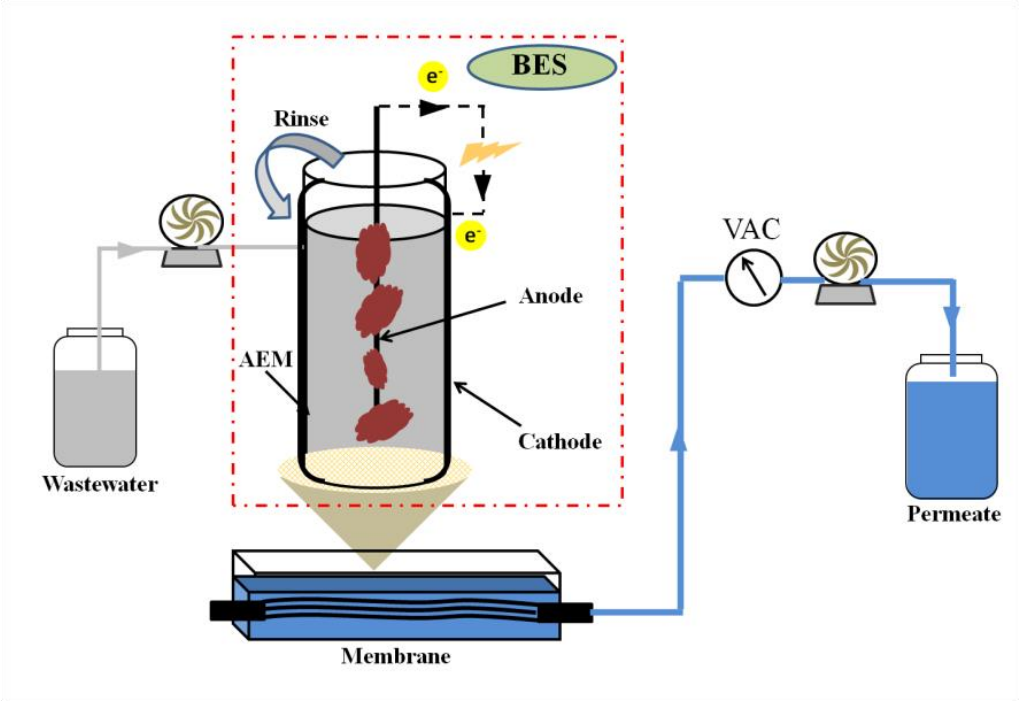

Figure 7.1 Schematic of the membrane electrochemical reactor (MBER) consisting of a tubular microbial fuel cell (MFC) and an external membrane module under MFC

7.2 Materials and Methods

7.2.1 MBER Setup

The proposed MBER system consisted of two units, an MFC and a (external) membrane module (Figure 7.1). The MFC was constructed as a tubular reactor (38 cm long and 5 cm in diameter) made of anion exchange membrane (AEM-Ultrex AMI 7001, Membrane International. Inc, Glen Rock, New Jersey, USA). A carbon brush was installed in the anodic chamber as an anodic electrode, resulting in a net liquid volume of 750 mL. Before use, the carbon brush was soaked in acetone overnight, and then heated for 30 min at 450 $^{\circ}$C. The cathode electrode was one piece of carbon cloth (Zoltek Corporation, St. Louis, MO, USA) coated with Pt/C powder (Etek, Somerest, NJ, USA) with a loading rate 0.2 mg Pt cm^{-2}. The cathode electrode wrapped the AEM membrane tube. The anode and cathode

electrodes were connected to a 10 Ω resistor. The external membrane module was made of thirteen 18-cm PVDF hollow fiber ultrafiltration membranes (15,000 Dalton, Litree Purifying Technology Co. China) that were installed in a 150 mL rectangular container, and was set up under the MFC to collect the catholyte.

7.2.2 Operating conditions

The MBER system was operated at room temperature. Its anode was fed with a synthetic solution containing (per L of tap water): glucose 0.25 g; NH_4Cl 0.15 g; NaCl 0.5 g; $MgSO_4$ 0.015 g; $CaCl_2$ 0.02 g; KH_2PO_4 0.53 g; K_2HPO_4 1.07 g; and 1mL trace elements. The anolyte was recirculated at 90, 50 and 20 mL min^{-1} on day 9, 55 and 74, respectively. The MBER was operated in a full loop mode, in which the synthetic solution was first fed into the anodic compartment and then the anodic effluent flowed to the cathode acting as a catholyte. There was no recirculation applied to the catholyte. The catholyte was collected by the membrane module, and the final permeate was extracted from the hollow-fiber membranes. The hollow fiber membrane module was operated in 4-min working/1-min relaxing mode; 1-min backwashing was applied in every 30-min from day 22 and in every 15-min from day 40, respectively. The flow rate of 1.25 mL min^{-1} was controlled by peristaltic pumps to achieve the desired anodic hydraulic retention time (HRT) at 10 h.

7.2.3 Measurements and analysis

The MFC voltage was recorded every 5 min by a digital multimeter (2700, Keithley Instruments, Cleveland, OH). The current and power density was normalized to the anode liquid volume. The pH was measured using a benchtop pH meter (Oakton Instruments, Vernon Hills, IL, USA). The conductivity was measured by a benchtop conductivity meter (Mettler-Toledo, Columbus, OH, USA). The concentration of chemical oxygen demand

(COD) was measured according to the manufacturer's procedure (Hach DR/890, Hach Company, Loveland, CO, USA). Transmembrane pressure (TMP) was recorded manually and the average value was reported in this study. Turbidity was measured using a turbidimeter (DRT 100B, HF Scientific, Inc, Fort Meyers, FL, USA). Energy recovery was evaluated by normalized energy recovery (NER) in kWh m^{-3} (Ge et al. 2013a, Xiao et al. 2014), a parameter for evaluating amount of energy can be generated for treating each m^3 of wastewater. The estimated energy consumption by the pumping system (for feeding, recirculating and membrane extracting) was calculated by the following equation (Kim et al. 2011). The energy consumption was expressed based on the volume of treated wastewater (kWh m^{-3}). The energy balance is the gap between energy recovery and consumption, which was also expressed based on the volume of treated wastewater (kWh m^{-3}).

7.2.4 Model formulation

A mathematical model is formulated by applying multiplicative Monod kinetics for microbial growth (Ping et al. 2014, Pinto et al. 2010). Intracellular redox mediator is assumed to be a key factor to aid electron transfer from substrate to an electrode, and a well-mixing condition is assumed in the anodic compartment. The overall cell voltage in MBER system is calculated by the difference between open circuit potential (V_{oc}) and potential loss, which includes overpotential from anode and cathode electrode, concentration overpotential and internal resistance. Because of the sufficient buffer solution and oxygen supply, the overpotential of the anode and the cathode electrodes has been neglected in this model. The estimated internal resistance includes mass transfer

resistance, ohmic resistance and activation resistance. More information about mass balance for substrate consumption, microorganism concentration, electron mediators and electrical production can be found in Table 7.1 and 7.2.

7.3 Results and Discussion

7.3.1 MBER performance of electricity generation and organic removal

The MBER system was fed with a synthetic solution for 101 days, and current generation is shown in Figure 7.2 A. The anolyte recirculation rate was gradually decreased from 90 (day 9), to 50 (day 55), and then to 20 mL min^{-1} (day 74). The MBER generated 7.1±0.5 A m^{-3} with the recirculation of 90 mL min^{-1}. Comparing to a previous MBER that was operated under a similar HRT (Li and He 2015b), the present MBER produced about 65.6% less electricity, possibly because that glucose used here is more complex than acetate used in the prior study and a lower COD concentration (250 vs. 350 mg L^{-1}) limits substrate transfer. Decreasing the anolyte recirculation rate to 50 mL min^{-1} resulted in current generation of 7.1±1.0 A m^{-3}, and further decrease to 20 mL min^{-1} produced current of 7.4±1.4 A m^{-3}. Unlike the prior study that shows improved electricity generation with the anolyte recirculation (Pham et al. 2008, Zhang et al. 2010) the present system was not obviously affected by the tested anolyte recirculation rates, most likely because of those recirculation rates are generally low. Significant improvement of the electricity generation was obtained with a high recirculation rate of 4-12 times of the anolyte volume per minute (Zhang et al. 2010), which is equivalent to 3,000 to 9,000 mL min^{-1} in the present system. Electrolyte recirculation has been identified as a major energy consumer in a bioelectrochemical system (Li and He 2015b, Zhang and He 2015) and thus low

recirculation rates are preferred from an aspect of low-energy operation. In fact, in our ongoing large MFC system (200-L), no anolyte recirculation is applied (data not shown).

The present MBER could effectively remove organic compounds (COD), through a staged removal in the anode, the cathode and the hollow-fiber membranes module. At the anodic HRT of 10 h and a recirculation rate of 90 mL min^{-1}, the anodic compartment removed 43.3±7.7% of total COD, and the cathode removed 48.2±7.2%; a final COD concentration in the membrane permeate was 4.0±3.8 mg L^{-1} , resulting in an overall COD removal efficiency of 98.4±1.5 % (Figure 7.2 B). The dripping cathode functioned as a secondary aerobic degradation process that polished the anode effluent by removing much of residual COD; such a removal would benefit the down-stream membrane module with less foulants. Thus, the membrane module acted mainly as a solid-liquid separation process without much biological reaction. Decreasing the anolyte recirculation rate to 50 or 20 mL min^{-1} actually enhanced the overall COD removal efficiency to 100.0±0.0%, benefited from the improved removal by the anode (TCOD removal of 74.9±0.6 or 72.4±18.4%). Such improvement might be related to the reduced oxygen leak into the anode through recirculation tubing at a lower rate, but the exact reasons are not clear at this moment and warrant further investigation. The turbidity of the membrane permeate was under 1 NTU.

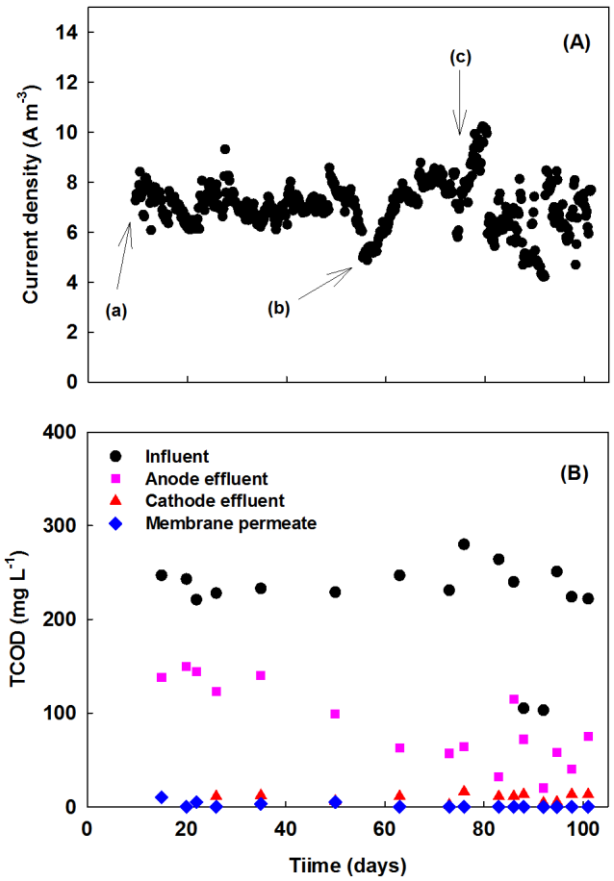

Figure 7.2 The performance of the MBER fed with synthetic wastewater: (A) Current density; (B) COD concentration in different liquid stream

7.3.2 Energy balance

The energy performance of the present MBER was evaluated through establishing an energy balance. The NER of the MBER was 0.004±0.001 kWh m^{-3} under the recirculation of 90 mL min^{-1} and the system would require 0.020 kWh energy to treat 1 m^3 of the synthetic solution; as a result, the overall energy balance was negative at -0.016±0.001 kWh m^{-3} (Figure 7.3). Decreasing the anolyte recirculation rate to 50 mL min^{-1} did not obviously change the NER but significantly decreased the energy consumption to 0.007

kWh m^{-3} , thereby achieving a final energy balance of -0.003±0.001 kWh m^{-3}. When the recirculation rate was further reduced to 20 mL min^{-1}, the NER was estimated to be 0.004±0.002 kWh m^{-3}, and the energy consumption was 0.001 kWh m^{-3}, which was only 5.0 and 14.3% of the two previous operational modes. Correspondingly, a slightly positive energy balance of 0.003±0.002 kWh m^{-3} was achieved. This result indicates that a low anolyte recirculation rate such as 20 or 50 mL min^{-1} could have been sufficient for substrate distribution in the anode chamber of the MBER, likely benefiting from its brush-containing space that has much room for liquid flow. Despite the positive energy balance at 20 mL min^{-1}, energy recovery was very low and must be further improved through adding more anode electrode materials (which could result in more impact of the anolyte recirculation rate on energy recovery), improving the catholyte catalysts, and optimizing the operating conditions (e.g., temperature). It is worth noting that the energy consumption due to backwashing for membrane fouling control was small and negligible in the energy balance calculation (estimated at 1.1×10^{-4} kWh m^{-3}). The energy consumption by the MBER is significantly lower than that of activated sludge (0.6 kWh m^{-3}(McCarty et al. 2011) , or aerobic MBRs (1.2-2.0 kWh m^{-3}(Martin et al. 2011)). The anaerobic MBRs (AnMBRs) could be energy positive, and it was estimated that a maximal 0.16 kWh energy can be produced to treat 1 m^3 wastewater by AnMBR (Smith et al. 2012); however, a strict

temperature control and proper strategies for extracting the dissolved methane will be important to maximize its energy recovery with biogas.

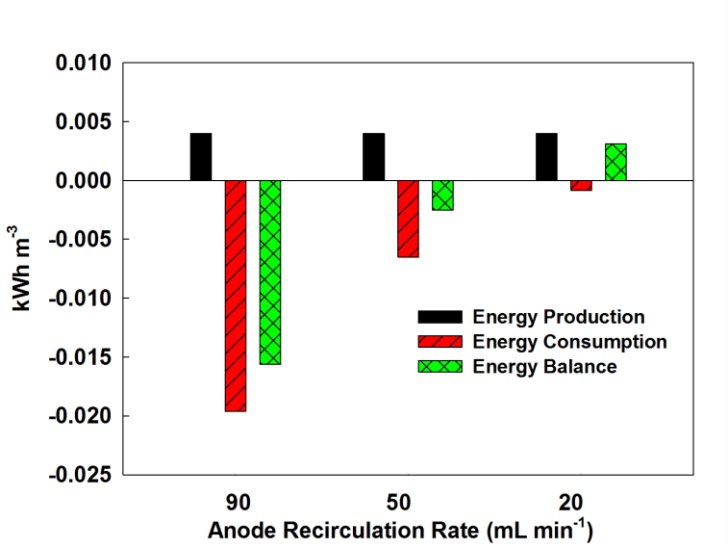

Figure 7.3 The energy production, consumption and balance of the MBER at different anolyte recirculation rates

7.3.3 Membrane performance

The TMP of the membrane module is shown in Figure 7.4 A, and the fouling control was conducted by membrane relaxation, backwashing, and offline cleaning. The offline cleaning was conducted by first applying soft brush to remove the attached foulants, and then rinsing the membrane surface with tap water until the cake layer mass was detached completely (based on visual judgment). The membrane module was connected to the MFC on day 12 of the operation under a 4-min work/1-min relax mode, and the serious fouling of the membrane was observed after only three days, when the TMP increased to 30 kPa on day 14, indicating a cake layer could accumulate rapidly by only applying a periodic relaxation to membrane. Offline cleaning was applied to reduce the TMP, which increased repeatedly in the subsequent weeks, which required offline cleaning on day 18 and 20.

From day 22, a regular backwashing flow at 2.5 mL min^{-1} (as double as membrane filtration flowrate) was applied for 1 min in every 30-min operation. This strategy has clearly delayed the TMP increase, which took about 10 days to reach 40 kPa on day 31, and after offline cleaning increased to 45 kPa on day 40. The frequency of backwashing was adjusted to 1 min in every 15-min permeation cycle and water flux was recorded from day 40 (Figure 7.4B). Such a change allowed the MBER to maintain its TMP under 40 kPa in the following 46 days without any offline cleaning. The water flux began to drop from 6 L m^{-2} h^{-1} (LMH) on day 40, due to the cake mass accumulation, to 2.8 LMH as the minimum on day 64. The TMP decrease and water flux increase on day 80 was related to the detachment of the cake mass due to the operational reasons.

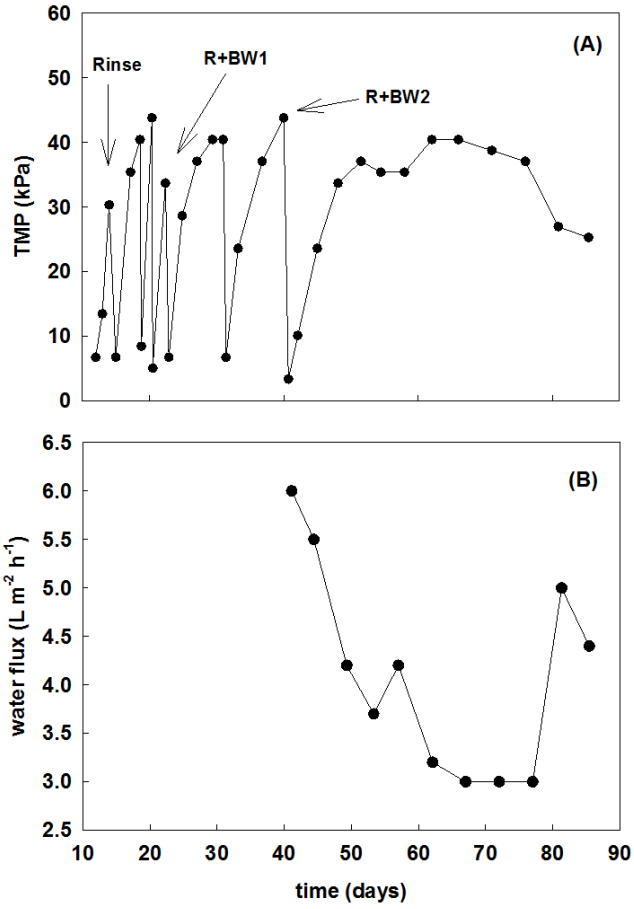

Figure 7.4 The variation of transmembrane pressure (TMP) (A) and water flux (B)

7.3.4 Model validation and prediction

The data used for parameter estimation were obtained under the experimental condition of varying either the anolyte COD concentration from 100 to 250 mg L^{-1}, or the anolyte flow rate from 1.3 to 2.1 mL min^{-1} (250 mg L^{-1} COD). The predicted current generation and organic concentration in the anode effluent were plotted along the experimental data in Figure 7.5. When varying the COD concentration, the model output of current generation generally followed the trend of experimental data that current generation was enhanced along with the increased substrate concentration (Figure 7.5 A). The relative root mean

square error (RMSE) showed that the simulated current generation was within 16.4% of their maximum value, affected by the fluctuation of experimental data. The model output of substrate concentration shared the same trend with the experimental measurement (Figure 7.5 B), with a relative RMSE of 36.9%, indicating large deviation existed between the simulation and the experimental data. Such a discrepancy can be from mismatch of current generation that at the early stage, the modeled current endured a sharp decrease and a temporal lagging period of bacteria growth could occur due to insufficient substrate supply; consequently, a lower COD concentration in the anode effluent was observed. The model output of the substrate concentration in the anode effluent began to increase as a response to the enhanced COD concentration in the influent, but overestimation was observed from the model simulation data, possibly due to the overestimated current generation from model simulation results with larger COD removal.

The model output of current generation affected by the anolyte flow rate had a high RMSE of 27.8%, because of the poor sensitivity of the MBER experiment (Figure 7.5 C). When the anolyte flow rate was changed from 1.3 to 2.1mL min^{-1}, the model current increased from 5.0 to 8.2 mA but the experimental data did not obviously respond. A similar phenomenon was reported in a model for microbial desalination cells (MDCs), suggesting that mathematical model has higher sensitivity to the change of substrate concentration when current generation is in a low range. Likewise, the experimental data of the COD concentration did not well respond to the change of the anolyte flow rate like that of the modeled value (Figure 7.5 D). The simulated substrate concentration shared a similar trend to the experimental data, with a relative RMSE of 32.1%. Enhancing the organic loading

rate (OLR) from 0.6 to 1.0 kgCOD m^{-3} day^{-1} by increasing the influent flowrate from 1.3 to 2.1 mL min^{-1} did not significantly change the COD concentration in the anode effluent, suggesting that more organics might have been consumed by the microorganisms other than electrogens at a higher COD loading rate. The modeled substrate concentration was lower than the experimental data, because of the overly estimated current generation.

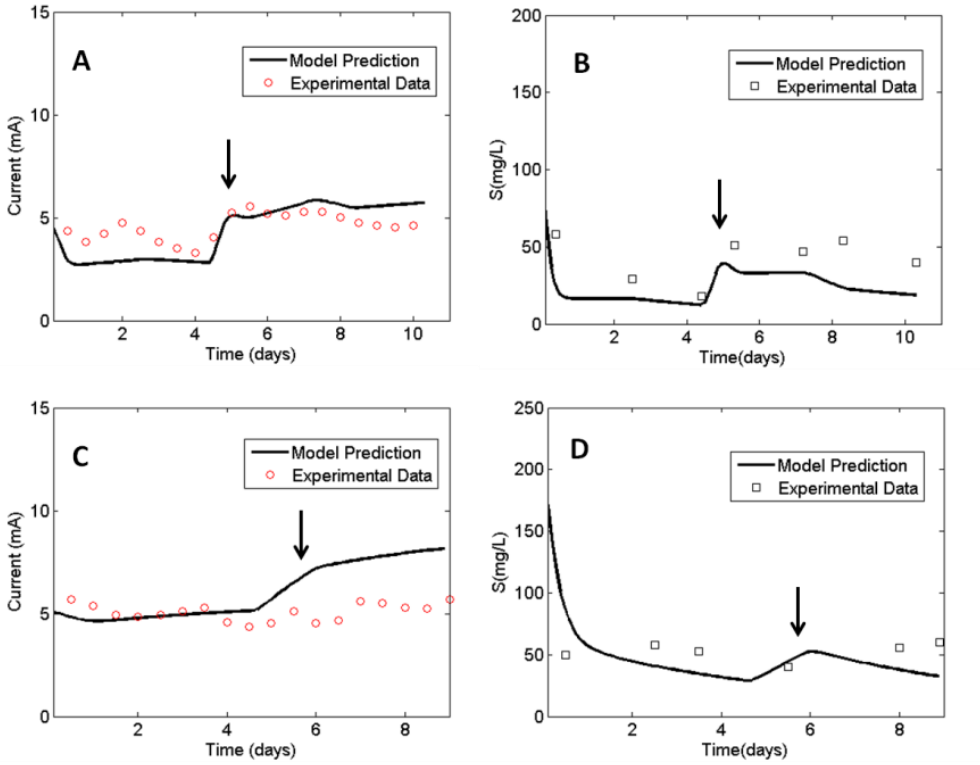

Figure 7.5 Model fitting under different testing conditions: (A) Current generation; (B) Substrate concentration in anode effluent by varying COD; (C) Current generation and (D) Substrate concentration in anode effleunt by varying feeding rate

The variation of TMP was also simulated and the model output could give a good prediction on TMP change (Figure 7.6). The model simulation has a relative RMSE of 16.0%, affected by inaccurate estimation of suspended solids concentration that could yield a deviated increase rate on membrane resistance. It is worth noting that membrane fouling is a consequence of a dynamic process, which includes both attachment and detachment of

the foulants. The attached foulants includes the suspended solids from the influent (from the MFC) and newly produced biomass within the membrane module; while the detachment occurs when physical fouling control such as air-bubble scrubbing or surface cross-flowing is provided. Water flux (J) and suspended solids (X) are two major components for simulating TMP (indicating membrane fouling) in the developed model, and result in a linear increase of TMP with time as shown in Figure 7.6.

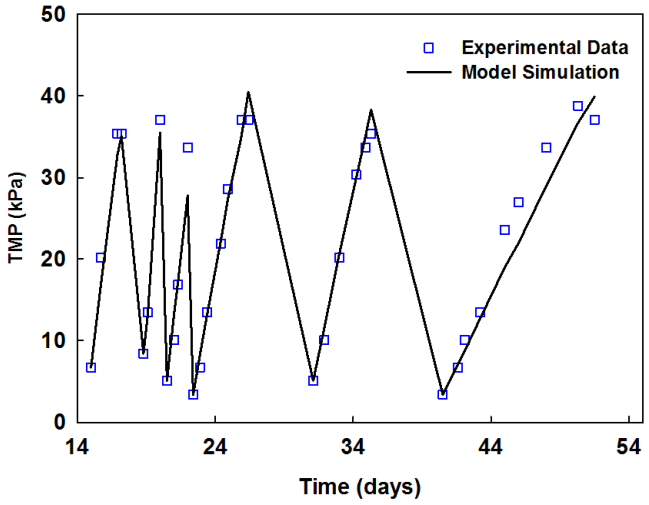

Figure 7.6 Model fitting of transmembrane pressure (TMP)

The model was used to predict the performance (current generation and COD removal) of the MBER affected by two factors, the influent COD concentration and the feeding rate of the anolyte (anodic HRT), both of which can affect the organic loading rate (OLR). It was found that current generation began to decline after the anodic HRT was extended (Figure 7.7 A) or influent COD was reduced (Figure 7.7 B). Insufficient organic supply for anodophillic bacteria was assumed to be a reason for such interactive effect. It also demonstrated that the anodic HRT has little impact on current generation after the influent

COD is beyond 2150 mg L^{-1}, indicating that the conversion rate of the substrate-to-electricity may have reached its maximum and additional substrate could not be converted to electricity. The relationship between current generation and organic loading rate (OLR) confirmed that the current generation could increase along with OLR in a logarithmic way with R^2 of 0.928 (Figure 7.7 C): current generation of 16.9 mA could be achieved after the OLR was increased to 11.4 kg COD m^{-3} day^{-1}, and further enhancing OLR had a marginal effect on current generation at a cost of worse organic removal performance. It is worth noting that to achieve same OLR, coupling high influent organic concentration with a longer anodic HRT could result in more current generation than that of low influent organic concentration with a shorter anodic HRT (Figure 7.7 D). For example, at an OLR of 2.4 kg COD m^{-3} day^{-1}, current generation of 10.7 mA could be achieved under the influent COD of 800 mg L^{-1} at an HRT of 8 h, but a higher current of 16.2 mA can be generated after the influent COD is changed to 1400 mg L^{-1} at HRT of 14 h (with the same OLR of 2.4 kg COD m^{-3} day^{-1}). The model indicated that such improvement could be related to more stimulated anodophillic bacteria activity.

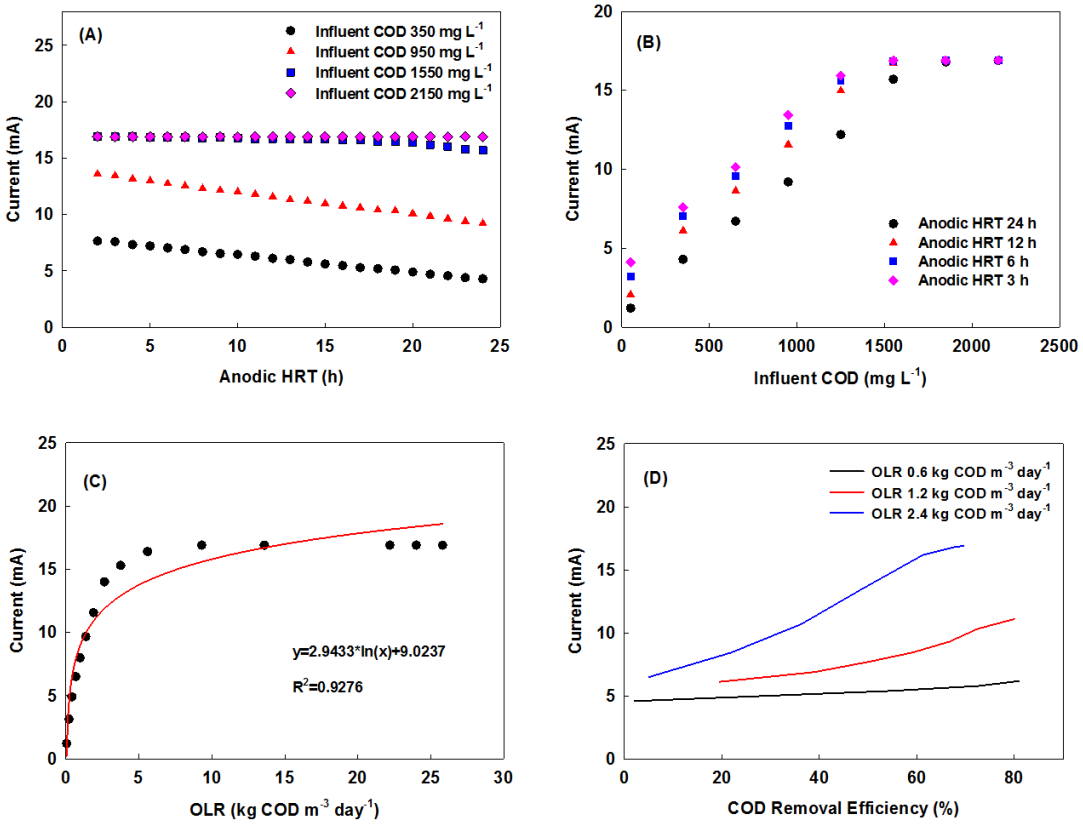

Figure 7.7 Model prediction for current generation affected by (A) Anodic HRT; (B) Influent COD; (C) Organic loading rate; and (D) COD removal efficiency

Table 7.1 Parameters for MBER electrical performance

Parameters	*Description*	*Value*	*Units*
F	Faraday constant	96,485	C mol^{-1}
R	Ideal gas constant	8.314	J K^{-1} mol^{-1}
T	Temperature	298.15	K
Y	Yield of anodophillic	4.44	mg-M mg-S^{-1}
Y_{CH4}	Methane Yield	0.3	mL CH_4 mg-S^{-1}
$q_{max,a}$	Maximum anodophillic reaction rate	5.32	mg-S mg-x^{-1} d^{-1}
$q_{max,m}$	Maximum methanogenic reaction rate	8.2	mg-S mg-x^{-1} d^{-1}
$\mu_{max,\,a}$	Maximum anodophillic growth rate	0.797	d^{-1}
$\mu_{max,\,m}$	Maximum methanogenic growth rate	0.1	d^{-1}
$K_{s,a}$	Half-rate constant of anodophillic	20	mg-S L^{-1}
$K_{s,m}$	Half-rate constant of methanogens	80	mg-S L^{-1}
m	Electrons transfer per mol of mediator	2	mol^{-1} mol mediator $^{-1}$
γ	Mediator molar mass	663,400	mg-M mol mediator^{-1}
M_{total}	Mediator fraction	0.05	mg-M mg-x^{-1}
K_M	Mediator half rate constant	0.01	mg-M L^{-1}
$K_{d,a}$	Decay rate of anodophillic microorganism	$0.02*\mu_{max,a}$	d^{-1}
$K_{d,m}$	Decay rate of methanogenic microorganism	$0.02*\mu_{max,m}$	d^{-1}
$X_{max,a}$	Anodophillic biofilm space limitation	512.5	mg-x L^{-1}
$X_{max,m}$	Methanogenic biofilm space limitation	525	mg-x L^{-1}
K_x	Steepness Factor	0.04	L mg-x^{-1}
R_{min}	Minimum internal resistance	31	Ω
R_{max}	Maximum internal resistance	2000	Ω
E_{min}	Minimum open circuit potential	0.1	V
E_{max}	Maximum open circuit potential	0.7	V
K_R	steepness factor correction coefficient	0.0818	L mg-x^{-1}

Table 7.2 Parameters for membrane performance

Parameters	*Description*	*Value*	*Units*
η	Water apparent viscosity	0.00089	Pa.S
A	Membrane surface area	0.013	m^{-2}
ρ	Specific cake resistance	100000000	$m\ g^{-1}$
α	Coefficient for TMP correction	1 (NO BW) 0.7 (BW1) 0.3 (BW2)	
Y	Yield coefficient of the substrate consumption	1.2	mg-Mmg-S^{-1}
$\mu_{s,max}$	Maximum growth rate	0.12	d^{-1}
J_{air}	Air crossflow	0	$m^3\ m^{-2}\ d^{-1}$
K_s	Half saturation of substrate	10	$g\ m^{-3}$
K_{air}	Half saturation of airflow	$4.6*10^{-5}$	$g\ m^{-3}$
β	Resistance of detachable cake by air crossflow	0.01	m^{-1}
Q_{out}	Outflow	0.0018	$m^3\ d^{-1}$
V	Volume of membrane module	0.00015	m^3

Note: **BW means backwashing; BW1 means 1-min backwashing in every 30-min operation; BW2 means 1-min backwashing in every 15-min operation.**

7.3.5 Perspectives

This is an early attempt to integrate experimental results with a mathematical model to optimize an MBER system. The present MBER is different from the prior MBERs in several aspects: (1) the external installation of the membrane module (through one-direction liquid flow connection) improves the flexibility of membrane module and decreases the effects of its operation/cleaning on the MFC unit; (2) the dripping method for supplying the cathode effluent can bring dissolved oxygen to the membrane module for additional aerobic treatment, which will be important when organic loading rate becomes higher; (3) aeration is eliminated from the cathode with its special configuration exposing the cathode surface to the air; and (4) the present MBER could theoretically achieve energy neutral. Both the findings of the influence of the anolyte recirculation rates and the mathematical model developed here can provide more insightful information on optimizing

MBER system. Future studies will investigate the improvement of energy recovery from organic conversion, possibly through adding the anode electrode materials and optimizing the system operating conditions such as temperature. Despite the low fouling of the present system, membrane fouling will be expected during a long-term operation with actual wastewater, and thus appropriate anti-fouling methods will still be needed. One of the interesting approaches for fouling control is to use in situ generated hydrogen peroxide for reducing fouling, and this will require precise control of oxygen reduction (via two electron reduction pathway for hydrogen peroxide production) on the cathode. In addition, system scaling up will remain a great challenge for developing MBERs.

7.4 Conclusions

This study has presented an MBER consisting of an MFC with an external membrane module, and the performance of this system was demonstrated through both the experiments and mathematical modeling. The external configuration allowed more flexibility in membrane cleaning without affecting the MFC unit. The anolyte recirculation was a major energy consumer in this system, and by decreasing the anolyte recirculation to 20 mL min^{-1}, the MBER could potentially be a net energy producer. Mathematical model was validated with experimental data and predicated that current generation by the MBER could reach a plateau of 16.9 mA after the OLR is increased to 11.4 kgCOD m^{-3} day^{-1}. The model may be further improved by considering heterogeneous substrate and microbial distribution.

CHAPTER 8

Investigation of Multiphysics in Tubular Microbial Fuel Cells by Coupled Computational Fluid Dynamics with Multi-Order Butler-Volmer Reactions

(This section has been published as: Zhao, L., Li, J., Battaglia, F. and He, Z.* (2016) Investigation of Multiphysics in Tubular Microbial Fuel Cells by Coupled Computational Fluid Dynamics with Multi-Order Butler-Volmer Reactions. **In Press.** DOI: http://dx.doi.org/10.1016/j.cej.2016.03.110)

Abstract

Microbial fuel cells (MFCs) are considered as an emerging concept for sustainable wastewater treatment with energy recovery. The anode of an MFC plays a key role in conversion of organic compounds to electricity, and thus understanding the multiphysics within the anodic compartment will be helpful with MFC optimization and scaling-up. In this study, a multi-order Butler-Volmer reaction model was proposed to compute organic consumption and energy recovery. Computational fluid dynamics (CFD) was applied to analyze the hydrodynamics and species transport inside the anodic compartment. By comparing to the experimental data, the reaction order of anodic surface reaction was determined as 6.4. The reaction model gave good agreement with experimental data when the influent sodium acetate was 1.0, 0.5 and 0.3 g L^{-1} at anodic hydraulic retention time (HRT) of 10 h, indicating the effectiveness of this multi-order Butler-Volmer reaction model. When the influent sodium acetate was 0.2 g L^{-1} or the anodic HRT was 15 h, the model exhibited discrepancies in predicting current generation and effluent chemical oxygen demand (COD) concentration, likely due to the interference of the decayed biomass and the activities of non-electroactive bacteria. The results of this study have demonstrated the viability of coupling CFD with a multi-order reaction model to understand the key operating factors of an MFC.

8.1 Introduction

Microbial fuel cells (MFCs) have emerged as a promising approach for sustainable wastewater treatment with bioenergy recovery (Li et al. 2014d). In MFCs, organic materials are biologically degraded and electrical energy is produced through interaction between microbes and solid electron acceptors (Logan et al. 2006b). Various configurations of MFCs have been developed to optimize organics removal, energy recovery and operational flexibility (He et al. 2006, Hernández-Fernández et al. 2015, Liu et al. 2004, You et al. 2006). Among these proposed configurations, tubular MFC systems have been studied in great detail because of its potential advantages in microbial and substrate distribution, short distance between anode and cathode electrodes, and large surface area of separator materials (Jacobson et al. 2015, Rabaey et al. 2005, Sun et al. 2015, Zhang et al. 2010). Interdependent multiphysics processes are present in tubular MFCs. For example, the hydrodynamics of electrolyte flow in the anodic chamber plays a key role in the substrate transport with associated effects on the activation overpotential distribution and chemical reactions, and vice versa. The activation overpotential and chemical reactions could contribute to the substrate consumption and transport, thereby impacting the flow field. Therefore, proper understanding of multiphysics phenomena in tubular MFCs can help guide the design and operation of such systems.

Mathematical modeling is a powerful tool to complement experiments and can be used to further understand the key processes that cannot be easily measured via experiments. Several models have been developed for studying metabolic pathway in anaerobic mixed culture fermentation and MFCs (González-Cabaleiro et al. 2015, Luo et al. 2015, Ortiz-Martínez et al. 2015), and among them, computational fluid dynamics (CFD) can be used

to numerically predict fluid flow, including mass transfer and reactions by solving various advection-diffusion equations. The application of CFD techniques in studying MFCs is still limited with very few publications in the past ten years. An early study combined MATLAB, COMSOL and a self-developed Java code to study the macro-scale homogeneous concentration evolution of soluble substrates and biomass in bulky liquid, and a micro-scale heterogeneous two dimensional biofilm model (Picioreanu et al. 2010). In this model, liquid velocity was calculated from the Navier-Stokes equations within a laminar flow regime, and it was found that localized proton accumulation was a rate-limiting factor on MFC output, and porous bio-electrode did not necessarily generate higher current as long as convective flow was absent. Unfortunately, those findings were not substantiated by any experimental results. Numerical simulations using CFD-ACE+ demonstrated in a Y-shape mixer with inset cylinders, a lower aspect ratio (micro-channel depth-to-width) and larger inlet Reynolds number ratio (Reynolds number ratio based on inlet streams) could enhance flow mixing efficiency, due to the increased side wall effect and shear stress (Wang et al. 2011a). COMSOL Multiphysics was used to simulate laminar incompressible fluid flow in an MFC and demonstrated that enlarged biofilm attachment and increased shear rate within helical flow pathways accounted for the enhanced MFC performance (Kim et al. 2012). Subsequently, three different helical flow channels (1.5, 5.4 and 10.8 mm, based on the spacing between helices) were experimentally investigated with a maximum power density of 11.63 W m^{-3} achieved in the smallest channel, which was confirmed by CFD modeling using a two layer k-ε eddy viscosity turbulence model (Michie et al. 2014). A recent study simulated a cubic-shaped MFC containing twelve different internal structures (*e.g.,* triangular/rectangular shape, number, length and

upward/downward orientation) using ANSYS CFX. (Kim et al. 2014a). Numerical results demonstrated that the maximum power density of 0.54 W m^{-2} could be achieved with the largest working space of 0.57 m^2. The CFD prediction using ANSYS Fluent 12.1 revealed that better water distribution and biomass attachment could be developed with granular graphite and stainless steel meshes due to the minimized occurrence of preferential flow ways (Vila-Rovira et al. 2015).

Although the aforementioned CFD-based MFC studies have provided useful information to understand MFC systems by analyzing micro- or macro-scaled flow conditions, there are still limitations with the CFD modeling that can be further addressed. For example, analyzing flow conditions alone fails to provide any information on activation overpotential and organic distribution, which can determine anodic surface reaction rate. A simplified electron transfer mechanism (e.g., external mediators) could be applied to electrochemically-active bacteria, which exists in a complex microbial community within the anodic chamber. Furthermore, time-dependent experimental data are essential to validate the model formulation. Herein, a coupled CFD and multi-order Butler-Volmer reaction model was proposed and validated to address some of the limitations, including a simple electron transfer mechanism, and an interaction between heterogeneous substrate and overpotential distribution on the anode surface. A direct contact electron transfer mechanism between microbes and the electrode surface was applied instead of an external mediator, because adding external mediator would not be feasible in wastewater treatments. Heterogeneous species distribution and electricity generation was predicted using the Butler-Volmer equations to include species concentration and activation overpotential on reaction rates. Real time-dependent experimental results were used for

model validation. The results of this work were expected to demonstrate the viability of using a high-fidelity CFD approach to model the complex reaction physics in a tubular MFC.

8.2 Materials and Methods

8.2.1 MFC setup and operation

The MFC was constructed as a tubular reactor (32 cm long and 3.8 cm inner diameter) made of anion exchange membrane (AEM-Ultrex AMI 7001, Membrane International. Inc, Glen Rock, New Jersey, USA), as shown in Fig 8.1. Carbon cloth (Zoltek Corporation, St. Louis, MO, USA) was used as the material for both the anodic and cathodic electrodes. Before use, the carbon cloth was soaked in acetone solvent overnight and then heated for 30 min at 450 $^{\circ}$C. The finished anode electrode (with effective surface dimensions of 22 cm-long and 2.9 cm-diameter) was installed along the inner surface of the AEM tube and supported by a plastic mesh, resulting in a net anodic liquid volume of 350 mL. The cathode electrode (23 cm × 12 cm) was coated with Pt/C powder (Etek, Somerrest, NJ, USA) at a loading rate 0.3 mg Pt cm^{-2}, and wrapped the AEM tube. The anode and cathode electrodes were connected to a 10 Ω resistor.

The MFC was operated at room temperature. Its anodic compartment was inoculated with anaerobic sludge from the Peppers Ferry Wastewater Treatment Plant (Radford, VA, USA) and operated with sodium acetate in a batch mode. During the start-up period, the external resistance was changed from 1000 to 10 Ω in a stepwise approach. After start-up, the system was fed with a synthetic solution containing (per L of tap water): sodium acetate 1 g (otherwise stated); NH_4Cl 0.15 g; NaCl 0.5 g; $MgSO_4$ 0.015 g; $CaCl_2$ 0.02 g; KH_2PO_4

0.53 g; K_2HPO_4 1.07 g; and 1 mL trace elements (He et al. 2006). No recirculation was applied to the anolyte, but the catholyte (50 mM phosphorus buffer solution) was recirculated at 5 mL min^{-1}. The catholyte was stored in a separate container (beneath the MFC reactor) and pumped to rinse the cathode surface constantly. The flowrate of the anolyte was controlled by a peristaltic pump to achieve the desired hydraulic retention time (HRT) of 10 h (otherwise stated). The Reynolds number is 0.42 based on the inlet velocity of 1.44×10^{-5} m s^{-1}.

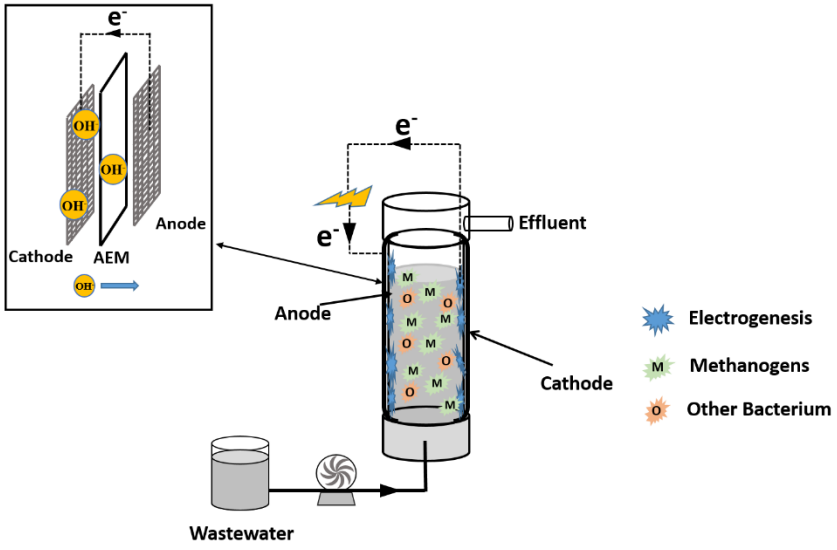

Figure 8.1 A schematic of a tubular microbial fuel cell (MFC) system used for developing CFD-multi-order Butler Volmer reaction model. Inset: enlarged arrangement of electrode and anion exchange membrane

8.2.2 Measurement and analysis

The MFC voltage was recorded every 5 min by a digital multimeter (2700, Keithley Instruments, Cleveland, OH). The pH was measured using a benchtop pH meter (Oakton Instruments, Vernon Hills, IL, USA). The conductivity was measured by a benchtop conductivity meter (Mettler-Toledo, Columbus, OH, USA). The concentration of chemical

oxygen demand (COD) was measured by using a colorimeter according to the manufacturer's procedure (Hach DR/890, Hach Company, Loveland, CO, USA).

8.3 Model formulation

8.3.1 Governing equation

For steady-state, laminar, incompressible flow, the continuity equation is

$$\nabla \cdot \vec{V} = 0 \tag{8.1}$$

where $\vec{V}$ is the velocity vector. The corresponding momentum equations for a Newtonian fluid are

$$\vec{V} \cdot \nabla(\rho\vec{V}) = -\nabla p + \nabla(\mu\nabla\vec{V}) + \rho\vec{g} \tag{8.2}$$

From left to right, the terms represent the momentum change in a control volume due to advection, pressure gradients, viscous diffusion, and gravity. In Eq. (8.1) and (8.2), the fluid properties, i.e., density ρ and dynamic viscosity μ, are calculated as volume-weighted mixture properties. However, due to the negligible amount of soluble substances and biomass in the bulk liquid, it is reasonable to assume that the mixture properties are equal to those of liquid water.

The heterogeneous species distribution is obtained by solving the species transport equation. For species *k*, the steady-state transport equation is given as:

$$\vec{V} \cdot \nabla C_k = D_k \nabla^2 C_k + S_k \tag{8.3}$$

The terms in Eq (3), from left to right, represent the molar concentration change in a control volume due to convection, diffusion and reactions, respectively. The reaction term can be further expressed as the summation of a series of reactions:

$$S_k = \sum_i r_{k,i} \tag{8.4}$$

where $r_{k,i}$ represents the production/consumption of species k in reaction i.

Because the flow under consideration is very laminar with a Reynolds number less than 1, the flow is assumed axisymmetric. The computational domain is discretized using a rectangular mesh with dimensions of 0.22 m × 0.145 m. A Dirichlet boundary condition is applied to the inlet with a fixed velocity (1.44×10^{-5} m s^{-1} for the base case) and sodium acetate concentration (0.5 g L^{-1} for the base case). The anode surface is modeled as a no-slip wall with surface reactions accounting for the mass flux. Fully developed flow, which implies zero gradient of velocity and species, is adopted at the outlet with a gage pressure of zero.

Fixed point iteration is used to solve the nonlinear system described using Eqs. (8.11) to (8.18), and is easy to implement into CFD calculations. However, the solution procedure requires strong under relaxation to ensure convergence. A finite volume method is used to discretize the governing equations using the commercial code ANSYS Fluent 15.0. User Defined Functions (UDF) are employed to incorporate correlations for the reaction rates.

8.3.2 Reaction models

In an effort to reduce the associated uncertainties in modeling bacterial activities, a two-population bacterium (methanogens and electrochemically-active microorganisms) community is assumed in the anode compartment.

8.3.2.1 Volumetric Reactions

Given the fact that various populations of bacteria exist in the bulk liquid, it is not easy to model each bacteria population separately. For simplicity, the microbes in the bulk liquid are simplified as the methanogens, which act as the catalysts in the methanogesis process, where

$$Acetate \xrightarrow{Methanogens} CH_4 + CO_2 \tag{8.5}$$

The methanogens are assumed to be uniformly distributed in the bulk liquid, and in this case the conventional Monod-limitation equation is applied to approximate the reaction rate as:

$$r_v = r_{v,0} \frac{C_{ac}}{C_{ac}+K_{ac}} \tag{8.6}$$

8.3.2.2 Anodic Reaction

Electrochemically-active bacteria are assumed to be evenly distributed on the anode surface. A generalized oxidation reaction catalyzed by electrochemically-active microorganisms (electrogens) is proposed (Logan et al. 2006a) and represented as:

$$\mathrm{CH_3COO^-} + 4\mathrm{H_2O} \xrightarrow{electrogens} 2\mathrm{HCO_3^-} + 9\mathrm{H^+} + 8e^- \tag{8.7}$$

Equation (7) is a chain-reaction and involves a series of sub-reactions. Based on the theory of reaction kinetics, the reaction rate of such a chain-reaction is determined in the following form:

$$r_a = kC_{ac}^{\gamma} C_{H_2O}^{\beta} \tag{8.8}$$

where superscripts γ and β are not necessarily equal to the stoichiometric coefficient, but the summation of γ and β defines the reaction order. The sub-reactions involved are regarded as the elementary equations, whose reaction orders equal the summation of the

stoichiometric coefficients of reactants. Focusing on the acetate removal and current generation, it is reasonable to use such a generalized reaction and corresponding reaction rate formula. In addition, given that the concentration of liquid water is constant, the reaction rate is then solely related to the concentration of acetate:

$$r_a = kC_{ac}^{\gamma} \tag{8.9}$$

where k is the rate constant and can be calculated as the function of activation overpotential η_{act}, temperature T and transfer coefficient α from Butler-Volmer equation (Picioreanu et al. 2007):

$$k = r_{a,0}(\exp\left(\frac{\alpha F\eta_{act}}{RT}\right) - \exp(\frac{(\alpha-1)F\eta_{act}}{RT})) \tag{8.10}$$

Combining Eq. (9) and (10) provides an estimate of the reaction rate of the anodic reaction:

$$r_a = r_{a,0}C_{ac}^{\gamma}(\exp\left(\frac{\alpha F\eta_{act}}{RT}\right) - \exp(\frac{(\alpha-1)F\eta_{act}}{RT})) \tag{8.11}$$

The relationship between reaction rate and current density is given:

$$i = nFr_a \tag{8.12}$$

where *n* is the stoichiometric coefficient of electrons in Eq (7) and *n*=8.

8.3.3 Electricity Generation

The generated current can be obtained by integrating current density on the entire anode surface:

$$I = \int idA \tag{8.13}$$

According to Ohm's Law, cell voltage is determined when the current passes through electrical resistance:

$$V = IZ_{ext} \tag{8.14}$$

The cell voltage is also the difference between the open circuit voltage (OCV) and the potential loss through internal resistance,

$$V = \mathrm{OCV} - IZ_{int} \tag{8.15}$$

where OCV is the theoretical potential difference between the anodic and cathodic electrodes: $OCV = E_c - E_a$ (8.16)

It should be noted that because the cathodic performance is beyond the scope of this study, the cathodic potential (i.e., oxygen reduction reaction) is fixed at 0.3 V (vs. Standard Hydrogen Electrode). However, the anodic potential can vary due to the concentration deviation. Activation polarization occurs to overcome the energy barriers when electrons are transferred from electrode donors to acceptors, *e.g.* acetate to anode. Hence, the anodic potential is given as:

$$E_a = E_{a,0} - \frac{RT}{8F}\ln\left(\frac{C_{ac}}{C_b^2 C_p^9}\right) + \eta_{act} \tag{8.17}$$

In summary, cell voltage can be represented as the summation of standard potential and irreversible losses,

$$V = E_c - E_{a,0} + \frac{RT}{8F}\ln\left(\frac{C_{ac}}{C_b^2 C_p^9}\right) - \eta_{act} - IZ_{int} \tag{8.18}$$

The internal resistance (Z_{int}) is constant due to the negligible resistance of the conducting wires and high solution conductivity. From Eq.18, concentration loss (third term on the right side) is mainly governed by organic strength. C_b and C_p are assumed to be constant due to the strong buffer solution in bulk liquid.

8.3.4 Model Correlations

Each component in the current modeling scheme is shown graphically in Fig 8.2. Any perturbation in the system input, for example the external resistance, HRT, organic feeding rate, and ambient temperature, will be directly reflected in the system output, *e.g.*, the substrate distribution, velocity field, potential distribution and electricity generation. Thus, the multiphysics processes involving hydrodynamics, mass transport, potential distribution and chemical reactions will be dynamically simulated.

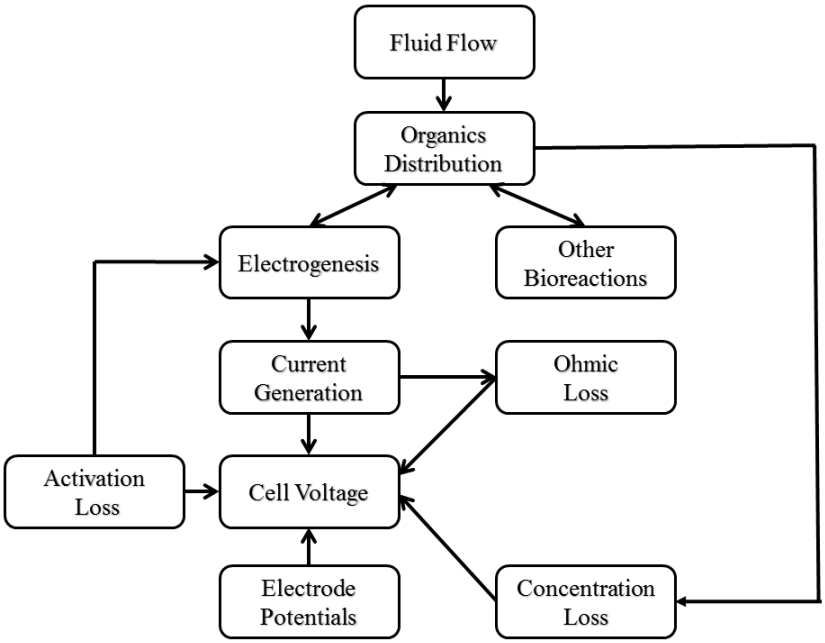

Figure 8.2 Modeling scheme connecting the reaction components

8.3.5 Determination of Reaction Order

As described in Section 8.3.2, Eq. 8.7 is actually a chain-reaction consisting of a series of elementary reactions due to the associated biochemical reactions occurring within the anodic compartment. The overall process is represented by a multi-order Butler-Volmer reaction model, whose most important parameter is the reaction order, as it correlates the

species distribution to both organic removal and electricity generation. By definition, the reaction order (γ) should equal the exponential number of the sodium acetate concentration in the reaction rate expression (Eq. 8.9). Thus, the reaction order could be determined either theoretically or experimentally. The theoretical reaction order can be calculated by combining reaction rates of each elementary reaction that comprise the overall acetate oxidization. However, the elementary processes, especially those occurring inside the microbes, are so complicated that the complete reaction path of the acetate oxidization is not well understood yet.

Another approach is to use the experimental data to find the reaction order. The simplest way to determine γ is by evaluating the reaction rate at different sodium acetate concentrations, while fixing other parameters, but this is not feasible experimentally. The acetate concentration cannot be measured on the anode surface experimentally, and it is not feasible to measure organic concentration on each single point on the anode surface without affecting normal operation. The activation overpotential is not constant along with the anode surface. Due to the heterogamous distribution of acetate on the anode surface, the concentration loss in Eq. 8.17 also varies. Correspondingly, the activation overpotential could be different at each single point on the surface area, because electrical potential should be identical throughout the anode surface. Rate constant *k*, another important parameter to determine reaction rate, is controlled by the value of activation overpotential (Eq. 8.11). Hence, because of the inaccessibities to acetate concentration and activation overpotential from anode surface, an alternative way should be attempted to learn the reaction order value.

Implicitly, the reaction order can be determined from numerical data by fitting to experimental data obtained from the polarization test. According to Eq. 8.13-8.18, by varying the external resistance, the activation overpotential will be changed too. Consequently, the surface reaction rate (Eq. 8.11) needs to be adjusted to fit this operational condition. It should be noted that the surface reaction acts as a boundary condition in species transport, and the species distribution within the anodic compartment is also changed. Eventually after a new equilibrium state is reached, the system will yield a different current generation, which is proportional to the surface reaction rate. Therefore, although implicit, the influence of the acetate concentration on the surface reaction rate could be reflected from the polarization test. A parameter estimation procedure was implemented to determine the reaction order (Stein et al. 2012, Zeng et al. 2010). The reaction order can be determined by gradually increasing the reaction order from unity to higher values and comparing the corresponding numerical data to the experimental polarization curve until there is an optimal fitting with a minimal root mean square deviation (RMSD).

8.4 Results and discussion

8.4.1 Determination of reaction order from polarization test

The results of the polarization test show that the current generation decreased from 27.3 to 4.8 mA after the external resistance was changed from 1 to 100 Ω sequentially, as shown in Fig. 8.3. By fitting an equation to the experimental polarization curve, the reaction order γ was estimated to be 6.4. The reaction order of 6.4 was used in the CFD simulations and the results are also shown in Fig. 8.3 as a symbol, with the average relative error of 7.4% between the experimental data and numerical predictions. In classical reaction kinetics, the

underlying assumption that chemical reactions are triggered by collisions of activated molecules implies that the reaction order is usually below 3, as the chance of more than 3 molecules colliding simultaneously is rare. However, this does not necessarily contradict with the curve-fitted reaction order of 6.4 in the current study. On one hand microbial reaction kinetics are primarily dominated by the microbial metabolism and the electrons are generated through an NADH-NAD^+ cycle and transferred to the electrode surface via outer membrane cytochromes (Lovley 2008). The reaction order of 6.4 also proves the correctness of the prior assumption that the anodic reaction is actually a chain reaction. On the other hand, the reaction order of 6.4 integrates the effects of concentration of both acetate and bacterium on reaction rate. A previous study showed the reaction rate could be determined by substrate and biomass concentration simultaneously (Zeng et al. 2010) of the form:

$$r_a = r_{a,0} \exp\left(\frac{\alpha F}{RT}\eta_{act}\right)\frac{C_{ac}}{C_{ac}+K_{ac}}X \tag{8.19}$$

where X represents the concentration of biomass. The transportation, production and consumption of biomass can be solved by adding another convective-diffusion equation into the governing equations. However, the concentration of biomass cannot be easily quantified from the experiment (in an attached biofilm system). Alternatively, a power law relationship $X \sim C_{ac}^n$ is assumed to eliminate the dependence of the reaction rate on biomass concentration because theoretically, biomass is inclined to accumulate in higher substrate regions. Equation 8.19 can be rewritten as:

$$r_a = r_{a,0} \exp\left(\frac{\alpha F}{RT}\eta_{act}\right)\frac{C_{ac}^{n+1}}{C_{ac}+K_{ac}} \tag{8.20}$$

which is the multi-order Butler-Volmer equation in the present study. The estimated reaction order will be used in the following validation tests.

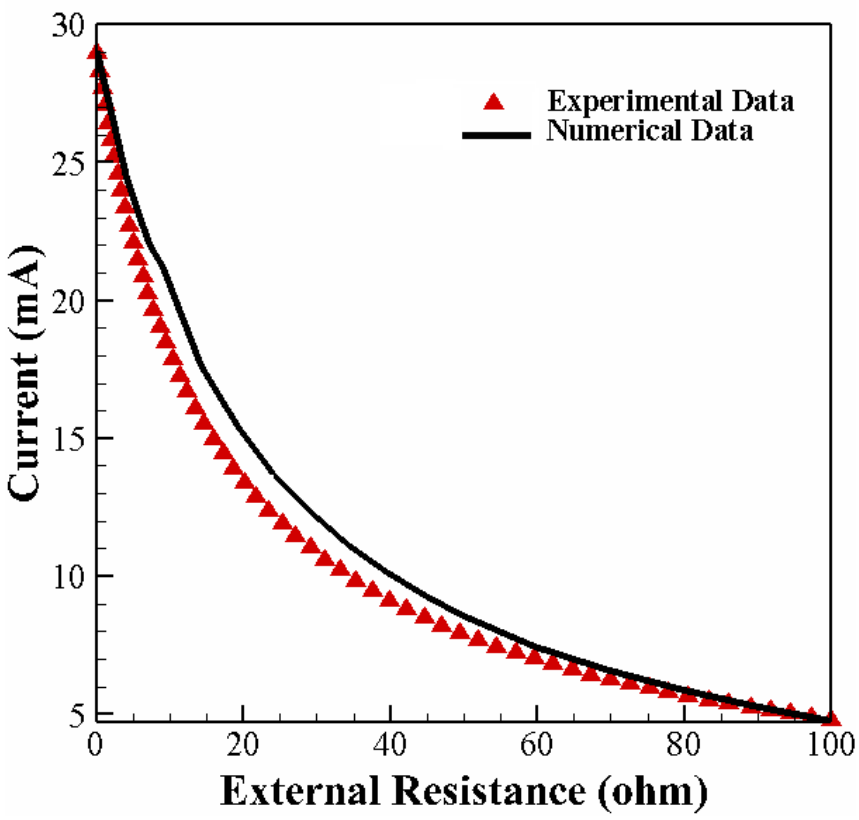

Figure 8.3 Experimental polarization curve and reaction model data for current generation under varied external resistance

Table 8.1 Model parameters and values

Parameters	Description	Value	Unit
D_{ac}	Mass diffusivity of acetate	7.523×10^{-9}	$m^2\ s^{-1}$
E_c	Cathode potential	0.3	V
$E_{a,0}$	Standard potential of anode	0.187	V
C_b	Bicarbonate concentration	0.0012	$kmol\ m^{-3}$
C_p	Proton concentration	1×10^{-7}	$kmol\ m^{-3}$
K_{ac}	Half saturation coefficient	7.3×10^{-5}	$kmol\ m^{-3}$
$r_{a,0}$	Anodic reaction constant	7.0×10^{5}	
$r_{v,0}$	Volumetric reaction constant	1.0×10^{-7}	
Z_{int}	Internal resistance	20	Ω
Z_{ext}	External resistance	10	Ω
α	Transfer coefficient	0.61	
γ	Reaction order	6.4	

8.4.2 Grid resolution study

To determine if the predictions are grid-independent, three grid resolutions (37 × 110, 73 × 220, and 145 × 440) are simulated and predictions of the acetate concentration and activation overpotential along the anodic surface are presented in Fig. 8.4 A and C. With increasing grid resolution, the acetate concentration and activation overpotential slightly decreased with average relative error lower than 0.3%. However, the average relative error is still inconclusive. To quantitatively specify the numerical uncertainties and mathematical correctness of the current model, the grid convergence index (GCI) (Celik et al. 2008, Roache 1994) was evaluated for the same grid resolutions (Fig. 8.4 B and D). The error bar denotes the possible range of exact numerical solution. Clearly, the numerical solution using the fine mesh falls within the error bars with the average GCI less than 0.1%.

Hence, the results from the grid resolution study indicate that a resolution of 145 × 440 is sufficient for the CFD simulation.

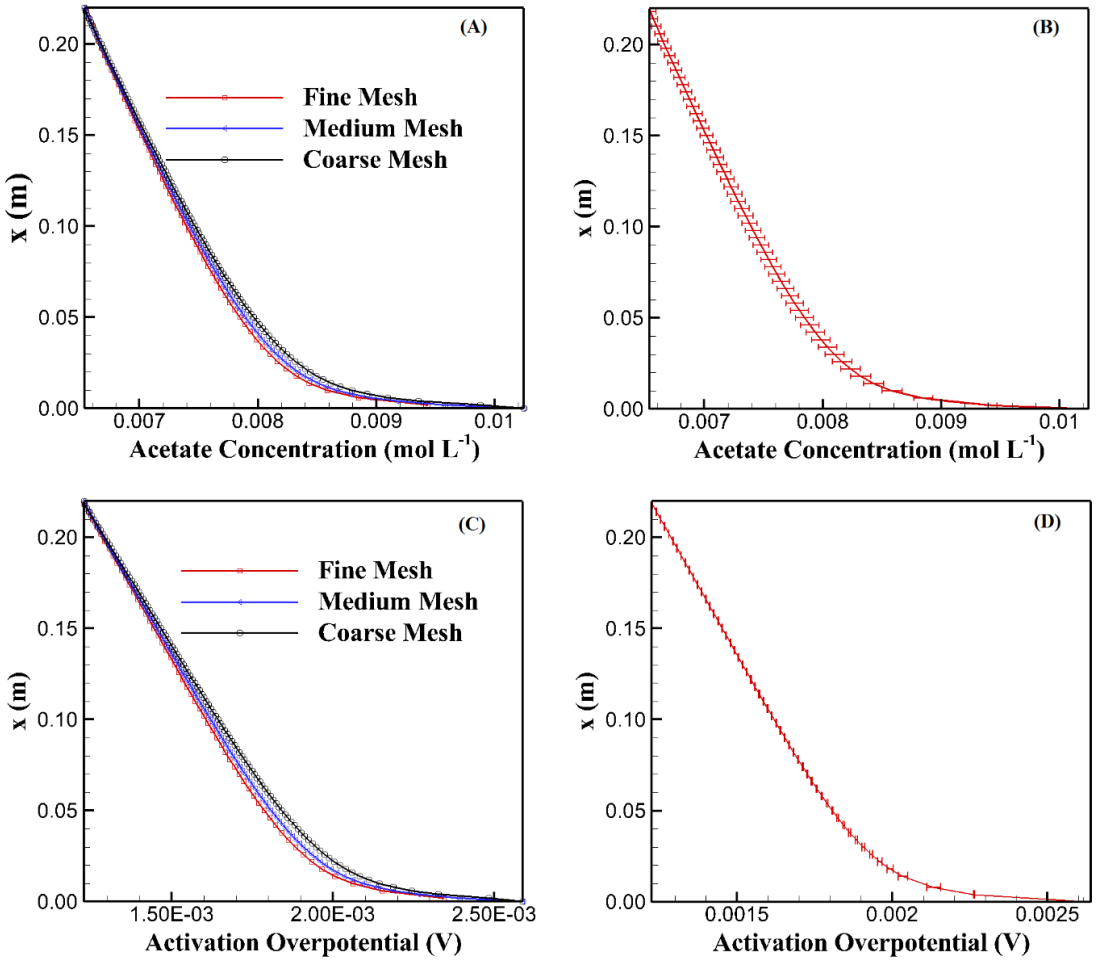

Figure 8.4 Grid independent study for (A) acetate concentration using three grid resolution; (B) error bars on acetate concentration; (C) activation overpotential three grid resolution and (D) error bars on activation overpotential

Table 8.2 Mean relative error for different grid resolution

	Coarse Mesh	Medium Mesh
Acetate Concentration	0.2%	0.1%
Activation Overpotential	0.06%	0.09%

Table 8.3 Mean GCI for different grid resolution

	Medium Mesh	Fine Mesh
Acetate Concentration	0.8%	0.8%
Activation Overpotential	0.5%	0.4%

8.4.3 Reaction model validation

Two independent operations were carried out to further validate the reaction model with different organic concentrations and flow rates of the influent solution. The operating parameters remained unchanged from Section 8.4.2 except for the target ones being studied.

The first test reduced the influent sodium acetate concentration in three steps from 1.0 to 0.5 to 0.3 to 0.2 g L^{-1} sequentially at an anodic HRT of 10 h. Figures 8.5 A and B present the experimental data and CFD predictions for current generation and total COD concentration in the effluent, respectively. In general, the CFD reaction model predictions for electricity generation were in good agreement with the experiments, indicating the effectiveness of the multi-order Butler-Volmer reaction model. However, at the lowest influent sodium acetate of 0.2 g L^{-1}, a discrepancy on the effluent COD occurred between the numerical and experimental data, which might be related to the low sodium acetate concentration from the influent. The CFD model calculated the effluent COD solely based on the residual sodium acetate by neglecting the decayed biomass, but the effects of the decayed biomass could become more significant when the influent organics are low. The decayed biomass could potentially be used as substrates and/or remain in the effluent, resulting in higher COD concentrations. The time scale of such a decay-conversion process

would play an important role in understanding its influence on the model prediction and warrants further investigation. Moreover, the slight discrepancy on current generation might result in an overestimation of COD removal.

Contour plots of the influent organic concentrations are shown in Fig. 8.6, and have been non-dimensionalized:

$$C_{ac}^{*} = \frac{C_{ac}}{C_{ac,0}} \tag{8.21}$$

where C_{ac}^{*} represents the nondimensional concentration of acetate, C_{ac} is the heterogeneous concentration of acetate, and $C_{ac,0}$ is the inlet acetate concentration. The organics were evenly distributed within the anodic compartment when the influent sodium acetate concentration is 1.0 g L^{-1}, and a decreased organic concentration from the influent is obtained with a lower influent organic concentration (Fig 8.6). The CFD predictions suggest that the anodic surface reaction occurred mainly below 13 cm after the influent organic concentration decreased to 0.2 g L^{-1}, indicating the system was not operated under the optimum condition for energy recovery.

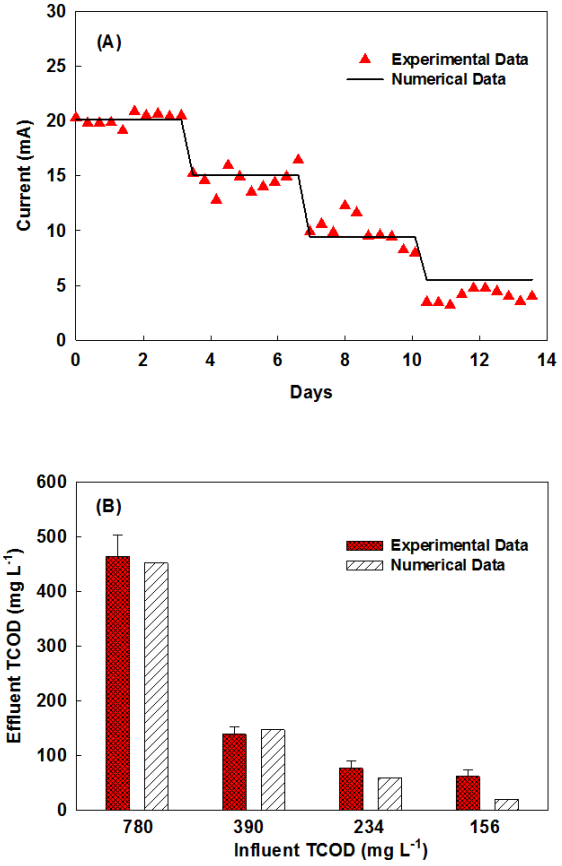

Figure 8.5 Comparison of experimental and reaction model data reducing influent COD from 780 to 390 to 234 to 156 mg L^{-1}: (A) Current generation and (B) COD concentration in effluent

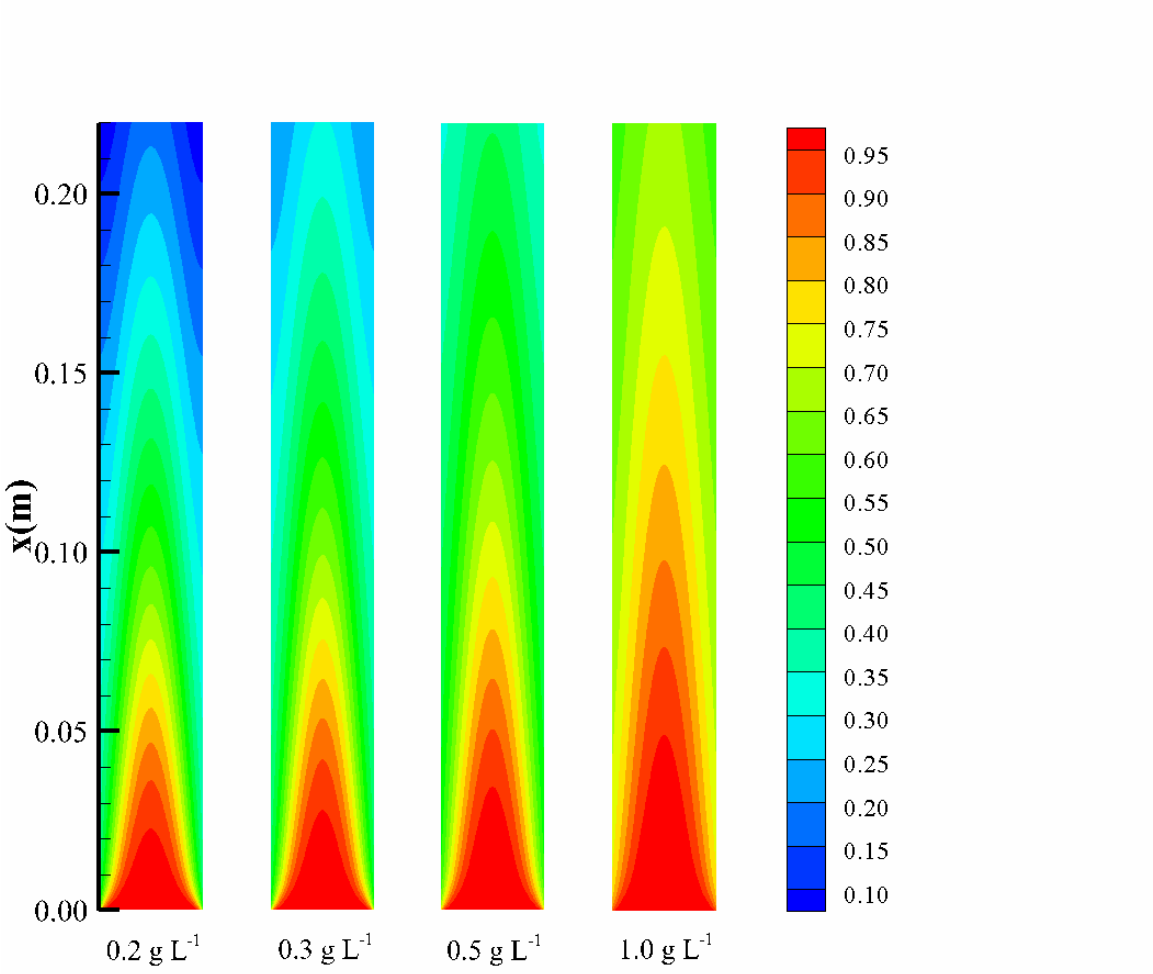

Figure 8.6 Heterogeneous distribution of nondimensional acetate concentration under different influent sodium acetate concentration

The second test was conducted by decreasing the influent flowrate from 1.17 mL min^{-1} (anodic HRT of 5 h) to 0.59 mL min^{-1} (anodic HRT of 10 h) to 0.39 mL min^{-1} (anodic HRT of 15 h), with the influent sodium acetate concentration fixed at 0.3 g L^{-1}, to replicate the strength of traditional municipal wastewater. The CFD predictions for current generation showed satisfactory agreement with the experiments for HRT of 5 and 10 h, as shown in Fig. 8.7, indicating effectiveness of the multi-order reaction model on the surface reaction. However, overestimation can be seen after HRT was extended to 15 h (Fig. 8.7 A), possibly

related to two reasons. First, more substrates are consumed by non-electroactive bacteria. The tubular MFC had two PVC caps as top/bottom ends, which contained no electrode materials and would allow the growth of non-electroactive microbial community. Consumption of organic compounds in such regions could become more dominant with an extended HRT, and as a consequence, less substrate was available for electrochemically-active microorganisms. Unfortunately, such effects were not simulated by the reaction model. Second, the conventional Monod-limitation equation may not be valid to describe methanogenic activity. In this study, the volumetric reaction rate was assumed to follow conventional Monod-limitation equation, in which the reaction rate was related to the sodium acetate concentration and half-reaction constant (Eq. 8.6) in a linear relationship; but actually, this could not occur ideally due to the fierce internal microbial competition with a low feeding rate. The numerical data exhibit good agreement with experimental data on the effluent COD concentration (Fig. 8.7 B), and predicted that the effluent COD is 148 mg L^{-1} at anodic HRT of 5 h, comparable to 134.7±26.4 mg L^{-1} obtained in the experiment. Reducing the influent feeding rate resulted in a lower effluent COD concentration, which was also predicted by the model that showed the effluent COD was reduced to 19 mg L^{-1} after the anodic HRT was extended to 15 h, within in the range of 27.3±19.3 mg L^{-1} obtained from the experiments.

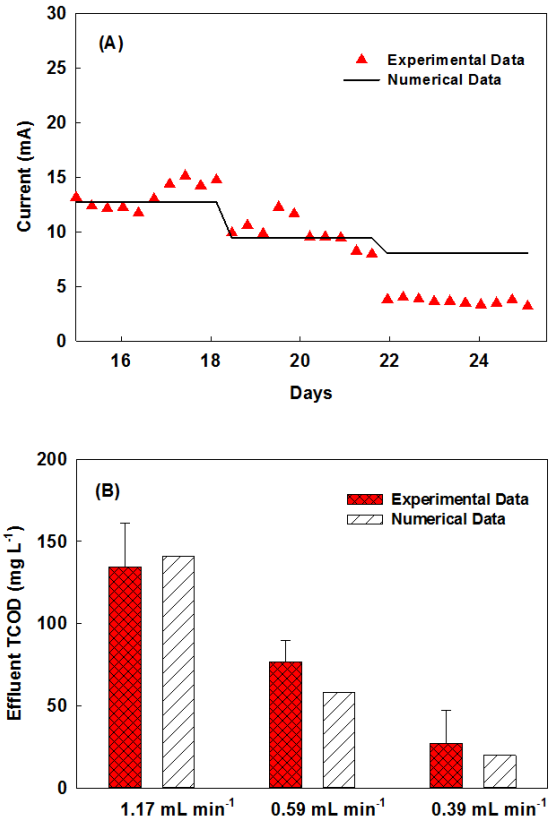

Figure 8.7 Comparison of experimental and reaction model data reducing flow rate of anolyte feeding from 1.17 to 0.59 to 0.39 mL min^{-1} sequentially: (A) Current generation and (B) Effluent total COD concentration

8.4.4 Perspectives

This study has demonstrated that the coupled CFD and multi-order Butler-Volmer model could effectively simulate the multiphysics (*e.g.*, hydrodynamics, species transport, electricity generation) in the anodic chamber of a tubular MFC. Comparing to the previous MFC modeling works (Li and He 2015a, Ping et al. 2014) that assumed homogeneous substrate distribution within anodic chamber and a constant overpotential on the anode surface, our work using a heterogeneous substrate distribution can deliver more accurate predictions for concentration loss, which in turn, affects the activation overpotential on

each geometric cell. The improvement using a heterogeneous model is especially useful for predicting large-scale MFC performance because the systems are not well-mixed due to the operational limitations. Moreover, although the Butler-Volmer- Monod equation has been applied in other published MFC models to represent substrate consumption, biomass growth, and electrochemical reactivity (Huang et al. 2014, Yan and Fan 2013, Zhao et al. 2014), a multi-order model has not been used in conjunction with CFD. Thus the coupling of CFD and the multi-order Butler-Volmer model presented in this paper can be used as a platform to accommodate more diverse electron transfer mechanisms and more complex flow conditions. For example, the addition of external mediator could stimulate biomass activity and enhance electricity generation. Such an operational change can be reflected by varying the exponential number in the multi-order reaction equation. In addition, the influence of substrate type on electricity generation can also be accomplished by modifying the multi-order reaction equation. More complex hydrodynamics (*e.g.*, tortuous internal structure, internal recirculation flow) could be achieved by adopting geometry change from meshing process and modifying inlet and outlet boundary conditions.

Several limitations may exist in the current model and should be addressed with future work. First, like many of the previously published MFC models, real wastewater containing complex substrates and low conductivity was not considered here, resulting in discrepancies between treatment performance and model prediction. Second, the influence of biofilm (*e.g.* thickness, conductivity, and capacity) was not well incorporated into the model formulation. In this study, the biofilm on the anode surface was assumed as an ideal conductive material, in which the produced electrons and protons could be transported

freely. Third, the current model did not involve temperature fluctuations, which may pose a significant influence on biomass activity and mass transport within the anodic compartment. This may be addressed by adding another convection diffusion equation into the governing equations. Last, biomass decay was not included in the model, and this could lead to deviations in the model predictions, especially when the organic concentration becomes low and the decayed biomass could be used as a substrate.

In addition to addressing the above limitations, further improvements may be achieved with knowledge of the electrochemically-active microorganism metabolic activities, which is necessary to determine the reaction order. A two-population microbial community could represent dominant species inside the anodic chamber, but it cannot exactly depict microbial activities. Thus, a complex bacteria community should be described in the model. Moreover, dynamic biomass attachment and detachment from the electrode surface should be considered because biomass thickness affects bacterial activity and diffusion on the substrate. Severe biomass detachment can cause operational issues, which may require a post treatment such as membrane separation process (Li et al. 2016). Thus, it is important to account for dynamic biofilm variation in the model. The reaction potential on the cathode surface should also be considered. For MFC applications, choosing a suitable electron acceptor for the cathode electrode is critical. Oxygen is a possible candidate due to its non-toxic and massive-available characteristics. A localized oxygen concentration can play a significant role in cathodic performance, but a high oxygen concentration may pose an unfavorable influence on the electrochemically-active microorganisms' activity, due to the cross-diffusion issue. Therefore, such a trade-off effect deserves further investigations.

8.5 Conclusions

A coupled CFD-multi-order Butler Volmer reaction model has been proposed and validated in the present work. Convective flow conditions and associated heterogeneous species distributions were simulated using the improved CFD reaction model. Comparing to the conventional Monod-limitation equation, the multi-order model was able to predict current generation and organics removal in a simplified way. The model was experimentally validated by varying organic concentrations and the anolyte flow rate. The CFD predictions demonstrate that the MFC system was not operated under the optimum condition for energy recovery and substrate supply could limit the anodic surface reaction in the higher zone of the reactor. Moreover, it is expected that this new model will not merely be specific to tubular MFC systems, and its application in other reactor configurations (*e.g.*, rectangular cross-section) will be of strong interest. The model can be improved by considering more diverse microbial communities, biomass decay, complex hydrodynamic conditions and dynamic cathodic reaction potentials.

CHAPTER 9

Conclusion

As described in this study, membrane bioelectrochemical reactors were proved to be a promising next-generation advanced wastewater treatment. The conventional membrane fouling issue has been alleviated by using different strategies without causing extra energy consumption. Nutrients removal, another common intrinsic issue associated with anaerobic treatment process, was addressed by taking advantage of anaerobic-aerobic condition between the anodic and cathodic compartments. In addition, overall carbon emission is reduced from this process.

However, several limitations still exist and need to be addressed. In the current work, all of attempted membrane fouling controls are based on the engineering perspective. Such engineering methods could provide straight-forward solutions, but based on the scaling-up perspective, some potential operational problems could emerge as well. For example, the fluidized GAC bed could function as an ideal surface for attached growth, which could result in a potential clogging issue. Alternatively, optimization of aeration in the cathodic chamber is required to minimize the energy demand, without influencing the normal operations. Besides controlling the membrane fouling, advanced membrane materials can be attempted, including applying more hydrophilic membrane by reducing contact angle or using a thinner and conductive polymeric material as a separator. In this way, less residual organics were left to cathodic compartment due to the less internal resistance. Last but not least, coating a layer of nano-silver particles onto membrane surface could be another option to control the fouling issue.

Moreover, the energy advantages of MBERs should be further optimized. This could be accomplished by using a more efficient electrode (*e.g* less overpotential from cathode materials) or optimizing the internal recirculation and aeration pattern. As described in the aforementioned chapter, adding recirculation could boost up electricity generation in an efficient way, but it also requires more energy to offset head pressure loss at inlet port. Such trade-off effects can be investigated by using computational fluid dynamics. Changing the hydrodynamics conditions to increase substrate mixing condition without incurring extra energy consumption could be attempted by adding filling materials within the anodic compartment. Optimizing aeration also could be achieved by using low intensity but coarse bubbling or precise controlling from membrane diffusion.

Direct/indirect wastewater reclamation and reuse from MBERs could be investigated towards agricultural activities, due to the less available freshwater resource. Comparing to the direct potable use, agriculture does not require high-quality water, but pathogen and organic matters should be given enough attention. MBERs can be an option to meet these requirements. Both the organics and pathogen could be effectively removed from membrane permeate by either biodegradation process or physical separation. While the nutrient elements such as potassium, nitrogen and phosphorus can be reused as a partial fertilizer to subsequent agricultural practice.

Last, but not least, a next-generation MBER model can be developed by taking account a more complex condition within the anodic compartment, such as heterogeneous biomass and substrate distribution, equilibrium between new biomass produced and decay, and

mixed bacterial consortium. The separator materials (either cation exchange membrane or anion exchange membrane) cannot prevent oxygen diffusion in an ideal way, which means some substrate can be utilized by aerobic bacteria, rather than electro-active bacteria. Therefore, aerobic bacteria activity should be taken into account in the next generation MBER model. Cathode performance should be considered in a next generation MBER model as well. Until now, most of microbial fuel cell modeling assumed an ideal and constant cathode performance, which does not always happen in actual operation. Oxygen diffusion toward cathode surface is an important factor to influence electricity generation. However, this has been seldom investigated in previous modeling studies.

Reference

Alonso, A. Camargo, J.A. 2006 Toxicity of nitrite to three species of freshwater invertebrates. *Environmental Toxicology*. **21**, 90-94.

Ang, W.L., Mohammad, A.W., Hilal, N. Leo, C.P. 2015 A review on the applicability of integrated/hybrid membrane processes in water treatment and desalination plants. *Desalination*. **363**, 2-18.

Angenent, L.T. Sung, S. 2001 Development of anaerobic migrating blanket reactor (AMBR), a novel anaerobic treatment system. *Water Research*. **35**, 1739-1747.

Arimi, M.M., Knodel, J., Kiprop, A., Namango, S.S., Zhang, Y. Geißen, S.-U. 2015 Strategies for improvement of biohydrogen production from organic-rich wastewater: a review. *Biomass and Bioenergy*. **75**, 101-118.

Asano, T. Cotruvo, J.A. 2004 Groundwater recharge with reclaimed municipal wastewater: health and regulatory considerations. *Water Research*. **38**, 1941-1951.

Borole, A.P. 2011 Improving energy efficiency and enabling water recycling in biorefineries using bioelectrochemical systems. *Biofuels, Bioproducts and Biorefining*. **5**, 28-36.

Bunani, S., Yörükoğlu, E., Yüksel, Ü., Kabay, N., Yüksel, M. Sert, G. 2015 Application of reverse osmosis for reuse of secondary treated urban wastewater in agricultural irrigation. *Desalination*. **364**, 68-74.

Cao, X., Huang, X., Liang, P., Xiao, K., Zhou, Y., Zhang, X. Logan, B.E. 2009 A New Method for Water Desalination Using Microbial Desalination Cells. *Environmental Science & Technology*. **43**, 7148-7152.

Celik, I.B., Ghia, U. Roache, P.J. 2008 Procedure for estimation and reporting of uncertainty due to discretization in CFD applications. *Journal of Fluid Mechanics Transaction-ASME*. **130**.

Chan, Y.J., Chong, M.F., Law, C.L. Hassell, D.G. 2009 A review on anaerobic–aerobic treatment of industrial and municipal wastewater. *Chemical Engineering Journal*. **155**, 1-18.

Cord-Ruwisch, R., Law, Y. Cheng, K.Y. 2011 Ammonium as a sustainable proton shuttle in bioelectrochemical systems. *Bioresource Technology*. **102**, 9691-9696.

Cusick, R.D., Ullery, M.L., Dempsey, B.A. Logan, B.E. 2014 Electrochemical struvite precipitation from digestate with a fluidized bed cathode microbial electrolysis cell. *Water Research*. **54**, 297-306.

Darton, R., Keairns, D., King, D. Kohlbrand, H. 2014 The Great Water-Energy-Food Challenge. *Chemical Engineering Progress*. **110**, 4-4.

Diez, V., Ezquerra, D., Cabezas, J., García, A. Ramos, C. 2014 A modified method for evaluation of critical flux, fouling rate and in situ determination of resistance and compressibility in MBR under different fouling conditions. *Journal of Membrane Science*. **453**, 1-11.

Freguia, S., Rabaey, K., Yuan, Z. Keller, J. 2007 Electron and carbon balances in microbial fuel cells reveal temporary bacterial storage behavior during electricity generation. *Environmental Science & Technology*. **41**, 2915-2921.

Ge, Z., Li, J., Xiao, L., Tong, Y. He, Z. 2013a Recovery of electrical energy in microbial fuel cells: brief review. *Environmental Science & Technology Letters*. **1**, 137-141.

Ge, Z., Ping, Q. He, Z. 2013b Hollow-fiber membrane bioelectrochemical reactor for domestic wastewater treatment. *Journal of Chemical Technology & Biotechnology*. **88**, 1584-1590.

Ge, Z., Zhang, F., Grimaud, J., Hurst, J. He, Z. 2013c Long-term investigation of microbial fuel cells treating primary sludge or digested sludge. *Bioresource Technology*. **136**, 509-514.

Ge, Z., Dosoretz, C.G. He, Z. 2014 Effects of number of cell pairs on the performance of microbial desalination cells. *Desalination*. **341**, 101-106.

Ge, Z. He, Z. 2015 An effective dipping method for coating activated carbon catalyst on the cathode electrodes of microbial fuel cells. *RSC Advances*. **5**, 36933-36937.

González-Cabaleiro, R., Lema, J.M. Rodríguez, J. 2015 Metabolic energy-based modelling explains product yielding in anaerobic mixed culture fermentations. *PLoS ONE*. **10**, e0126739.

He, Z., Wagner, N., Minteer, S.D. Angenent, L.T. 2006 An upflow microbial fuel cell with an interior cathode: assessment of the internal resistance by impedance spectroscopy. *Environmental Science & Technology*. **40**, 5212-5217.

He, Z. Mansfeld, F. 2009 Exploring the use of electrochemical impedance spectroscopy (EIS) in microbial fuel cell studies. *Energy & Environmental Science*. **2**, 215-219.

Hernández-Fernández, F.J., Pérez de los Ríos, A., Salar-García, M.J., Ortiz-Martínez, V.M., Lozano-Blanco, L.J., Godínez, C., Tomás-Alonso, F. Quesada-Medina, J. 2015 Recent progress and perspectives in microbial fuel cells for bioenergy generation and wastewater treatment. *Fuel Process Technology*. **138**, 284-297.

Huang, H., Wang, X., Gong, X. You, S. 2014 Numerical anodic mass transfer of redox mediators in microbial fuel cell, Materials for Renewable Energy and Environment (ICMREE), 2013 International Conference on, IEEE 298-302.

Jacobson, K.S., Kelly, P.T. He, Z. 2015 Energy balance affected by electrolyte recirculation and operating modes in microbial fuel cells. *Water Environment Research*. **87**, 252-257.

Judd, S. 2008 The status of membrane bioreactor technology. *Trends in Biotechnology*. **26**, 109-116.

Judd, S. (2010) The MBR book: principles and applications of membrane bioreactors for water and wastewater treatment, Elsevier.

Kelly, P.T. He, Z. 2014 Nutrients removal and recovery in bioelectrochemical systems: A review. *Bioresource Technology*. **153**, 351-360.

Khan, S.J., Visvanathan, C. Jegatheesan, V. 2009 Prediction of membrane fouling in MBR systems using empirically estimated specific cake resistance. *Bioresource Technology*. **100**, 6133-6136.

Kim, B., Kim, H., Kim, J. Yu, J. 2014a Computational fluid dynamic analysis in microbial fuel cells with different anode configurations. *Water Science and Technology*. **69**, 1447-1452.

Kim, J., Kim, K., Ye, H., Lee, E., Shin, C., McCarty, P.L. Bae, J. 2011 Anaerobic fluidized bed membrane bioreactor for wastewater treatment. *Environmental Science & Technology*. **45**, 576-581.

Kim, J.R., Boghani, H.C., Amini, N., Aguey-Zinsou, K.-F., Michie, I., Dinsdale, R.M., Guwy, A.J., Guo, Z.X. Premier, G.C. 2012 Porous anodes with helical flow pathways in bioelectrochemical systems: The effects of fluid dynamics and operating regimes. *Journal of Power Sources*. **213**, 382-390.

Kim, K.-Y., Chae, K.-J., Choi, M.-J., Yang, E.-T., Hwang, M.H. Kim, I.S. 2013 High-quality effluent and electricity production from non-CEM based flow-through type microbial fuel cell. *Chemical Engineering Journal*. **218**, 19-23.

Kim, K.-Y., Yang, E., Lee, M.-Y., Chae, K.-J., Kim, C.-M. Kim, I.S. 2014b Polydopamine coating effects on ultrafiltration membrane to enhance power density and mitigate biofouling of ultrafiltration microbial fuel cells (UF-MFCs). *Water Research*. **54**, 62-68.

Knowles, R. 1982 Denitrification. *Microbiological reviews*. **46**, 43.

Krzeminski, P., van der Graaf, J.H. van Lier, J.B. 2012 Specific energy consumption of membrane bioreactor (MBR) for sewage treatment. *Water Science and Technology*. **65**, 380.

Li, J., Ge, Z. He, Z. 2014a A fluidized bed membrane bioelectrochemical reactor for energy-efficient wastewater treatment. *Bioresource Technology*. **167**, 310-315.

Li, J., Ge, Z. He, Z. 2014b Advancing membrane bioelectrochemical reactor (MBER) with hollow-fiber membranes installed in the cathode compartment. *Journal of Chemical Technology & Biotechnology*. **89**, 1330-1336.

Li, J. He, Z. 2015a Development of a dynamic mathematical model for membrane bioelectrochemical reactors with different configurations. *Environmental Science and Pollution Research*. **23,** 3897-3906.

Li, J. He, Z. 2015b Optimizing the performance of a membrane bio-electrochemical reactor using an anion exchange membrane for wastewater treatment. *Environmental Science: Water Research & Technology*. **1**, 355-362.

Li, J., Zhu, Y., Zhuang, L., Otsuka, Y., Nakamura, M., Goodell, B., Sonoki, T. He, Z. 2015 A novel approach to recycle bacterial culture waste for fermentation reuse via a microbial fuel cell-membrane bioreactor system. *Bioprocess and biosystems engineering*. **38,** 1795-1802.

Li, J., Rosenberger, G. He, Z. 2016 Integrated experimental investigation and mathematical modeling of a membrane bioelectrochemical reactor with an external membrane module. *Chemical Engineering Journal*. **287**, 321-328.

Li, W.-W., Yu, H.-Q. He, Z. 2014c Towards sustainable wastewater treatment by using microbial fuel cells-centered technologies. *Energy & Environmental Science*. **7**, 911-924.

Liu, H., Ramnarayanan, R. Logan, B.E. 2004 Production of electricity during wastewater treatment using a single chamber microbial fuel cell. *Environmental Science & Technology*. **38**, 2281-2285.

Liu, H., Grot, S. Logan, B.E. 2005 Electrochemically assisted microbial production of hydrogen from acetate. *Environmental Science & Technology*. **39**, 4317-4320.

Liu, R., Huang, X., Sun, Y.F. Qian, Y. 2003 Hydrodynamic effect on sludge accumulation over membrane surfaces in a submerged membrane bioreactor. *Process Biochemistry*. **39**, 157-163.

Liu, Z.-h., Yin, H., Dang, Z. Liu, Y. 2014 Dissolved methane: a hurdle for anaerobic treatment of municipal wastewater. *Environmental Science & Technology*. **48**, 889-890.

Logan, B.E., Hamelers, B., Rozendal, R., Schröder, U., Keller, J., Freguia, S., Aelterman, P., Verstraete, W. Rabaey, K. 2006a Microbial fuel cells: methodology and technology. *Environmental Science & Technology*. **40**, 5181-5192.

Lovley, D.R. 2008 The microbe electric: conversion of organic matter to electricity. *Current Opinion in Biotechnology*. **19**, 564-571.

Luo, S., Sun, H., Ping, Q., Jin, R. He, Z. 2015 A review of Modeling Bioelectrochemical System (BES): Engineering and Statistical Aspects. *Energies*. 9: 111

Malaeb, L., Katuri, K.P., Logan, B.E., Maab, H., Nunes, S.P. Saikaly, P.E. 2013 A hybrid microbial fuel cell membrane bioreactor with a conductive ultrafiltration membrane biocathode for wastewater treatment. *Environmental Science & Technology*. **47**, 11821-11828.

Marcus, A.K., Torres, C.I. Rittmann, B.E. 2007 Conduction-based modeling of the biofilm anode of a microbial fuel cell. *Biotechnology & Bioengineering*. **98**, 1171-1182.

Martin, I., Pidou, M., Soares, A., Judd, S. Jefferson, B. 2011 Modelling the energy demands of aerobic and anaerobic membrane bioreactors for wastewater treatment. *Environmental Technology*. **32**, 921-932.

Matos, C., Pereira, S., Amorim, E., Bentes, I. Briga-Sá, A. 2014 Wastewater and greywater reuse on irrigation in centralized and decentralized systems—An integrated approach on water quality, energy consumption and CO 2 emissions. *Science of the Total Environment*. **493**, 463-471.

McCarty, P.L., Bae, J. Kim, J. 2011 Domestic wastewater treatment as a net energy producer–can this be achieved? *Environmental Science & Technology*. **45**, 7100-7106.

Melin, T., Jefferson, B., Bixio, D., Thoeye, C., De Wilde, W., De Koning, J., Van der Graaf, J. Wintgens, T. 2006 Membrane bioreactor technology for wastewater treatment and reuse. *Desalination*. **187**, 271-282.

Meng, F., Chae, S.-R., Drews, A., Kraume, M., Shin, H.-S. Yang, F. 2009 Recent advances in membrane bioreactors (MBRs): Membrane fouling and membrane material. *Water Research*. **43**, 1489-1512.

Michie, I.S., Kim, J.R., Dinsdale, R.M., Guwy, A.J. Premier, G.C. 2014 The influence of anodic helical design on fluid flow and bioelectrochemical performance. *Bioresource Technology*. **165**, 13-20.

Mohsen, M.S. Jaber, J.O. 2003 Potential of industrial wastewater reuse. *Desalination*. **152**, 281-289.

Morris, J.M., Jin, S., Crimi, B. Pruden, A. 2009 Microbial fuel cell in enhancing anaerobic biodegradation of diesel. *Chemical Engineering Journal*. **146**, 161-167.

Ng, A.N. Kim, A.S. 2007 A mini-review of modeling studies on membrane bioreactor (MBR) treatment for municipal wastewaters. *Desalination*. **212**, 261-281.

Nges, I.A., Wang, B., Cui, Z. Liu, J. 2015 Digestate liquor recycle in minimal nutrients-supplemented anaerobic digestion of wheat straw. *Biochemical Engineering Journal*. **94**, 106-114.

Nozzi, N.E., Desai, S.H., Case, A.E. Atsumi, S. 2014 Metabolic engineering for higher alcohol production. *Metabolic Engineering*. **25**, 174-182.

Ortiz-Martínez, V.M., Salar-García, M.J., de los Ríos, A.P., Hernández-Fernández, F.J., Egea, J.A. Lozano, L.J. 2015 Developments in microbial fuel cell modeling. *Chemical Engineering Journal*. **271**, 50-60.

Otsuka, Y., Nakamura, M., Shigehara, K., Sugimura, K., Masai, E., Ohara, S. Katayama, Y. 2006 Efficient production of 2-pyrone 4, 6-dicarboxylic acid as a novel polymer-based material from protocatechuate by microbial function. *Applied Microbiology and Biotechnology*. **71**, 608-614.

Palachek, R.M. Tomasso, J.R. 1984 Nitrite toxicity to fathead minnows: Effect of fish weight. *Bulletin of Environmental Contamination and Toxicology*. **32**, 238-242.

Passanha, P., Kedia, G., Dinsdale, R.M., Guwy, A.J. Esteves, S.R. 2014 The use of NaCl addition for the improvement of polyhydroxyalkanoate production by Cupriavidus necator. *Bioresource Technology*. **163**, 287-294.

Pham, H.T., Boon, N., Aelterman, P., Clauwaert, P., De Schamphelaire, L., Van Oostveldt, P., Verbeken, K., Rabaey, K. Verstraete, W. 2008 High shear enrichment improves the performance of the anodophilic microbial consortium in a microbial fuel cell. *Microbial biotechnology*. **1**, 487-496.

Picioreanu, C., Head, I.M., Katuri, K.P., van Loosdrecht, M.C.M. Scott, K. 2007 A computational model for biofilm-based microbial fuel cells. *Water Research*. **41**, 2921-2940.

Picioreanu, C., van Loosdrecht, M.C.M., Curtis, T.P. Scott, K. 2010 Model based evaluation of the effect of pH and electrode geometry on microbial fuel cell performance. *Bioelectrochemistry.***78**, 8-24.

Ping, Q., Zhang, C., Chen, X., Zhang, B., Huang, Z. He, Z. 2014 Mathematical model of dynamic behavior of microbial desalination cells for simultaneous wastewater

treatment and water desalination. *Environmental Science & Technology*. **48**, 13010-13019.

Pinto, R., Srinivasan, B., Manuel, M.-F. Tartakovsky, B. 2010 A two-population bio-electrochemical model of a microbial fuel cell. *Bioresource Technology*. **101**, 5256-5265.

Qin, M. He, Z. 2014 Self-supplied ammonium bicarbonate draw solute for achieving wastewater treatment and recovery in a microbial electrolysis cell-forward osmosis-coupled system. *Environmental Science & Technology Letters*. **1**, 437-441.

Rabaey, K., Clauwaert, P., Aelterman, P. Verstraete, W. 2005 Tubular microbial fuel cells for efficient electricity generation. *Environmental. Science & Technology*. **39**, 8077-8082.

Rabaey, K. Verstraete, W. 2005 Microbial fuel cells: novel biotechnology for energy generation. *Trends in Biotechnology*. **23**, 291-298.

Ren, L., Ahn, Y. Logan, B.E. 2014 A two-stage microbial fuel cell and anaerobic fluidized bed membrane bioreactor (MFC-AFMBR) system for effective domestic wastewater treatment. *Environmental Science & Technology*. **48**, 4199-4206.

Rezania, B., Oleszkiewicz, J. Cicek, N. 2007 Hydrogen-dependent denitrification of water in an anaerobic submerged membrane bioreactor coupled with a novel hydrogen delivery system. *Water Research*. **41**, 1074-1080.

Roache, P.J. 1994 Perspective: a method for uniform reporting of grid refinement studies. *Journal of Fluid Engineering*. **116**, 405-413.

Rosa, P.R.F., Santos, S.C., Sakamoto, I.K., Varesche, M.B.A. Silva, E.L. 2014 Hydrogen production from cheese whey with ethanol-type fermentation: Effect of hydraulic retention time on the microbial community composition. *Bioresource Technology*. **161**, 10-19.

Sato, O., Suzuki, Y., Sato, Y., Sasaki, S. Sonoki, T. 2015 Water-insoluble material from apple pomace makes changes in intracellular NAD+/NADH ratio and pyrophosphate content and stimulates fermentative production of hydrogen. *Journal of Bioscience and Bioengineering*. **119**, 543-547.

Shin, C., McCarty, P.L., Kim, J. Bae, J. 2014 Pilot-scale temperate-climate treatment of domestic wastewater with a staged anaerobic fluidized membrane bioreactor (SAF-MBR). *Bioresource Technology*. **159**, 95-103.

Smith, A.L., Stadler, L.B., Love, N.G., Skerlos, S.J. Raskin, L. 2012 Perspectives on anaerobic membrane bioreactor treatment of domestic wastewater: A critical review. *Bioresource Technology*. **122**, 149-159.

Sonoki, T., Morooka, M., Sakamoto, K., Otsuka, Y., Nakamura, M., Jellison, J. Goodell, B. 2014 Enhancement of protocatechuate decarboxylase activity for the effective production of muconate from lignin-related aromatic compounds. *Journal of Biotechnology*. **192**, 71-77.

Souza, C., Chernicharo, C. Aquino, S. 2011 Quantification of dissolved methane in UASB reactors treating domestic wastewater under different operating conditions. *Water Science & Technology*. **64**, 2259-2264.

Stein, N.E., Hamelers, H.M., van Straten, G. Keesman, K.J. 2012 On-line detection of toxic components using a microbial fuel cell-based biosensor. *Journal of Process Control*. **22**, 1755-1761.

Sun, H., Luo, S., Jin, R. He, Z. 2015 Multitask lasso model for investigating multimodule design factors, operational factors, and covariates in tubular microbial fuel cells. *ACS Sustainable Chemical Engineering*. **3**, 3231-3238.

Sun, Z., Ramsay, J.A., Guay, M. Ramsay, B.A. 2007 Carbon-limited fed-batch production of medium-chain-length polyhydroxyalkanoates from nonanoic acid by Pseudomonas putida KT2440. *Applied Microbiology and Biotechnology*. **74**, 69-77.

Tian, Y., Li, H., Li, L., Su, X., Lu, Y., Zuo, W. Zhang, J. 2015 In-situ integration of microbial fuel cell with hollow-fiber membrane bioreactor for wastewater treatment and membrane fouling mitigation. *Biosensors and Bioelectronics*. **64**, 189-195.

Vardon, D.R., Franden, M.A., Johnson, C.W., Karp, E.M., Guarnieri, M.T., Linger, J.G., Salm, M.J., Strathmann, T.J. Beckham, G.T. 2015 Adipic acid production from lignin. *Energy & Environmental Science*. **8**, 617-628.

Vila-Rovira, A., Puig, S., Balaguer, M.D. Colprim, J. 2015 Anode hydrodynamics in bioelectrochemical systems. *RSC Advances*. **5**, 78994-79000.

Wang, C., Li, Q., Wang, D. Xing, J. 2014a Improving the lactic acid production of Actinobacillus succinogenes by using a novel fermentation and separation integration system. *Process Biochemistry*. **49**, 1245-1250.

Wang, C.T., Shaw, C.K. Hu, T.Y. 2011a Optimization of flow in microbial fuel cells: an investigation into promoting micro-mixer efficiency with obstacle. *Tamkang Journal Science Engineering.* **14**, 25-31.

Wang, H. Ren, Z.J. 2013 A comprehensive review of microbial electrochemical systems as a platform technology. *Biotechnology Advances*. **31**, 1796-1807.

Wang, H., Luo, H., Fallgren, P.H., Jin, S. Ren, Z.J. 2015 Bioelectrochemical system platform for sustainable environmental remediation and energy generation. *Biotechnology Advances*. **33**, 317-334.

Wang, X., Yue, X. Guo, Q. 2014b Production of electricity during wastewater treatment using fluidized - bed microbial fuel cells. *Chemical Engineering & Technology*. **37**, 703-708.

Wang, Y.-K., Sheng, G.-P., Li, W.-W., Huang, Y.-X., Yu, Y.-Y., Zeng, R.J. Yu, H.-Q. 2011b Development of a novel bioelectrochemical membrane reactor for wastewater treatment. *Environmental Science & Technology*. **45**, 9256-9261.

Wang, Y.-K., Sheng, G.-P., Shi, B.-J., Li, W.-W. Yu, H.-Q. 2013 A novel electrochemical membrane bioreactor as a potential net energy producer for sustainable wastewater treatment. *Scientific reports*. **3**.

Wang, Y.-P., Liu, X.-W., Li, W.-W., Li, F., Wang, Y.-K., Sheng, G.-P., Zeng, R.J. Yu, H.-Q. 2012 A microbial fuel cell–membrane bioreactor integrated system for cost-effective wastewater treatment. *Applied Energy*. **98**, 230-235.

Xiao, L., Damien, J., Luo, J., Jang, H.D., Huang, J. He, Z. 2012 Crumpled graphene particles for microbial fuel cell electrodes. *Journal of Power Sources*. **208**, 187-192.

Xiao, L., Ge, Z., Kelly, P., Zhang, F. He, Z. 2014 Evaluation of normalized energy recovery (NER) in microbial fuel cells affected by reactor dimensions and substrates. *Bioresource Technology*. **157**, 77-83.

Xu, K. Xu, P. 2014 Betaine and beet molasses enhance L-lactic acid production by Bacillus coagulans. *PloS One*. **9**(6): e100731

Xu, L., Zhao, Y.Q., Doherty, L., Hu, Y.S. Hao, X.D. 2016 The integrated processes for wastewater treatment based on the principle of microbial fuel cells: A review. *Critical Review Environmental Science & Technology*. **46**, 60-91.

Yadav, S., Rawat, G., Tripathi, P. Saxena, R. 2014 Dual substrate strategy to enhance butanol production using high cell inoculum and its efficient recovery by pervaporation. *Bioresource Technology*. **152**, 377-383.

Yan, M., Fan, L. 2013 Constant voltage output in two-chamber microbial fuel cell under fuzzy PID control. *International Journal of Electrochemical Science*. **8**, 3321-3332.

Yan, Q., Zheng, P., Tao, S.-T. Dong, J.-J. 2014 Fermentation process for continuous production of succinic acid in a fibrous bed bioreactor. *Biochemical Engineering Journal*. **91**, 92-98.

Yang, W., Cicek, N. Ilg, J. 2006 State-of-the-art of membrane bioreactors: Worldwide research and commercial applications in North America. *Journal of Membrane Science*. **270**, 201-211.

Yano, K. Nishi, T. 1980 pKJ1, a naturally occurring conjugative plasmid coding for toluene degradation and resistance to streptomycin and sulfonamides. *Journal of Bacteriology*. **143**, 552-560.

You, S., Zhao, Q., Zhang, J., Jiang, J. Zhao, S. 2006 A microbial fuel cell using permanganate as the cathodic electron acceptor. *Journal of Power Sources*. **162**, 1409-1415.

Yuan, H., Abu-Reesh, I.M. He, Z. 2015 Enhancing desalination and wastewater treatment by coupling microbial desalination cells with forward osmosis. *Chemical Engineering Journal*. **270**, 437-443.

Yuan, H. He, Z. 2015 Integrating membrane filtration into bioelectrochemical systems as next generation energy-efficient wastewater treatment technologies for water reclamation: A review. *Bioresource Technology*. **195**, 202-209.

Zeng, Y., Choo, Y.F., Kim, B.-H. Wu, P. 2010 Modelling and simulation of two-chamber microbial fuel cell. *Journal of Power Sources*. **195**, 79-89.

Zhang, F., Jacobson, K.S., Torres, P. He, Z. 2010 Effects of anolyte recirculation rates and catholytes on electricity generation in a litre-scale upflow microbial fuel cell. *Energy & Environmental Science*. **3**, 1347-1352.

Zhang, F. He, Z. 2012a Simultaneous nitrification and denitrification with electricity generation in dual-cathode microbial fuel cells. *Journal of Chemical Technology & Biotechnology*. **87**, 153-159.

Zhang, F. He, Z. 2012b Integrated organic and nitrogen removal with electricity generation in a tubular dual-cathode microbial fuel cell. *Process Biochemistry*. **47**, 2146-2151.

Zhang, F., Ge, Z., Grimaud, J., Hurst, J. He, Z. 2013a Improving electricity production in tubular microbial fuel cells through optimizing the anolyte flow with spiral spacers. *Bioresource Technology*. **134**, 251-256.

Zhang, F., Ge, Z., Grimaud, J., Hurst, J. He, Z. 2013b Long-term performance of liter-scale microbial fuel cells treating primary effluent installed in a municipal wastewater treatment facility. *Environmental Science & Technology*. **47**, 4941-4948.

Zhang, F. He, Z. 2015 Scaling up microbial desalination cell system with a post-aerobic process for simultaneous wastewater treatment and seawater desalination. *Desalination*. **360**, 28-34.

Zhao, L., Brouwer, J., Naviaux, J. Hochbaum, A. (2014) Modeling of polarization losses of a microbial fuel cell. ASME 2014 12th International Conference on Fuel Cell Science, Engineering and Technology collocated with the ASME 2014 8th International Conference on Energy Sustainability, American Society of Mechanical Engineers, 2014.

Zuriaga-Agustí, E., Bes-Piá, A., Mendoza-Roca, J.A. Alonso-Molina, J.L. 2013 Influence of extraction methods on proteins and carbohydrates analysis from MBR activated sludge flocs in view of improving EPS determination. *Separation and Purification Technology*. **112**, 1-10.

Zuthi, M., Ngo, H., Guo, W., Nghiem, L., Hai, F., Xia, S., Zhang, Z. Li, J. 2015 Biomass viability: An experimental study and the development of an empirical mathematical model for submerged membrane bioreactor. *Bioresource Technology*. **190**, 352-358.